Ground-state Overlaps and Topological Phase Transitions

by

Jiahua Gu

A dissertation submitted in partial fulfillment
of the requirements for the degree of
Doctor of Philosophy
(Physics)
in The University of Michigan
2019

Doctoral Committee:

Associate Professor Kai Sun, Chair
Professor Cagliyan Kurdak
Associate Professor Lu Li
Professor James Liu

Jiahua Gu

jiahuagu@umich.edu

ORCID: 0000-0001-5516-8845

ACKNOWLEDGEMENTS

First I would like to thank my advisor, Professor Kai Sun, for his generous support and education in the past 7 years. I made my mind to work with him in my first semester here in Michigan. During our first meeting, he was so kind that he even analyzed for me what would be the pros and cons to choose a young advisor. I knew he would be a great advisor from then. Indeed, later on, he not only supported my research, but also encouraged me to attend more than 10 conferences and summer schools. With these great resources, I gradually built up a general view of condensed matter physics and also made a lot of peer friends. My advisor also has great insights over nearly every corner of physics. So I could always get help from him whenever I stuck with some problems. He also gave me enough freedom on what I would like to research on. Without his support, this thesis would not be possible. All in all, I learned both physics and communication with him. This great experience would be precious for my future career development.

I am grateful to the committee. Although the end of the semester is extremely busy for them, they are still willing to spend time attending my defense, reading my thesis and providing critical comments.

I would also like to thank my family for their love and care in both my everyday life and education. My parents worked in the health center in our town. They have been working diligently in the past few decades to provide me the best education and life that they could afford. I still remember my mother came back very late in the night and kissed me and my sleeping brother during the 2003 SARS period in China.

Even in such a busy time, my father still remembered to discuss my study with my teachers. He bought me the exercise book on Geometry in my middle school. Those problems are so interesting that I was fascinated by the beauty of geometry. This placed in my heart a seed for my later interest in topology and physics. My mother is kind and beautiful. She fed me very well and told me not to worry about anything. So I could focus on my study without being disturbed.

Last but not least, I owe a debt of gratitude to my girl friend and all other friends I met in Michigan. They made my life colorful in the 7 years' PhD study.

TABLE OF CONTENTS

LIST OF FIGURES

Figure

LIST OF APPENDICES

Appendix

ABSTRACT

For decades, Landaus theory of phase transition has provided a successful classification for quantum and classical states of matter based on their symmetry broken patterns, except for certain exotic quantum states such as the fractional quantum Hall (FQH) effect. However, such exotic phenomena are crucial for a complete understanding of the nature. This thesis explores new physical principles emerging from topology and topological states.

First, we use an example to demonstrate Landaus theory by studying a pair-density wave system, where the symmetry-breaking paradigm is applicable. It turns out that such a system exhibits the Kosterlitz-Thouless (KT) transition, a phase transition driven by the proliferation of topological defects, i.e. vortex-antivortex pairs. For topological systems, where symmetry broken pattern cannot be used as a classification tool, we prove a theorem that two gapped systems with non-vanishing ground-state overlap must be adiabatically connected, and thus are necessarily in the same topological phase. This theorem provides a simple and generic approach to classify topological band insulators/superconductors, without the needs to calculate any known or yet-to-known topological indices. Once the overlap is found nonzero, the two systems must be topologically identical. After presenting a generic proof, the theorem is also verified through calculating the overlap for several milestone topological band insulators and certain interacting systems.

Such an overlap technique is then generalized to $(2 + 1)$-D strongly-interacting topological systems at fixed points, including both symmetry-protected topological

(SPT) states and intrinsic topological states like FQH. For interacting topological states, the main challenge of utilizing wave-function overlaps to classify them lies in the famous Anderson orthogonality catastrophe (AOC), which states that two different many-body wave functions must have zero overlap in the thermodynamic limit. In this thesis, we found that wave-function overlaps indeed carry critical information about the topological nature of quantum states and this information can be extracted from the finite-size scaling of the overlaps. In the finite-size scaling analysis, we found a universal topological response term as a sub-leading contribution. This term depends on both the central charge of the corresponding conformal field theory (CFT) and the Euler characteristics of the underlying manifolds on which the system is defined. This term reveals a fundamental connection between ground-state overlaps and CFTs. In addition, surprisingly, the overlap between an intrinsic topological state and a topologically trivial product state shows a decay faster than the exponential behavior expected via a typical AOC analysis. Such finite-size scaling behaviors could be utilized to theoretically detect the gapless edge modes, and to distinguish the topology of quantum states or serve as a signature of topological phase transitions. Possible generalization to higher dimensions and generic non-fixed-point topological systems is also discussed.

CHAPTER I

Introduction

1.1 Translational symmetry and band theories

Symmetry lies on the root of physics. One most common symmetry in condensed matter systems is the discrete translational symmetry, i.e., periodicity. In a material without boundary, electrons feel the same random Coulomb potential from all other electrons, as well as a periodic attractive interaction from all the ions. As we know, the dispersion relation of a single free electron is quadratic in momentum,

$$E = \frac{\boldsymbol{p}^2}{2m} = \frac{\hbar^2 \boldsymbol{k}^2}{2m}. \tag{1.1}$$

The periodicity of the ion potential leads to a periodic dispersion relation for the electrons (see Fig. 1.1). And interactions lift the degeneracy of such dispersion relation on high symmetry points [1]. So periodicity and interaction together create the bands in the energy dispersion of electronic systems. Actually, a comprehensive theory based on symmetries has been developed to derive the dispersion of bands in each lattice [2].

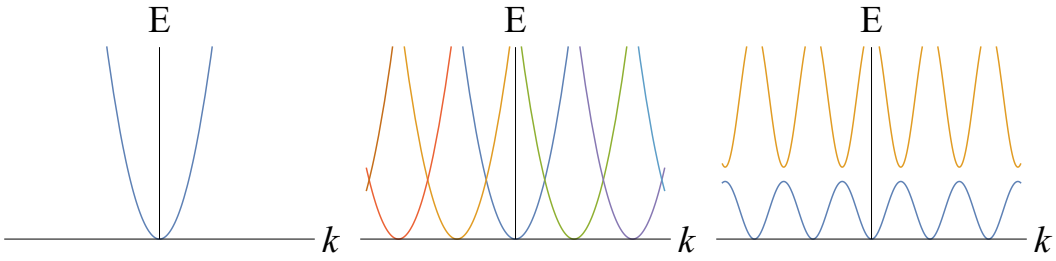

Figure 1.1: (Left) Dispersion relation of free electrons; (Middle) Dispersion relation of electrons in periodic potential; (Right) Interaction lifts the degeneracy.

Due to Pauli exclusion principle, each quantum state could only hold one electron [1]. With all the states on different bands available, electrons in the condensed matter system start to fill in from lowest energy to higher energy. Since in materials the number of electrons is finite while the number of energy levels is infinite, there is naturally an uppermost energy level that electrons could reach, called Fermi level. Bands are filled below this level and empty above. If the Fermi level lies in the gap between two bands, the material would be an insulator (at low temperature). The reason is that electrons would need to overcome an energy gap to hop to a different quantum state. But there is no extra energy for electrons to accomplish that at low enough temperature (Superconductivity is out of our scope of discussion). So their mobility in the material is restricted. This kind of materials does not conduct electricity and hence becomes an insulator. Otherwise, if it crosses one or more of the bands, the material is a metal because electrons close to the Fermi level could move to the next state on the same band via paying infinitesimal energy penalty. This energy might come from thermal fluctuations. Of course, if the energy gap is small enough, we may define a semiconductor. When the temperature is high enough and electrons have enough energy to overcome the energy gap, a semiconductor could be turned into a (poor) conductor. Strictly speaking, a semiconductor is still an insulator since the definitions are assuming no thermal fluctuations.

1.2 Symmetry and Landau theory for insulators

Besides band theories, symmetry is also the key to Landau theory of phase transitions [3–5]. In different phases of matter, electrons form different patterns. Each pattern is invariant under certain symmetry groups. Some symmetry groups are subgroups of others. It was realized that the change of electron configuration patterns are related to symmetry breaking. And a symmetry-breaking theory of phase transition is thus formulated.

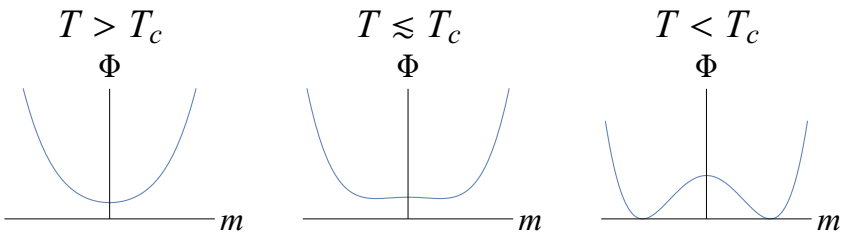

Figure 1.2: Spontaneous symmetry breaking in Ising model. From left to right the temperature is decreased gradually.

One simplest example is Ising magnets. At higher temperature the spins of electrons point to random directions and the system has no net magnetic moment. In this phase the $\mathbb{Z}_2$ spin-flip symmetry is conserved. At lower temperature, electron spins are aligned and the system shows a macroscopic magnetic moment. There is obviously no $\mathbb{Z}_2$ symmetry in the system anymore. So if we consider the procedure of lowering the temperature, the system must undergo a phase transition where the $\mathbb{Z}_2$ symmetry is spontaneously broken (see Fig. 1.2). This behavior can be captured by an order parameter, the magnetic moment m, and the Landau free energy $\Phi(m, T)$. Because the magnetic moment m is almost zero around the phase transition point, the Landau free energy could be expanded as a Taylor series of m.

$$\Phi(m, T) = \Phi(0, T) + \frac{1}{2}a(T)m^2 + \frac{1}{4}b(T)m^4 + \cdots . \tag{1.2}$$

The odd powers of m vanish because of the $\mathbb{Z}_2$ symmetry, that is, transforming m to $-m$ should not result in any change towards the total Landau free energy. The ground state could be found by minimizing the Landau free energy. We truncate the series to the fourth order since this is enough to illustrate the physics. But in principle higher-order terms could exist, except that they might be irrelevant (in renormalization group sense). To make sure the system is stable, the coefficient of the highest order term should be positive. Here we require $b(T) > 0$. Taking the derivative of $\Phi(m, T)$ with respect to m and setting it to 0 we find the value of m.

$$m = \begin{cases} 0 & \text{if } a(T) \geq 0 \\ \pm\sqrt{-\frac{a(T)}{b(T)}} & \text{if } a(T) < 0 \end{cases} \tag{1.3}$$

Based on experimental values for the magnetization, the common choice of the coefficients are $a(T) = a_0(T - T_c), b(T) = b_0$ where a_0, b_0 are constants and T_c is the critical temperature. Under this set of coefficients, the order parameter m is 0 when $T > T_c$, and nonzero when $T < T_c$. There is clearly a phase transition at the critical temperature T_c. To determine the order of the phase transition at $T = T_c$, we notice that the second derivative of the free energy $\frac{\partial^2 \Phi(m,T)}{\partial T^2}$ is a continuous function of order parameter m and the order parameter m is a continuous function of T. So $\frac{\partial^2 \Phi(m,T)}{\partial T^2}$ is a continuous function of T in the ground state and the phase transition is continuous.

Since its discovery, Landau theory has been utilized to explain different kinds of phase transitions. It has been extended to inhomogeneous systems with spatial variations. By adding the term $(\nabla\psi(\boldsymbol{x}))^2$, one can construct the so-called Ginzburg-Landau theory. Such a theory is still a mean-field theory. For systems with continuous symmetry groups, fluctuations could be introduced to create new physics like spin waves [6]. Even beyond the fluctuations are topological theories of defects and critical phenomena described by conformal field theories (CFT's) [7]. In summary, Landau

theory is the starting point to study phase transitions and it has been one important pillar of condensed matter physics.

1.3 Beyond symmetry: the rise of topology

Landau's paradigm of symmetry breaking has been successful in explaining phase transitions in most experiments. However, in the experiments of quantum Hall effect [8–12], there is no symmetry breaking in the transitions between states with different Hall conductance. The study of such experiments has led to the theory of topological orders [13–16].

Topological orders are categorized as symmetry-protected topological (SPT) order and intrinsic topological order [17, 18]. Superficially, the distinction between these two concepts lies in the role of symmetries in quantum phase transitions. Essentially, it is the entanglement of the ground states that distinguishes them. SPT states are short-range entangled while intrinsic topological states are long-range entangled. In SPT systems, one can find a smooth path to adiabatically tune an SPT state to a trivial product state. But during such a procedure the symmetries are garanteed to be broken. If we preserve the symmetries, then it is not possible to find any path adiabatically connecting SPT states and trivial product states. On the other hand, there is no smooth path connecting systems with intrinsic topological orders and trivial product states, no matter whether the symmetries are preserved or not. Therefore, some authors [19] consider the intrinsic topological order as the *true* topological order whereas the SPT order as *symmetry-protected trivial* order.

In other words, SPT states must be protected by certain symmetries. Local unitary transformations [17] could transform SPT states to trivial product states. But SPT phases are still different from conventional phases because no such transformation could be found while preserving the symmetries. Examples of SPT states include Haldane chain [20–22], AKLT model [23] and topological insulators [24–38].

One of the most important experimental signatures of an SPT state would be localized edge/surface modes. In $(2+1)$-D SPT systems, it has been shown [18, 39] that gapless edge modes must exist in both bosonic and fermionic case. But in higher dimensions, the surface states could be gapped either due to undergoing a symmetry breaking or due to having intrinsic topological order.

Conversely, intrinsic topological states could not be connected with trivial product states via any local unitary transformation [17, 18]. Symmetry is not required to define topological orders. But it still has a role in such phases. With the presence of symmetries, intrinsic topological orders could be enriched to even more diverse phases. Typical intrinsic topological phases arise in strongly-correlated systems such as quantum spin liquids [40–44] and fractional quantum Hall (FQH) states [9–11, 45–47]. There are two defining signatures for intrinsic topological order. One is the robust ground-state degeneracy depending on topology of the manifold where the system lives on [15, 16]. The other is the quantized non-Abelian geometric phases of the ground states.

The outburst in this field comes around the year of 2005 when Kane and Mele proposed the time reversal topological insulator [24, 25]. Such topological Insulators could be understood with simple band theories. After that, there has been many efforts to classify topological orders [48–56]. Among them, group cohomology seems to comprehensively classify SPT states. Along the same line, a classification for the intrinsic topological phases is also quite fruitful. Now it has been clear that symmetry-breaking paradigm is not the full story for phase transitions, but at most a half. In topological world, there are equally abundant phases as in Landau symmetry-breaking world.

1.4 Organization of this thesis

In this thesis, I will follow the same logic flow as in the introduction.

A Landau theory of pair density wave (PDW) state is constructed and investigated in Chapter II. In that chapter, we will encounter an infinite order phase transition, Kosterlitz-Thouless (KT) transition [57]. There we will pick up where we left in the discussion of Landau theory and go beyond fluctuation to see the topological effect.

In Chapter III, a generic theorem is constructed and proved to show the connection among adiabatic continuity, ground-state overlaps and topological phase transitions.

In Chapter IV, I will review the milestone topological band insulators in 1D, 2D and 3D. And these will serve as examples to illustrate the overlap theorem in Chapter III.

In Chapter V, the overlap calculation is extended to a large class of *many-body* ground states in SPT systems and FQH systems. I will show that a topological response term exists for the many-body overlaps.

Finally, in Chapter VI I will conclude this thesis and discuss some possible open problems for future work.

All the chapters are self-contained and could be understood without relying on other chapters too much.

CHAPTER II

Pair-density waves on lattices with 6-fold rotational symmetry

2.1 Introduction

In this chapter, I will study the pair-density wave (PDW) systems on (stacked) triangular lattices. I will start with constructing the Landau free energy via symmetry considerations. Then I will map such PDW systems to the fully-frustrated XY (FFXY) models. In this way, we could utilize all the literature on FFXY models to understand the physics in PDW systems.

Throughout this procedure, Landau theory of symmetry breaking would be the basis. We will also need to go beyond and do the renormalization group (RG) analysis to obtain the final phase diagram. Quite surprisingly, the 2D PDW system on triangular lattice shows an Ising-type phase transition. Even more interestingly, a KT transition beyond Landau symmetry breaking paradigm shows up.

2.2 The Landau free energy

The order parameter of PDW in momentum space is

$$\Delta(\boldsymbol{k}) = \sum_{\boldsymbol{q}} \langle c^\dagger_{\boldsymbol{q}\uparrow} c^\dagger_{\boldsymbol{k}-\boldsymbol{q}\downarrow} \rangle \tag{2.1}$$

It is clear that $\Delta(\boldsymbol{k})^* \neq \Delta(-\boldsymbol{k})$. So for the lattice with C_6 rotational symmetry, there should be 6 independent complex order parameters $\Delta_1, \Delta_2, \ldots, \Delta_6$ corresponding to the vectors $\boldsymbol{k}_i$ where $i \in \{1, 2, 3, 4, 5, 6\}$. Note that each $\boldsymbol{k}_i$ could be obtained by acting a group element in C_6 on another $\boldsymbol{k}_j$.

If the momentum happens to be on the $\boldsymbol{K}, \boldsymbol{K}' = -\boldsymbol{K}$ points, then we are left with two independent complex order parameters (because others could be obtained by translating the momentum by a reciprocal lattice vector). The triangular lattice has a D_6 symmetry group. Since the two wave vectors still have residual D_3 rotational symmetry, the symmetry breaking pattern from high-temperature disordered phase to low-temperature PDW phase is $\mathbb{T} \times \mathbb{Z}_2 \times U(1)$, where $\mathbb{T}$ is the translational symmetry, $\mathbb{Z}_2 = D_6/D_3$ is the inversion symmetry group and $U(1)$ is the gauge symmetry that leads to particle conservation.

There will be three constraints for the Landau free energy from these three decoupled broken symmetries. Here we only treat the sixth order terms as an example. Suppose the powers of $\Delta_1, \Delta_1^*, \Delta_2, \Delta_2^*$ are u, v, x, y respectively. Then we immediately have $u + v + x + y = 6$. Translational symmetry gives the second constraint that the total momentum should be 0 or equal to a reciprocal lattice vector due to translational symmetry. So $u - v - x + y = 3n$ where n is an integer (actually $n = 0, \pm 2$ in this case). The reason why the right-hand-side should be $3n$ is that the vector $\boldsymbol{K} = (\frac{4\pi}{3}, 0)$ and $3n\boldsymbol{K}$ should be a reciprocal lattice vector. A third constraint is that the number of $c^\dagger$ and c should be the same for a single term in the Hamiltonian, i.e. $u - v + x - y = 0$ due to $U(1)$ gauge symmetry. Then solving the three equations

one would get all the possible terms. Finally the sixth order terms would be all combinations of these permissible terms that are invariant under the point group D_6 (or inversion symmetry). In this way we find the Landau free energy to be

$$\begin{aligned} F =& t(|\Delta_1|^2 + |\Delta_2|^2) + u_1(|\Delta_1|^4 + |\Delta_2|^4) + u_2|\Delta_1|^2|\Delta_2|^2 + v_1(|\Delta_1|^6 + |\Delta_2|^6) \\ &+ v_2(|\Delta_1|^4|\Delta_2|^2 + |\Delta_1|^2|\Delta_2|^4) + v_3|\Delta_1|^3|\Delta_2|^3\cos[3(\phi_1 - \phi_2)] + \cdots \end{aligned} \tag{2.2}$$

2.3 Map to the FFXY models

Now we are in the position to solve this Landau theory. In both 2D and 3D, this free energy turns out to be the same as the antiferromagnetic XY model on triangular lattices, one of those fully-frustrated XY (FFXY) models [58, 59]. Hereafter we will provide an argument for both dimensions.

This could easily be done with the help of the antiferromagnetic XY model on a (stacked) triangular lattice (see GL theory construction in [60, 61]). The Hamiltonian of this model is

$$H = J\sum_{\langle ij\rangle}^{xy} \boldsymbol{s}_i \cdot \boldsymbol{s}_j - J'\sum_{\langle ij\rangle}^{z} \boldsymbol{s}_i \cdot \boldsymbol{s}_j, \tag{2.3}$$

where $J, J' > 0$, $\boldsymbol{s}_i = (\cos(\theta_i), \sin(\theta_i))$ is the planar vector spin on the xy plane and $\langle ij\rangle$ indicates the summation over nearest-neighbour spins along the xy plane or z direction. This is essentially a 3D antiferromagnetic XY-model with ferromagnetic interaction in the third direction. If $J' = 0$ then we are back to the 2D case. So this model is appropriate for our purpose of illustrating the equivalence between our PDW model and FFXY systems in both dimensions. The low energy modes could be found by Fourier transformation, after which the Hamiltonian becomes

$$H = \sum_{\boldsymbol{q}} J(\boldsymbol{q})\boldsymbol{s}(\boldsymbol{q}) \cdot \boldsymbol{s}(-\boldsymbol{q}), \tag{2.4}$$

where $J(\boldsymbol{q}) = J[\cos(q_x) + 2\cos(q_x/2)\cos(\sqrt{3}q_y/2)] - J'\cos(q_z)$. The eigenfunction

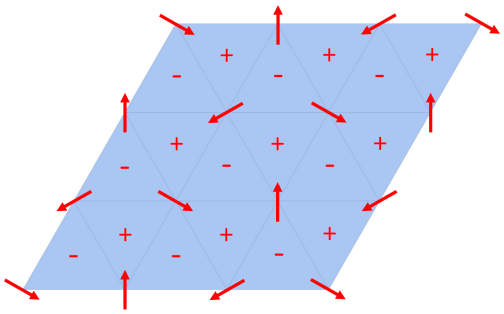

Figure 2.1: Ground state configuration of antiferromagnetic XY model on a triangular lattice, the sign on each plaquette denotes the chirality

$J(\boldsymbol{q})$ is minimized at two inequivalent momentum points $(\pm 4\pi/3, 0, 0)$ in the first Brillouin zone [$(\pm 4\pi/3, 0)$ if $J' = 0$ or in 2D]. So the order parameters are 2 two-component vectors $\boldsymbol{\phi} = (\phi_1, \phi_2), \boldsymbol{\psi} = (\psi_1, \psi_2)$ corresponding to the two inequivalent wave-vectors. In fact, there is a correspondence between the order parameters in the two systems.

$$\begin{aligned} \Delta_1 &\leftrightarrow \phi_1 + i\phi_2, \\ \Delta_2 &\leftrightarrow \psi_1 + i\psi_2. \end{aligned} \tag{2.5}$$

Now that the number of order parameters (4 real or 2 complex) are the same and the wave vector responsible for the low energy modes are the same, the last thing we need to check is that they share the same symmetry-breaking pattern. To this end, we note that in the ground state the in-plane spin vectors exhibit a 120° angle difference from each of their nearest neighbours. A typical ground-state configuration is shown in Fig. 2.1 [62]. Other ground states could be obtained by globally rotating the spins on each site or doing an inversion with any site being the inversion center (but note that spins are internal degrees of freedom and will not change directions after inverting the spatial degree of freedom). So besides the translational symmetry $\mathbb{T}$, the ground states break the point group symmetry D_6 down to D_3 and break the internal spin rotational symmetry $SO(2)$ completely. Since we know $SO(2) \cong U(1)$, the broken symmetry here is $\mathbb{T} \times \mathbb{Z}_2 \times U(1)$ where $\mathbb{Z}_2$ is the inversion symmetry (the same symmetry-breaking pattern as in the FFXY literature except there $\mathbb{Z}_2$ represents

chiral symmetry). Therefore this symmetry breaking pattern is exactly the same as the PDW case and they should lie in the same universality class as well. Indeed, the antiferromagnetic XY model on a triangular lattice shares the same Landau free energy [61] with the PDW free energy in Eq. (2.2).

The analysis above is true for both vanishing and nonvanishing J' and thus applies to both 2D and 3D systems. From the symmetry point of view, our PDW system is equivalent to the thoroughly studied FFXY models. So we only need to review what happens in FFXY models in order to understand our PDW systems.

2.4 Phase transitions and universality classes in FFXY models

In this section, I will study the FFXY models in both 2D and 3D based on historical investigations.

2.4.1 2D case

In 2D, the FFXY model is just the anti-ferromagnetic XY model. And its Hamiltonian is given by

$$H = J \sum_{\langle ij \rangle} \boldsymbol{s}_i \cdot \boldsymbol{s}_j = J \sum_{\langle ij \rangle} \cos(\theta_i - \theta_j) \tag{2.6}$$

where $J > 0$ is the antiferromagnetic coupling between nearest neighbours on the triangular lattice. A generalized model could be written as

$$H = -J \sum_{\langle ij \rangle} \cos(\theta_i - \theta_j + A_{ij}) \tag{2.7}$$

where $J > 0$ and A_{ij} is the bond angle such that the sum over all bonds on a plaquette is a constant

$$\sum A_{ij} = 2\pi f. \tag{2.8}$$

This model describes the high-capacitance-limit Josephson-junction array in the transverse magnetic field B ([63] and references therein). The relation between B and f is

$$f = BA_P/\Phi_0 \tag{2.9}$$

where A_P is the plaquette area and $\Phi_0 \equiv hc/(2e)$ is the flux quantum. Note that when $f = 1/2$ the generalized model is clearly reduced to the fully frustrated XY model defined initially. So the FFXY models on the triangular or square lattice could be realized through coupled Josephson-junction arrays in a transverse magnetic field [64, 65]. Actually the same free energy also describes helimagnets [60, 66, 67], the phase transition of dipole-locked phase A of Helium-3 [68]. The following form of the Landau free energy is more popular in the literature, especially for FFXY models on (stacked) square lattice (see, for example, [60, 61, 66, 69–73]).

$$F = \frac{1}{2}\{r_0(\boldsymbol{a}^2 + \boldsymbol{b}^2) + u(\boldsymbol{a}^2 + \boldsymbol{b}^2)^2 + v[(\boldsymbol{a}\cdot\boldsymbol{b})^2 - \boldsymbol{a}^2\boldsymbol{b}^2]\}, \tag{2.10}$$

where $\boldsymbol{a}, \boldsymbol{b}$ are the real two-component-vector order parameters. But after the transformation

$$\begin{aligned} \Delta_1 &\leftrightarrow \frac{a_x + b_y}{\sqrt{2}} + i\frac{a_y - b_x}{\sqrt{2}}, \\ \Delta_2 &\leftrightarrow \frac{a_y + b_x}{\sqrt{2}} - i\frac{a_x - b_y}{\sqrt{2}}, \end{aligned} \tag{2.11}$$

it becomes

$$\begin{aligned} F =& \frac{1}{2}[r_0(|\Delta_1|^2 + |\Delta_2|^2) + (u - \frac{1}{4}v)(|\Delta_1|^4 + |\Delta_2|^4) + 2(u + \frac{1}{4}v)|\Delta_1|^2|\Delta_2|^2)] \\ =& t\Delta^2 + (u - \frac{1}{8}v)\Delta^4 + \frac{1}{8}v\Delta^4\cos(4\theta), \end{aligned} \tag{2.12}$$

where we have defined $|\Delta_1| = \Delta\cos(\theta), |\Delta_2| = \Delta\sin(\theta)$ and $\theta \in [0, \pi/2]$. Clearly this is equivalent to what we wrote down for the PDW systems up to quartic order. We will show that higher-order terms actually are irrelevant later on.

To have a stable system, the coefficients of the quartic terms should satisfy

$$u > 0, 4u - v > 0. \tag{2.13}$$

For the case $v < 0$, in order to minimize the free energy the order parameters $\boldsymbol{a}, \boldsymbol{b}$ tends to be (anti)parallel with each other. So the free energy describes the normal continuous phase transition from the paramagnetic state to the sinusoidal state [66, 72]. The transition point is at $r_0 = 0$. In terms of PDW order parameters, $|\Delta_1| = |\Delta_2| = \frac{1}{\sqrt{2}}\Delta$ in the low temperature phase. One can see there is no double degeneracy for the ground state in this case since θ must be $\pi/4$. So there is also no issue whether $\mathbb{Z}_2$ symmetry breaks first or $U(1)$ gauge symmetry breaks first, consistent with our expectation of a single continuous phase transition.

For the case $v > 0$ describing the frustrated models [74, 75], it was shown by M. Yosefen and E. Domany using the Polyakov $2 + \epsilon$ expansion that all the terms of order higher than four are irrelevant [60]. In this case, the FFXY model order parameters $\boldsymbol{a}, \boldsymbol{b}$ tends to be orthogonal to each other, hence also called "non-collinear order" [66, 72, 76, 77]. In our PDW systems, it corresponds to $\Delta_1 = \Delta, \Delta_2 = 0$ or vice versa, i.e., $\theta = 0, \pi/2$. So there is a double degeneracy of the ground state due to $\mathbb{Z}_2$ symmetry breaking. The total broken symmetry, as we discussed above, is $\mathbb{T} \times \mathbb{Z}_2 \times U(1)$. The $\mathbb{Z}_2$ symmetry breaking can also be seen from the appearance of a four-state clock term. The four-state clock model is known to be reducible to $q = 2$ Potts model (Ising model) [78] and this is valid for all lattices [79]. So such a term is responsible for an Ising-type phase transition. The KT transition may happen before or after the Ising symmetry breaking as we decrease the temperature. And it is also equally possible that they happen at the same temperature and the fluctuation of Δ serves as the trigger for the Ising transition. What's more, the two transitions may even be coupled to form a new universality class, where the possibility of first order

transition is also not excluded. So it is a quite complicated but interesting system.

Such phase transition(s) and universality class(es) for breaking $\mathbb{Z}_2 \times U(1)$ symmetry in 2D was under debate for about three decades (see the review [70]). Now there is a consensus [70, 80–87] that for the FFXY models with the same ground-state degeneracy, antiferromagnetic XY model on a triangular lattice or FFXY model on a square lattice [58, 59, 64] for example, the temperature for $\mathbb{Z}_2$ chiral symmetry breaking is strictly higher than that for the $U(1)$ symmetry breaking. And after some controversy [70] it was shown that the phase transition for the $\mathbb{Z}_2$ symmetry breaking is in the Ising universality class and that for the $U(1)$ symmetry breaking in the 2D XY universality class [57, 88, 89]. This two-phase-transition scenario is supported by the argument based on the unbinding of kink-antikink pairs [85, 90]. The same free energy could also describe a single first order phase transition upon tuning the positive parameter v to be large enough [69–71] (see Fig. 2.2).

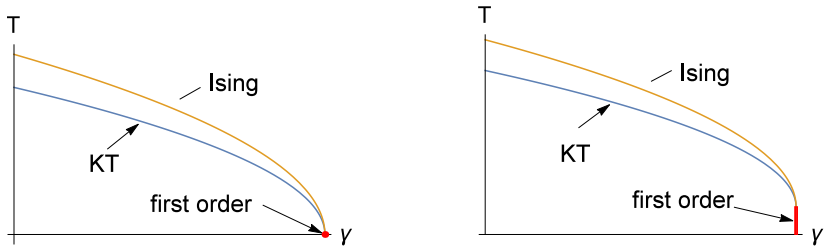

Figure 2.2: Possible phase diagrams for 2D quantum system exhibiting PDW order in low temperature. γ represents some interaction parameter.

2.4.2 3D case

In 3D systems, the expression of Landau free energy turns out to be the same as in 2D. Simple dimensional analysis suggests that terms beyond sixth order are all irrelevant in 3D. For the sixth order, one can do a $4 - \epsilon$ expansion [91] for generic

models as below

$$\begin{aligned} F = t(|\Delta_1|^2 + |\Delta_2|^2) + u_1(|\Delta_1|^4 + |\Delta_2|^4) + u_2|\Delta_1|^2|\Delta_2|^2 + \\ v_1(|\Delta_1|^6 + |\Delta_2|^6) + v_2(|\Delta_1|^4|\Delta_2|^2 + |\Delta_1|^2|\Delta_2|^4) + w_n[(\Delta_1\Delta_2^*)^n + h.c] \end{aligned} \tag{2.14}$$

where $n \geq 3$ is an integer. The RG equations for the quartic terms are

$$\begin{aligned} \frac{du_1}{dl} =& \epsilon u_1 - 20u_1^2 + \dots, \\ \frac{du_2}{dl} =& \epsilon u_2 - 4u_2^2 - 16u_1u_2 + \dots, \end{aligned} \tag{2.15}$$

where we have omitted all higher order terms, including terms like tu_1, tu_2. The argument is that for RG equations close to the Gaussian point, $t = O(\epsilon^2)$ and any coefficient u_1, u_2 multiplied by t would be of order $O(\epsilon^3)$. So to the order of ϵ, the fixed points are

$$\begin{cases} u_1 = 0, \\ u_2 = 0, \end{cases} \quad \begin{cases} u_1 = 0, \\ u_2 = \frac{\epsilon}{4}, \end{cases} \quad \begin{cases} u_1 = \frac{\epsilon}{20}, \\ u_2 = 0, \end{cases} \quad \begin{cases} u_1 = \frac{\epsilon}{20}, \\ u_2 = \frac{\epsilon}{20}. \end{cases} \tag{2.16}$$

The first fixed point is just the trivial Gaussian fixed point and others are the Wilson-Fisher fixed pints.

The higher order terms have the following RG equations

$$\begin{aligned} \frac{dv_1}{dl} =& (6-2d)v_1 - 8u_1^2 - 96u_1v_1 - 4u_2v_2 - 336v_1^2 + \dots, \\ \frac{dv_2}{dl} =& (6-2d)v_2 - 8u_1u_2 - 40u_1v_2 - 2u_2^2 - 18u_2v_1 \\ & - 16u_2v_2 - 72v_1v_2 - 64v_2^2 + \dots, \\ \frac{dw_n}{dl} =& (6-2d)w_n - 4n(n-1)u_1w_n - 2n^2u_2w_n \\ & - 4n(n-1)(n-2)v_1w_n - 4n^2(n-1)v_2w_n + \dots. \end{aligned} \tag{2.17}$$

Again we have omitted all the terms proportional to t since that will be at least of

order $O(\epsilon^3)$.

Now it is clear that when $d = 3$ the scaling dimensions of v_1 and v_2 are negative after the fixed-point solutions being inserted into the RG equations. So those terms are marginally irrelevant. The scaling dimension of the coefficient w_n of the generic coupling term can be read off from the RG equations as

$$(6 - 2d) - 4n(n-1)u_1 - 2n^2u_2. \tag{2.18}$$

Note that $d = 4 - \epsilon$. Insert the u_1, u_2 values for different Wilson-Fisher fixed points and extrapolate the scaling dimension to 3D ($\epsilon = 1$). Then we find that the scaling dimensions of the coupling terms are all negative for $n \geq 3$ in our assumption. Therefore all terms beyond quartic order are irrelevant. Of course this expansion to first order is not reliable for $\epsilon = 1$. But as we have analyzed the broken symmetry does not contain a $\mathbb{Z}_3$ group, the three-state clock term should be irrelevant. Besides the symmetry argument, one can also refer to a recent numerical result which shows that the quartic order termination of the free energy produces the same conclusion as the original microscopic model [92]. For a review on the phase transition of FFXY models in 3D, see [73]. So we conclude the sixth order terms are indeed irrelevant and the free energy in 3D is thus the same as the 2D case [Eq. (2.12)]. Therefore we are led to the difficulty of understanding the intertwined order due to discrete $\mathbb{Z}_2$ symmetry breaking and the continuous $U(1)$ symmetry breaking again.

For the non-frustrated case $v < 0$, it was pointed out that the system does not have any fixed point [60, 66]. So it could only undergo a first order transition although mean field analysis gives a continuous transition.

For the frustrated $v > 0$ case, similar to the 2D situation, the issue also continues for more than three decades. Even in 2016, there is still a paper [77] trying to clarify this point using functional renormalization groups.

On the numerical side, consistent results have been shown by multiple groups [62, 92–97]. It is fairly clear that there is a single first order transition from disordered phase to the chiral noncollinear phase.

On the theoretical side, the $4-\epsilon$ renormalization-group studies [66, 73] on the Ginzburg-Landau theory of N-component-spin generalizations show that there is one critical number of components N_c, above which the system experiences a second order phase transition and below which the transition is of first order. The three-loop calculation shows that such a critical number is given by [98].

$$N_c = 21.80 - 23.43\epsilon + 7.088\epsilon^2 + O(\epsilon^3). \tag{2.19}$$

Even though the perturbative approach seems to give the same result (first order transition) as numerics, the coefficients are not decreasing fast enough. A six-loop calculation [99, 100] found a fixed point in contrast with the three-loop order result. However, the critical exponents not only strongly depend on the perturbation series resummation procedure [101] but are also incompatible with experiments [102]. So it seems the fixed point is spurious. Then nonperturbative RG was utilized to find again a first order transition [102–104]. Besides that, the authors also solved the problem that the critical exponents seem to be non-universal. According to their result, the RG flow is so slow at around the points describing stacked XY antiferromagnets and helimagnets that the systems seem to exhibit a "pseudo"-critical behaviour.

So most evidences are showing that the phase transition in 3D FFXY systems (if exists) should be first order.

2.5 Conclusions and implications for PDW systems

The discussion of FFXY models in previous section indicates that 2D systems may show more interesting physics (see Fig. 2.2) while 3D systems most likely only

exhibit first order transitions.

Imagine that we have a 2D PDW quantum system with 6-fold rotational symmetry. Suppose the ground states fall on the $\boldsymbol{K}$ and $\boldsymbol{K}' = -\boldsymbol{K}$ points in the hexagonal first Brillouin zone. Then the phase diagram is very similar to the antiferromagnetic XY model. There will be an intermediate phase with Ising order only and a low temperature phase with both Ising order and XY order. If we could tune the interaction terms in Eq. (2.2) through some parameter γ, then at zero temperature there will only be a first order transition (see Fig. 2.2).

In experiments, one can stack a piece of 2D material on a conventional superconductor and utilize the proximity effect to realize such a PDW system. The 2D material should be on a triangular lattice with D_6 symmetry.

CHAPTER III

Adiabatic continuity, wave-function overlap and topological phase transitions

3.1 Introduction

In quantum many-body systems, quantum phase transitions are among the most fascinating phenomena [105]. From the point of view of adiabatic continuity, a quantum phase transition can be characterized by the absence of an adiabatic path between ground states of quantum systems. Consider two quantum many-body systems in their ground states. If an adiabatic path can be constructed to smoothly deform one system into the other without any singularity, these two quantum states can be classified into the same quantum phase. On the other hand, if it is impossible to adiabatically deform one quantum system into the other, without going through some singular point (or some intermediate phase), these two quantum states belong to different quantum phases of matter and the singular point, which arises when we try to deform one system into the other, is a quantum phase transition point.

In general, quantum phase transitions can be largely classified into two categories, Landau-type and topological, depending on the origin of the singularity. In the first category, the two quantum phases separated by a quantum phase transition have different symmetries, i.e. certain symmetry is broken spontaneously as we move across

the phase boundary. Similar to a classical (thermal) phase transition, the difference in symmetry implies that it is impossible for these two quantum states to smoothly evolve into each other without undergoing a quantum phase transition. In the second category, the two quantum phases have the same symmetry, but their ground-state wave functions have different topological structures. For a gapped quantum system, where a finite energy gap exists between the ground state and the excited ones, the topology of the ground-state wave function cannot change in any adiabatic procedure without closing the excitation gap. Thus, if the ground-state wave functions of two gapped quantum systems have different topology, as we try to deform one into the other, a singularity point must arise, at which the energy gap closes and the ground-state wave function changes its topology. This singular point is known as a topological phase transition. Such a topological transition can take place even in the absence of interactions, e.g. in non-interacting band insulators [14, 54, 106–111].

In this chapter, we study adiabatic continuity between quantum states in gapped quantum systems focusing on the following question: *for two (arbitrary) quantum states, how can we determine whether a gapped adiabatic path between these two states exists or not*? More precisely, we want to determine, for two quantum states $|\psi_1\rangle$ and $|\psi_2\rangle$, whether it is possible or not to construct a gapped Hamiltonian $H(\alpha)$, where α is some control parameter, such that as we tune the value of the control parameter α, the ground state of the Hamiltonian changes smoothly from $|\psi_1\rangle$ to $|\psi_2\rangle$. It must be emphasized that here we require the Hamiltonian remains gapped for this adiabatic procedure, i.e., the energy gap between the ground and excited states never vanishes. As discussed above, the answer to this question is of direct relevance to the study of quantum phase transitions between gapped quantum systems, including topological phase transitions.

For band-insulators, we find that regardless of the symmetry and microscopic details, as long as the Bloch wave functions (of the valence bands) of two insulators

have finite wave function overlap, an adiabatic path can be constructed, connecting the two insulators without closing the insulating gap. For the study of topological band insulators, this conclusion implies that two band insulators with finite wave function overlap must have the same topology, i.e, all topological indices take the same value in the two insulators. This result also implies that for two insulators with different topology, there must exist at least one momentum point in the Brillouin zone, at which the Bloch waves in these two insulators are orthogonal to each other, i.e. the wave functions have zero overlap.

This conclusion can be easily generalized to interacting systems, i.e., if two quantum states have finite wave function overlap, regardless of microscopic details, a gapped adiabatic path can be defined to connect these two states. However, as pointed out below, this conclusion cannot be applied to study generic quantum many-body systems and quantum phase transitions, due to the orthogonality catastrophe [112], which says that in the thermodynamic limit, even for two quantum states in the same quantum phase, the wave function overlap will vanish due to the infinite size of the system. As a result, the wave function overlap, which is always zero in the thermodynamic limit, doesn't carry useful information about quantum phases and adiabatic continuity. This is in sharp contrast to noninteracting systems, e.g. band insulators discussed above, where we can utilize single-particle Bloch waves, which do not suffer from the orthogonality catastrophe. We will try to extract more generic information from the orthogonality catastrophe in next chapter. For this chapter, we limit ourselves to certain interacting systems, including integer and fractional quantum Hall systems [8, 9], and integer and fractional Chern insulators [14, 113–121], utilizing various schemes, e.g., by studying systems with finite size or factorizing the many-body wave function.

This chapter focuses on arguments and proofs. Examples will be provided in next chapter. We study adiabatic continuity in band insulators in Sec. 3.2. Then

in Sec. 3.3, we generalize the conclusion to interacting systems. In Sec. 3.4, we study how to utilize this result to study quantum phase transitions in the presence of interactions. Finally, we conclude the chapter by discussing possible implications in experimental and numerical studies. Details about the calculations and proofs are shown in Appendix A.

3.2 Band insulators

For band insulators, if we only focus on the qualitative properties, interactions can often be ignored. Within the non-interacting approximation, the quantum wave function of a band insulator is the (antisymmetrized) product of Bloch-wave states. Because of momentum conservation, Bloch states with different momenta decouple from one another. Therefore, we can examine wave function overlap at each momentum point separately.

In this section, we focus on the non-interacting regime. First, we prove that for two band insulators, the wave function overlap between the many-body ground states factorizes into the product of (Bloch-wave function) overlaps at each momentum point. Then, we will show that if the overlap remains finite for all momenta, the two insulators are adiabatically connected, i.e. we can adiabatically deform the ground-state wave function of one insulator into the other without closing the insulating gap or breaking any symmetries.

This conclusion immediately implies that (a) if two band insulators belong to two different quantum phases (i.e. it is impossible to deform one state into the other without closing the insulating gap), there must exist (at least) one momentum point $\boldsymbol{k}^*$, at which the (Bloch-wave function) overlap between the two insulators vanishes, and (b) if the Bloch wave functions of two band insulators have finite overlap at all momenta, this two insulators must belong to the same quantum phase.

We start the discussion by considering insulators with only one valence band

(Sec. 3.2.1). Then in Sec. 3.2.2, we will generalize the conclusions to generic cases with multiple valence bands.

3.2.1 Insulators with one valence band

In this section, we considering two band insulators, dubbed insulator I and insulator II, each of which has only one valence band. More generic situations (with more than one valence bands) will be studied in the next section.

3.2.1.1 Wave function overlap

Within the non-interacting approximation, the many-body ground states of these two insulators can be written as

$$|\mathrm{G_I}\rangle = \prod_{\boldsymbol{k}} c^\dagger_{\boldsymbol{k}} |0\rangle \tag{3.1}$$

$$|\mathrm{G_{II}}\rangle = \prod_{\boldsymbol{k}} d^\dagger_{\boldsymbol{k}} |0\rangle \tag{3.2}$$

where $|\mathrm{G_I}\rangle$ and $|\mathrm{G_{II}}\rangle$ are the (many-body) ground states of the two insulators respectively. $|0\rangle$ represents the vacuum, i.e. the quantum state with no electrons. $c^\dagger_{\boldsymbol{k}}$ ($d^\dagger_{\boldsymbol{k}}$) is the creation operator which creates a particle in the Bloch state of the valence band in insulator I (insulator II) at crystal momentum $\boldsymbol{k}$. $\prod_{\boldsymbol{k}}$ represents the product over all momenta in the Brillouin zone.

It is straightforward to verify that the overlap between the two ground states factorizes as

$$|\langle \mathrm{G_I}|\mathrm{G_{II}}\rangle| = \prod_{\boldsymbol{k}} |\phi(\boldsymbol{k})| \tag{3.3}$$

where $\phi(\boldsymbol{k})$ is the overlap between Bloch waves at crystal momentum $\boldsymbol{k}$

$$\phi(\boldsymbol{k}) = \langle 0 | c_{\boldsymbol{k}} d^{\dagger}_{\boldsymbol{k}} | 0 \rangle \tag{3.4}$$

In the language of first quantization, this Bloch-wave overlap is

$$\phi(\boldsymbol{k}) = \langle \psi^{\mathrm{I}}(\boldsymbol{k}) | \psi^{\mathrm{II}}(\boldsymbol{k}) \rangle \tag{3.5}$$

where

$$|\psi^{\mathrm{I}}(\boldsymbol{k})\rangle = c^{\dagger}_{\boldsymbol{k}} |0\rangle \tag{3.6}$$

$$|\psi^{\mathrm{II}}(\boldsymbol{k})\rangle = d^{\dagger}_{\boldsymbol{k}} |0\rangle \tag{3.7}$$

are the Bloch waves of the valence bands in insulators I and II respectively.

3.2.1.2 The adiabatic path between two insulators

Define a new Bloch state

$$|\Psi(\boldsymbol{k}, \alpha)\rangle = \frac{(1-\alpha)\,|\psi^{\mathrm{I}}(\boldsymbol{k})\rangle + \alpha\;\phi(\boldsymbol{k})^{*}\,|\psi^{\mathrm{II}}(\boldsymbol{k})\rangle}{\mathcal{N}}, \tag{3.8}$$

Here, $|\psi^{\mathrm{I}}(\boldsymbol{k})\rangle$ and $|\psi^{\mathrm{II}}(\boldsymbol{k})\rangle$ are the Bloch wave functions of the valence bands for insulators I and II respectively [Eqs. (3.6) and (3.7)]. $\phi(\boldsymbol{k})^{*} = \langle \psi^{\mathrm{II}}(\boldsymbol{k}) | \psi^{\mathrm{I}}(\boldsymbol{k}) \rangle$ is the complex conjugate of the overlap between the two Bloch states as defined in Eq. (3.5). The control parameter α is a real number between 0 and 1. The denominator $\mathcal{N}$ is a normalization factor,

$$\mathcal{N} = \sqrt{(1-\alpha)^2 + \alpha(2-\alpha)|\phi(\boldsymbol{k})|^2} \tag{3.9}$$

which enforces the normalization condition $\langle\Psi(\boldsymbol{k},\alpha)|\Psi(\boldsymbol{k},\alpha)\rangle = 1$. It is easy to prove that as long as the overlap is nonzero $\phi \neq 0$, $\mathcal{N}$ is positive and thus the denominator will not introduce any singularity.

When $\alpha = 0$, the Bloch state defined above coincides with $|\psi^{\mathrm{I}}(\boldsymbol{k})\rangle$, i.e. the Bloch state for insulator I. At $\alpha = 1$, the Bloch state becomes that of insulator II, up to an unimportant phase factor,

$$|\Psi(\boldsymbol{k},\alpha=0)\rangle = |\psi^{\mathrm{I}}(\boldsymbol{k})\rangle \tag{3.10}$$

$$|\Psi(\boldsymbol{k},\alpha=1)\rangle = \frac{\phi(\boldsymbol{k})^*}{|\phi(\boldsymbol{k})^*|}\,|\psi^{\mathrm{II}}(\boldsymbol{k})\rangle \tag{3.11}$$

Therefore, by varying the parameter $0 \leq \alpha \leq 1$, Eq. (3.8) defines a path between the two insulators.

As proved in Appendix A.2, if insulators I and II preserve certain symmetries (e.g., the time-reversal symmetry, lattice symmetries or some internal symmetries), the Bloch state $|\Psi(\boldsymbol{k},\alpha)\rangle$ will preserve the same symmetry. In other words, the path defined above preserves all necessary symmetries. This is very important for the study of symmetry-protected topological states.

3.2.1.3 The insulating gap

Now, we explore one key problem for the study of adiabatic continuity: *is it possible to use the path defined in Eq.* (3.8) *to deform insulator* I *into insulator* II *without closing the insulating gap?*. The answer to this question is yes, as long as the wave function overlap remains finite for all momenta, $\phi(\boldsymbol{k}) \neq 0$. To prove this conclusion, we construct the following hermitian operator, which will serve as the Hamiltonian for an insulator,

$$H(\alpha) = -\sum_{\boldsymbol{k}} |\Psi(\boldsymbol{k},\alpha)\rangle\,\langle\Psi(\boldsymbol{k},\alpha)|\,. \tag{3.12}$$

This Hamiltonian has one control parameter $0 \leq \alpha \leq 1$. It has one flat band with energy $E = -1$ and the Bloch wave for this band is $|\Psi(\boldsymbol{k}, \alpha)\rangle$. All other bands in the system have energy $E = 0$. If we set the Fermi energy to be between -1 and 0, this Hamiltonian defines a band insulator with one valence band. The band gap for this insulator is 1.

When $\alpha = 0$, the valence band has the same Bloch wave function as insulator I, and for $\alpha = 1$, the valence-band Bloch wave function coincides with that of insulator II. For $0 < \alpha < 1$, the Hamiltonian defines an insulator with a finite insulating gap, and the gap never closes. As a result, by varying the value of α, the Hamiltonian shown in Eq. (3.12) defines an adiabatic path between the two insulators.

In the language of topological phase transitions, this observation implies that the two band insulators must belong to the same quantum phase (i.e. have the same topological indices), as long as the wave function overlap $\phi(\boldsymbol{k})$ remains finite for all $\boldsymbol{k}$. For two insulators with different topology (i.e. if some topological index takes different values in the two insulators), there must be at least one momentum point, at which the overlap vanishes.

3.2.1.4 The complex $U(1)$ phase

In Eq. (3.8), we introduced a factor $\phi(\boldsymbol{k})^*$ in the definition of $|\Psi(\boldsymbol{k}, \alpha)\rangle$. This factor is necessary in order to preserve the $U(1)$ phase symmetry, which is also known as the $U(1)$ gauge symmetry for band insulators [122]. In a band insulator, it is known that if we multiply a $U(1)$ phase to a Bloch wave function, the new wavefunciton still describes the same Block state, i.e. $|\psi^{\mathrm{I}}(\boldsymbol{k})\rangle$ and $e^{i\varphi}|\psi^{\mathrm{I}}(\boldsymbol{k})\rangle$ describe the same Bloch state in insulator I, where φ is an arbitrary $U(1)$ phase. Similarly, $|\psi^{\mathrm{II}}(\boldsymbol{k})\rangle$ and $e^{i\varphi'}|\psi^{\mathrm{II}}(\boldsymbol{k})\rangle$ correspond to the same Bloch state in insulator II. In other words, when we write down the Bloch states $|\psi^{\mathrm{I}}(\boldsymbol{k})\rangle$ and $|\psi^{\mathrm{II}}(\boldsymbol{k})\rangle$ for the insulators, there is a freedom to choose an arbitrary phase factor for each of these states. In order

to ensure that physical observables [e.g. the Hamiltonian $H(\alpha)$] *does not* depend on this arbitrary phase choice, the factor $\phi(\boldsymbol{k})^*$ is necessary. It is straightforward to verify that with the help of this factor, the Hamiltonian $H(\alpha)$ defined in Eq. (3.12) is independent of the phase choice, i.e. it is invariant under the transformation

$$|\psi^{\mathrm{I}}(\boldsymbol{k})\rangle \to e^{i\varphi}\,|\psi^{\mathrm{I}}(\boldsymbol{k})\rangle \tag{3.13}$$

$$|\psi^{\mathrm{II}}(\boldsymbol{k})\rangle \to e^{i\varphi'}\,|\psi^{\mathrm{II}}(\boldsymbol{k})\rangle \tag{3.14}$$

In addition, as shown in Appendix A.2, this factor $\phi(\boldsymbol{k})^*$ also help to ensure that the adiabatic path preserves the same symmetries as insulators I and II.

3.2.2 Insulators with multiple bands

Now we consider band insulators with more than one valence bands.

3.2.2.1 Wave function overlap

For an insulator with N valence bands, in the non-interacting limit, the ground-state wave function is

$$|\mathrm{G_I}\rangle = \prod_{n=1}^{N}\prod_{\boldsymbol{k}} c^\dagger_{n,\boldsymbol{k}}\,|0\rangle \tag{3.15}$$

Here, we follow the same convention as utilized in Eqs. (3.1) and (3.2), except that the creation operators $c^\dagger_{n,\boldsymbol{k}}$ now have one extra subindex n, which labels the valence bands ($n = 1, 2, \ldots, N$), and $\prod_{n=1}^{N}$ represents the product for all occupied bands.

Consider another insulator with the same number of valence band, whose ground-state wave function is

$$|\mathrm{G_{II}}\rangle = \prod_{n=1}^{N}\prod_{\boldsymbol{k}} d^\dagger_{n,\boldsymbol{k}}\,|0\rangle \tag{3.16}$$

where $d^\dagger_{n,\boldsymbol{k}}$ is the creation operator for the Bloch waves in this insulator. The quantum overlap between the two ground states of these two insulators factorizes (similar to the case with one valence band)

$$|\langle \mathrm{G_I}|\mathrm{G_{II}}\rangle| = \prod_{\boldsymbol{k}} |\phi(\boldsymbol{k})| \tag{3.17}$$

where the Bloch-wave overlap at each momentum point is

$$\phi(\boldsymbol{k}) = \langle 0| \prod_{n=1}^{N} c_{n,\boldsymbol{k}} \prod_{m=1}^{N} d^\dagger_{m,\boldsymbol{k}} |0\rangle \tag{3.18}$$

In the first-quantization language, $\phi(\boldsymbol{k})$ is the determinant of the overlap matrix $\mathcal{F}(\boldsymbol{k})$

$$\phi(\boldsymbol{k}) = \det \mathcal{F}(\boldsymbol{k}) \tag{3.19}$$

where $\mathcal{F}(\boldsymbol{k})$ is an $N \times N$ matrix with matrix elements

$$\mathcal{F}_{n,m}(\boldsymbol{k}) = \langle 0| c_{n,\boldsymbol{k}} d^\dagger_{m,\boldsymbol{k}} |0\rangle = \langle \psi^{\mathrm{I}}_n(\boldsymbol{k})|\psi^{\mathrm{II}}_m(\boldsymbol{k})\rangle \tag{3.20}$$

where

$$|\psi^{\mathrm{I}}_n(\boldsymbol{k})\rangle = c^\dagger_{n,\boldsymbol{k}} |0\rangle \tag{3.21}$$

$$|\psi^{\mathrm{II}}_m(\boldsymbol{k})\rangle = d^\dagger_{m,\boldsymbol{k}} |0\rangle \tag{3.22}$$

are the Bloch wave functions of the valence bands for insulators I and II respectively, and the subindices n and m are band indices for valence bands in these two insulators.

We emphasize that the overlap matrix $\mathcal{F}(\boldsymbol{k})$ is a function of the crystal momentum $\boldsymbol{k}$. However, to simplify the formulas, in this chapter we will use $\mathcal{F}$ to represent the matrix without showing explicitly that this matrix is a function of $\boldsymbol{k}$.

3.2.2.2 The adiabatic path

In this section, we will assume that the overlap between the two insulators, i.e. $\phi(\boldsymbol{k})$ defined in Eq. (3.18), is finite for all momentum points, and then defines an adiabatic path between the two insulators.

According to Eq. (3.19), $\phi(\boldsymbol{k}) \neq 0$ implies that the overlap matrix $\mathcal{F}$ [Eq. (3.20)] has a nonzero determinant. As shown in Appendix A.1.2, because $\mathcal{F}\mathcal{F}^\dagger$ is a hermitian matrix, we can find a unitary matrix $\mathcal{U}$, which diagonalizes $\mathcal{F}\mathcal{F}^\dagger$, i.e. $\mathcal{U}\mathcal{F}\mathcal{F}^\dagger\mathcal{U}^\dagger$ is a diagonal matrix. Utilizing the matrices $\mathcal{F}$ and $\mathcal{U}$, we can define N quantum states

$$|\Psi_l(\boldsymbol{k},\alpha)\rangle = \frac{(1-\alpha)\,\mathcal{U}^*_{l,n}\,|\psi^{\mathrm{I}}_n(\boldsymbol{k})\rangle + \alpha\,\mathcal{U}^*_{l,n}\mathcal{F}^*_{nm}\,|\psi^{\mathrm{II}}_m(\boldsymbol{k})\rangle}{\mathcal{N}_l}, \tag{3.23}$$

where $*$ represents complex conjugate; $0 \leq \alpha \leq 1$ is a control parameter and the subindex $l = 1, 2, \ldots, N$. In this chapter, we adopt the Einstein summation convention. Unless claimed otherwise, repeated band indices will be summed over, and this sum only goes over all valence bands with band indicies between 1 and N, while conduction bands (with band indices larger than N) will not be included in the sum. The denominator $\mathcal{N}_l$ is the normalization factor, which ensures that the quantum state is properly normalized, $\langle\Psi_l\Psi_l\rangle = 1$, and the valule of this normalization function is shown in Eq (A.19). In the Appendix A.1.4, we proved that this normalization factor $\mathcal{N}_l$ never reaches zero, as long as the overlap is nonzero $\phi(\boldsymbol{k}) \neq 0$, which ensures that Eq. (3.23) is singularity free.

We will prove in the next section that as long as the overlap $\phi(\boldsymbol{k})$ remains finite, the states defined in Eq. (3.23) are orthonormal

$$\langle\Psi_l(\boldsymbol{k},\alpha)|\Psi_{l'}(\boldsymbol{k},\alpha)\rangle = \delta_{l,l'} \tag{3.24}$$

As a result, we can design an insulator with N valence bands and utilize these or-

thonormal states as the Bloch states of the valence bands, and this insulator will serve as an adiabatic path between insulators I and II. Here, we define the Hamiltonian of this insulator

$$H(\alpha) = -\sum_{l=1}^{N}\sum_{\boldsymbol{k}} |\Psi_l(\boldsymbol{k},\alpha)\rangle \langle\Psi_l(\boldsymbol{k},\alpha)| \tag{3.25}$$

Because $|\Psi_l(\boldsymbol{k},\alpha)\rangle$ are orthonormal for $l = 1, 2, \ldots, N$, it is straightforward to verify that $|\Psi_l(\boldsymbol{k},\alpha)\rangle$ are eigenstates of the Hamiltonian with eigenenergy $E = -1$, and all other single-particle states orthogonal to $|\Psi_l(\boldsymbol{k},\alpha)\rangle$ have eigenenergy $E = 0$, i.e., this Hamiltonian has N (flat) energy bands with energy $E = -1$ and all other energy bands have energy $E = 0$. If the Fermi energy is between -1 and 0, this Hamiltonian defines a band insulator with band gap $\Delta = 1$, and $|\Psi_l(\boldsymbol{k},\alpha)\rangle$ are the Bloch waves of the valence bands. As will be shown in the next section, for $\alpha = 0$ ($\alpha = 1$), the ground-state wave function of this insulator coincides with that of insulator I (insulator II). And thus $H(\alpha)$ defines an adiabatic path between the two insulators.

3.2.2.3 Proof for the adiabatic path

In this section, we prove the conclusions presented in Sec. 3.2.2.2. We will first prove that the quantum states defined in Eq. (3.23) are indeed orthonormal, i.e., $\langle\Psi_l(\boldsymbol{k},\alpha)|\Psi_{l'}(\boldsymbol{k},\alpha)\rangle = \delta_{l,l'}$ Then, we will show that the Hamiltonian defined in Eq. (3.25) is the Hamiltonian for an insulator with N valence bands, and we will further prove that for $\alpha = 0$ ($\alpha = 1$), the ground state recovers that of the insulator I (II).

It turns out that it is easier to present the proof using the language of second quantization, so here we will reformulate the same Bloch states and the Hamiltonian utilizing creation/annihilation operators defined in Eqs. (3.15) and (3.16), i.e. the creation operator $c^\dagger_{n,\boldsymbol{k}}$ ($d^\dagger_{m,\boldsymbol{k}}$) adds one electron to the nth (mth) valence band of insulator

I (II) at crystal momentum $\boldsymbol{k}$. Since electrons are fermions, the creation/annihilation operators satisfy the canonical anticommutation relation

$$\{c_{n,\boldsymbol{k}}, c^{\dagger}_{n',\boldsymbol{k}'}\} = \delta_{n,n'}\delta_{\boldsymbol{k},\boldsymbol{k}'} \tag{3.26}$$

$$\{d_{m,\boldsymbol{k}}, d^{\dagger}_{m',\boldsymbol{k}'}\} = \delta_{m,m'}\delta_{\boldsymbol{k},\boldsymbol{k}'} \tag{3.27}$$

where δ is the Kronecker delta. For the anticommutators between c's and d's, it is straightforward to prove that

$$\{c_{n,\boldsymbol{k}}, d^{\dagger}_{m,\boldsymbol{k}'}\} = \mathcal{F}_{n,m}\delta_{\boldsymbol{k},\boldsymbol{k}'} \tag{3.28}$$

$$\{d_{m,\boldsymbol{k}}, c^{\dagger}_{n,\boldsymbol{k}'}\} = \mathcal{F}^{*}_{n,m}\delta_{\boldsymbol{k},\boldsymbol{k}'} \tag{3.29}$$

and all other anticommutators vanish(See Appendix A.1.1 for details).

Utilizing these creation and annihilation operators, as well as the matrices $\mathcal{F}$ and $\mathcal{U}$ defined in Sec 3.2.2.2, we can define creation operators

$$a^{\dagger}_{l,\boldsymbol{k}} = \frac{(1-\alpha)\,\mathcal{U}^{*}_{l,n}c^{\dagger}_{n,\boldsymbol{k}} + \alpha\,\mathcal{U}^{*}_{l,n}\mathcal{F}^{*}_{nm}d^{\dagger}_{m,\boldsymbol{k}}}{\mathcal{N}_l}, \tag{3.30}$$

Here, repeated indices are summed over, the same as in Eq. (3.23). It is straightforward to verify that this creation operator creates the Bloch state $|\Psi_l(\boldsymbol{k},\alpha)\rangle$ defined in Eq. (3.23), i.e. $|\Psi_l(\boldsymbol{k},\alpha)\rangle = a^{\dagger}_{l,\boldsymbol{k}}|0\rangle$. In Appendix A.1.3, we proved that as long as the overlap $\phi(\boldsymbol{k})$ is nonzero, these $a^{\dagger}_{l,\boldsymbol{k}}$ operators, and the corresponding annihilation operators, satisfies canonical anticommutation relations

$$\{a_{l,\boldsymbol{k}}, a^{\dagger}_{l',\boldsymbol{k}}\} = \delta_{l.l'} \tag{3.31}$$

The anticommutation relation implies that the quantum states defined in Eq. (3.23)

are orthonormal, because

$$\delta_{l,l'} = \langle 0|\{a_{l,\boldsymbol{k}}, a^{\dagger}_{l',\boldsymbol{k}}\}|0\rangle = \langle \Psi_l(\boldsymbol{k},\alpha)|\Psi_{l'}(\boldsymbol{k},\alpha)\rangle \tag{3.32}$$

Now we examine the Hamiltonian defined in Eq.(3.25) and rewrite it in the second-quantization language

$$H(\alpha) = -\sum_{l=1}^{N}\sum_{\boldsymbol{k}} a^{\dagger}_{l,\boldsymbol{k}} a_{l,\boldsymbol{k}} \tag{3.33}$$

Along with the anticommutation relation [Eq. (3.31)], it is easy to verify that this Hamiltonian describes a band insulator with N valence bands. $a^{\dagger}_{l,\boldsymbol{k}}$ are the creation operators for the Bloch states in the valence bands ($l = 1, 2, \ldots, N$). All the valence bands in this insulator have energy -1, while the conduction bands have energy 0. Here, we set the Fermi energy into the band gap, i.e., between -1 and 0. For any values of $0 \leq \alpha \leq 1$, the insulating gap never closes and the value remains 1.

For $\alpha = 0$, we know from Eq. (3.30) that

$$a^{\dagger}_{l,\boldsymbol{k}} = \mathcal{U}^{*}_{l,n} c^{\dagger}_{n,\boldsymbol{k}} \tag{3.34}$$

Because $\mathcal{U}$ is an unitary matrix (i.e. $\mathcal{U}^{*}_{l,n}\mathcal{U}_{l,n'} = \delta_{n,n'}$), the Hamiltonian at $\alpha = 0$ is

$$H(\alpha = 0) = -\sum_{n=1}^{N}\sum_{\boldsymbol{k}} c^{\dagger}_{n,\boldsymbol{k}} c_{n,\boldsymbol{k}} \tag{3.35}$$

Therefore, the ground state is identical to that of insulator I, i.e., all Bloch states created by $c^{\dagger}_{n,\boldsymbol{k}}$ for $n = 1, 2, \ldots, N$ are occupied.

For $\alpha = 1$, Eq. (3.30) implies that

$$a^{\dagger}_{l,\boldsymbol{k}} = \frac{1}{\mathcal{N}_l}\mathcal{U}^{*}_{l,n}\mathcal{F}^{*}_{n,m} d^{\dagger}_{m,\boldsymbol{k}}. \tag{3.36}$$

Thus the Hamiltonian becomes

$$H(\alpha=1) = -\sum_{\boldsymbol{k}} \frac{\mathcal{F}^*_{n,m}\mathcal{U}^*_{l,n}\mathcal{U}_{l,n'}\mathcal{F}_{n',m'}}{\mathcal{N}_l^2} d^\dagger_{m,\boldsymbol{k}} d_{m',\boldsymbol{k}} \tag{3.37}$$

As proved in Appendix A.1.2,

$$\frac{\mathcal{F}^*_{n,m}\mathcal{U}^*_{l,n}\mathcal{U}_{l,n'}\mathcal{F}_{n',m'}}{\mathcal{N}_l^2} = \delta_{m,m'} \tag{3.38}$$

and thus this Hamiltonian can be simplified

$$H(\alpha=1) = -\sum_{m=1}^{N}\sum_{\boldsymbol{k}} d^\dagger_{m,\boldsymbol{k}} d_{m,\boldsymbol{k}}. \tag{3.39}$$

The ground state for this Hamiltonian coincides with that of the insulator II, i.e., all Bloch states created by $d^\dagger_{m,\boldsymbol{k}}$ for $m = 1, 2, \ldots, N$ are occupied.

3.2.2.4 Insulators with different numbers of valence bands

Consider two insulators with different numbers of valence bands. It is easy to realize that these two insulators are *not* adiabatically connected, because it is impossible to change the number of valence bands in a band insulator without closing the band gap.

At the same time , we know that the overlap function also vanishes. Utilizing the overlap function defined in Eq. (3.18), we know that

$$\phi(\boldsymbol{k}) = \langle 0| \prod_{n=1}^{N} c_{n,\boldsymbol{k}} \prod_{m=1}^{N'} d^\dagger_{m,\boldsymbol{k}} |0\rangle \tag{3.40}$$

where N and N' are the number of valence bands for the two insulators respectively. It is transparent that $\phi(\boldsymbol{k}) = 0$, if $N \neq N'$.

In summary, for two insulators with different numbers of valence bands, the two

insulators are not adiabatically connected, and the wave function overlap is zero.

3.2.3 Symmetry-protected topological states

As have been mentioned above and proved in Appendix A.2, if insulators I and II preserves certain symmetry, the adiabatic path that we defined will preserve the same symmetry. This property is very important for the study of symmetry-protected topological states, where the topological index can only be defined in the presence of certain symmetries. There, when we discuss about adiabatic paths that connect two quantum states, we must ensure that the symmetry that are utilized to define the topological index is preserved along the path. And the adiabatic path that we constructed above indeed preserves the symmetry, as long as the symmetry is preserved in insulators I and II.

3.2.4 Insulators with different lattice structures

In the previous sections, we assumed that the two insulators (I and II) have the same Brillouin zone, and thus we can use the same momentum points in both insulators to calculate the wave function overlap. This assumption is not necessary, and all the conclusions above can be generalized, even if two insulators have different lattice structures, and thus different Brillouin zones.

This is because topology of a band insulator remains invariant as we adiabatically deform the lattice structure (For certain topological states, e.g. topological crystalline insulators [111], the symmetry of the underlying lattice plays an essential role in the definition of the topological structure. There, as long as the deformation of the lattice structure preserves the essential symmetry, the topological structure also remains invariant). Thus, we can deform adiabatically the crystal structure of one insulator into the structure of the other insulator, and then all the conclusions above can be generalized.

Finally, we emphasize that the adiabatic deformation discussed here is not unique. Instead, there exists a vast number of different paths to deform the crystal structure. As long as the deformation is adiabatic, our conclusion will remain the same.

In next chapter, we will provide one example to compare the Bloch waves in two insulators with different lattice structures.

3.2.5 Adiabatic band flattening

Above, we defined a Hamiltonian with flat bands to demonstrate the adiabatic continuity. This band structure (with flat bands) is different from that of a real insulator, where the energy bands are in general not flat and not degenerate. However, for the study of adiabatic continuity and/or topological phase transitions, this difference doesn't play any essential role. This is because in an arbitrary band insulator, we can adiabatically flatten all the bands and adjust the energy of each band without changing the Bloch wave functions. The adiabatic flattening of energy bands are widely utilized in the study of topological insulator/superconductors, and it is known that topological properties remain invariant as we flatten the bands in a band insulator, as long as the band gap remains open (See for example Refs. [54] and [109]).

3.3 Interacting systems

In the presence of interactions, we can no longer utilize single-particle (Bloch) states to characterize the ground state of a many quantum system. However, we can prove a similar theorem for generic quantum systems, which reveals a universal relation between adiabatic continuity and the wave function overlap.

Theorem III.1. *For any two quantum states with nonzero overlap, i.e., $|\psi\rangle$ and $|\psi'\rangle$ with $\langle\psi|\psi'\rangle \neq 0$, a Hamiltonian $H(\lambda)$ can be defined, such that by turning the control parameter λ, the ground state of the Hamiltontian evolves adiabatically from $|\psi\rangle$ to*

$|\psi'\rangle$. During this adiabatic procedure, the energy gap between the ground and excited states remains finite.

It must be emphasized that although this theorem shares some similarities with what was discussed above for band insulators (and the proof is along the same line of thinking as will be shown below), this theorem is fundamentally different from the conclusions shown in the previous section. This theorem covers a wider range of systems (interacting and non-interacting), but it is a weaker statement in comparison to what we have proved in the previous section for band insulators. For noninteracting band insulators, we showed that the adiabatic path can be achieved using a non-interacting Hamiltonian. But for more general situations considered in the theorem above, the Hamiltonian that describes the adiabatic path may contain interactions, i.e., we have to enlarge the scope of Hamiltonians in order to construct the adiabatic path for generic systems. Proving that two states are connected by a non-interacting Hamiltonian is a stronger statement than proving that they are connected by a Hamiltonian, without the non-interacting constraint. Another way to see this difference is by examining the adiabatic path. As will be shown below, the Hamiltonian that we constructed to prove this theorem contains interactions. Even in the non-interacting limit, in general, it will not recover the non-interacting Hamiltonian utilized in the previous section.

In this section, we prove this theorem, and its implications for quantum phase transitions will be discussed in the next section. As will be shown in the next section, for topological phase transitions, there exist major differences between interacting and non-interacting systems. In particular, in the presence of strong interactions, the connection between our theorem and quantum phase transitions becomes much more complicated in comparison to non-interacting systems discussed in the previous section. As a result, we can only apply this theorem for the study of certain interacting topological systems.

3.3.1 Adiabatic path connecting two quantum states

Consider two quantum states $|\psi\rangle$ and $|\psi'\rangle$. Here $|\psi\rangle$ and $|\psi'\rangle$ are generic quantum states, instead of single-particle states. We can define overlap between the two states as

$$\phi = \langle\psi|\psi'\rangle \tag{3.41}$$

Define a new quantum state

$$|\Psi(\alpha)\rangle = \frac{(1-\alpha)\ |\psi\rangle + \alpha\ \phi^*\,|\psi'\rangle}{\mathcal{N}}, \tag{3.42}$$

where $0 \leq \alpha \leq 1$ is a real number between 0 and 1 and ϕ^* is the complex conjugate of the wave function overlap. The denominator $\mathcal{N}$ is a normalization factor,

$$\mathcal{N} = \sqrt{(1-\alpha)^2 + \alpha(2-\alpha)|\phi|^2} \tag{3.43}$$

which ensures the normalization condition $\langle\Psi(\alpha)|\Psi(\alpha)\rangle = 1$. Utilizing this wave function, we can define a hermitian quantum operator

$$H(\alpha) = -\,|\Psi(\alpha)\rangle\,\langle\Psi(\alpha)|\,, \tag{3.44}$$

and this quantum operator will serve as our Hamiltonian.

If $H(\alpha)$ is a Hamiltonian and α is a control parameter, the energy spectrum of the system can be figured out immediately. The ground state of the system is $|\Psi(\alpha)\rangle$ with eigen-energy -1

$$H(\alpha)\,|\Psi(\alpha)\rangle = -\,|\Psi(\alpha)\rangle\,\langle\Psi(\alpha)|\Psi(\alpha)\rangle = -\,|\Psi(\alpha)\rangle\,, \tag{3.45}$$

All other eigenstates of H have eigenenergy 0, which are the excited states. In other

words, this Hamiltonian defines a gapped system with a unique ground state, while all the excited states are separated by an energy gap.

When $\alpha = 0$, the ground state is $|\Psi(0)\rangle = |\psi\rangle$. At $\alpha = 1$, the ground state is $|\Psi(1)\rangle = |\psi'\rangle$. For $0 < \alpha < 1$, the energy gap between the ground and excited states always remain finite ($\Delta = 1$), and thus as we tune α from 0 to 1, it offers an adiabatic path to deform (adiabatically) a quantum state $|\psi\rangle$ into a different quantum state $|\psi'\rangle$ without closing the excitation gap.

For quantum phase transitions, the existence of such an adiabatic path implies that $|\psi\rangle$ and $|\psi'\rangle$ belongs to the same quantum phase, i.e. we can go from one to the other without going through a quantum phase transition. This conclusion remains valid as long as the overlap remains finite $\langle\psi|\psi'\rangle \neq 0$.

As shown in Appendix A.2, this adiabatic path preserves the same symmetry as $|\psi\rangle$ and $|\psi'\rangle$.

3.3.2 $U(1)$ phase symmetry

In Eq. (3.42), a factor $\phi^* = \langle\psi|\psi'\rangle$ is introduced in the definition of $|\Psi(\alpha)\rangle$. This factor is necessary in order to preserve the $U(1)$ phase symmetry. Because the proof is in strong analogy to the non-interacting case discussed discussed in Sec. 3.2.1.4, here we will not repeat the analysis, and it is straightforward to verify that with the help of this $\langle\psi'|\psi\rangle$ factor, the Hamiltonian $H(\alpha)$ defined in Eq. (3.45) is independent of the phase choice, i.e. $H(\alpha)$ is invariant under the transformation

$$|\psi\rangle \to e^{i\phi} |\psi\rangle \tag{3.46}$$

$$|\psi'\rangle \to e^{i\phi'} |\psi'\rangle . \tag{3.47}$$

3.4 Applications to quantum phase transitions

For the study of quantum phase transitions, this theorem has two immediate implications: (1) if two quantum states belong to two different quantum phases, i.e. it is impossible to go from one to the other adiabatically without going through a quantum phase transition point, the overlap between the two quantum wave functions must be strictly zero, i.e. the two wave function must be orthogonal to each other; and (2) if two quantum states have finite overlap, they must belong to the same quantum phase, i.e., one can turn a state into the other adiabatically without going through a quantum phase transition.

This observation enforces a strong constraint on quantum wave functions in different quantum phases. However, before we can apply this knowledge to the study of quantum phase transitions, one challenge has to be resolved, the *orthogonality catastrophe*. Based on the orthogonality theorem from Anderson, in the thermodynamic limit, the overlap between two different quantum wave functions shall vanish due to the infinite degrees of freedom [112]. To utilize the theorem discussed above to study quantum phase transitions, it is necessary to find a way to distinguish zero overlap caused by Anderson's orthogonality theorem and zero overlap caused by the absence of an adiabatic path. In general, there are three ways to taken care of the orthogonality catastrophe:

- Utilizing another zero to cancel the zero induced by the orthogonality theorem. One technique that can achieve this objective is the strange correlator as shown in Ref. [123].

- Separate an infinite system into smaller subsystems with finite degrees of freedom, and then investigate the overlap in each subsystem, which doesn't suffer from the orthogonality catastrophe. This technique is applicable for non-interacting systems and certain interacting systems.

- Study finite-size systems and then extrapolate to the infinite-size limit via finite size scaling. This last approach is directly relevant to numerical studies.

In next chapter, we will give some examples to demonstrate the second and the third techniques.

3.5 Discussion

In this chapter, we explored the relation between wave function overlap and adiabatic continuity in (non-interacting) band insulators and interacting quantum systems. Our results can be utilized to simplify certain problems in the study of topological states. For example, in the study of band insulators, a large number of topological indices have been defined (e.g. the Chern number, the $\mathbb{Z}_2$ topological index, the mirror Chern number, the spin Chern number, the Hopf index), and more topological indices can be defined, if we enforce additional symmetries (e.g. space-group symmetries). As a result, to fully determine the topological property of an insulator becomes a nontrivial task. In principle, it is necessary to compute *all* these topological indices in order to achieve such an objective. The conclusions reported in this chapter offer an alternative approach. Instead of trying to compute all known topological indices, one can utilize some known insulators as reference systems, whose wave functions and topological properties are well understood. If the Bloch wave of a new insulator has nonzero overlap with some reference insulator, we immediately know the topological properties of this new insulator, which must be identical to the reference insulator. If the new insulator has zero Bloch-wave function overlap with all known reference insulators, then this insulator might be a new topological state, and it requires further investigation to understand its topological structure.

It is worthwhile to notice that a nonzero wave-function overlap is a sufficient condition for topologically equivalence, but it is not necessary. For example, two

topologically equivalent states may accidentally have wave-functions that are orthogonal to each other. Such an accidental vanishing wave function overlap is typically not stable and will be removed by small perturbations, while the topologically-protected zero wave-function overlap is stable and cannot be removed.

For interacting systems, our theorem can be easily generalized. However, it cannot be applied to generic interacting systems because of the orthogonality catastrophe. On the other hand, in the study of interacting topological states, many numerical methods can only handle finite-size systems (e.g. exact diagonalization or density matrix renormalization group). There, our conclusions will not suffer from the orthogonality catastrophe, and thus could benefit some of the numerical investigations. This point will be further illustrated in next two chapters.

Above, we proved that if we have two insulators with different topology, there must exist (at least) one momentum point, at which the overlap of the wave function vanishes. The vanishing overlap has direct experimental implications, if we consider tunneling between these two insulators, i.e. the vanishing wave function overlap can prohibit tunneling between the two insulators at certain momentum point. In Ref. [124], it is shown that this is indeed the case when one studies tunneling between Chern insulators and conventional insulators, and between time-reversal invariant topological insulators and conventional insulators. Our results suggest that similar physics could be generalized for more generic topological states.

CHAPTER IV

Examples on the overlap theorem

4.1 Introduction

In last chapter, we proved a theorem to find an adiabatic path between two topologically equivalent band insulators. Our main result is that, if the overlap of two bands is non-zero in the whole first Brillouin zone (1BZ) then these two bands are topologically equivalent or adiabatically connected. In other words, topologically different bands must produce 0 overlap at some momentum in 1BZ. As an application, this conclusion could be used to find signatures of quantum phase transition, since two topologically different insulators must have no adiabatic path in between. For band insulators, the experimental implications of our theorem are also immediate. By Fermi's golden rule, it is clear the transition rate between topologically different bands vanishes at some momentum and the correspondent modes are protected from hybridization by topology. To get a better intuition for this result, recall that distance for two quantum states $|u(\boldsymbol{k})\rangle, |v(\boldsymbol{k})\rangle$ is defined by $\mathcal{D}(\boldsymbol{k}) = \arccos(|\langle v(\boldsymbol{k})|u(\boldsymbol{k})\rangle|)$. So our result just means that topologically different bands are separated by $\max_{\boldsymbol{k}\in 1BZ} \mathcal{D}(\boldsymbol{k}) = \pi/2$, the largest possible quantum distance.

Our result above was generalized to the following cases.

a) Multi-band ground states. Considering the fact that creation and annihilation operators for Fermions subject to anticommutation relation, we write the ground

states with n-band degeneracy using creation operators as $a_1^\dagger(\boldsymbol{k})a_2^\dagger(\boldsymbol{k})\ldots a_n^\dagger(\boldsymbol{k})\,|0\rangle$ and $b_1^\dagger(\boldsymbol{k})b_2^\dagger(\boldsymbol{k})\ldots b_n^\dagger(\boldsymbol{k})\,|0\rangle$, where $|0\rangle$ is the vacuum state. The overlap of these two ground states was shown to be

$$\phi(\boldsymbol{k}) := \det(\langle v_i(\boldsymbol{k})|u_j(\boldsymbol{k})\rangle) = \det(\mathcal{F}). \tag{4.1}$$

where $\mathcal{F}$ is the overlap matrix with each entry shown in the above equation. Then the result above shows that topological difference in multiband ground states implies 0-determinant of the $n \times n$ overlap matrix $\langle v_i(\boldsymbol{k})|u_j(\boldsymbol{k})\rangle$ at some momentum.

b) Beyond band insulators. P. W. Anderson [112] pointed out that the overlap between ground states of a Fermionic system and the system with finite-range scattering potential tends to vanish as the system size approaches infinity, which is called Anderson Orthogonality Catastrophe (AOC). Being generic for infinite-size systems, vanishing of overlap has nothing to do with topology of the many-body ground states. However, for finite-size systems twisted boundary conditions [125] could be introduced to interpret topological properties of some interacting systems. A second case that our result could apply is when the system could be divided into small systems. Then the orthogonality catastrophe is gone. Even for those systems that do not fall into these two categories, analytic or numerical results for finite-size scaling could still provide us a lot of information about quantum phases. Details will be discussed in next chapter.

In this chapter, we will provide examples on various systems, including single valence-band systems, multi-valence-band systems and interacting systems. Examples on systems with different symmetries are also considered.

4.2 Band insulators with the same symmetry

In this section, we consider several well-known topological indices and corresponding band insulators to verify our results above. These models range from one dimension (1D) to three dimensions (3D).

4.2.1 Berry phase and Su-Schrieffer-Heeger model

4.2.1.1 Review

Su-Schrieffer-Heeger (SSH) model [126], proposed as a theoretical model for polyacetylene, is a 1D chain with two different bonds. Suppose the couplings for these bonds are t_1 and t_2 ($t_1 \neq t_2$). Then the Hamiltonian is:

$$H = \sum_i (t_1 a_i^\dagger b_{i-1} + t_2 a_i^\dagger b_i) + h.c., \tag{4.2}$$

where the summation is over each unit cell containing site a_i and site b_i.

After Fourier transform, the Bloch Hamiltonian can be put into a 2×2 matrix in momentum space:

$$\mathcal{H} = \mathcal{H}_x \sigma_x + \mathcal{H}_y \sigma_y, \tag{4.3}$$

where σ_x and σ_y are Pauli matrices and if a is lattice constant,

$$\begin{aligned} \mathcal{H}_x &= t_1 \cos(ka) + t_2, \\ \mathcal{H}_y &= t_1 \sin(ka). \end{aligned} \tag{4.4}$$

It is straightforward to find the band gap to be $2|t_1 - t_2|$ and this model describes an insulator. Recall that Berry connection is defined by

$$\mathcal{A}_\mu(\boldsymbol{k}) = -i \langle u(\boldsymbol{k}) | \partial_\mu | u(\boldsymbol{k}) \rangle , \tag{4.5}$$

where $\partial_\mu = \frac{\partial}{\partial k_\mu}$ and $|u(\boldsymbol{k})\rangle$ is the ground state of this model. Since SSH model is 1D, here Berry connection only has one component. And the Berry flux $\oint_{1BZ} dk\mathcal{A}(k)$ can be easily calculated to be π if $t_1 > t_2$ and 0 if $t_1 < t_2$. Intuitively, consider the 2D parameter space formed by $\mathcal{H}_x$ and $\mathcal{H}_y$. From the equations above,

$$(\mathcal{H}_x - t_2)^2 + \mathcal{H}_y^2 = t_1^2, \tag{4.6}$$

which is a circle with radius t_1 centered at $(t_2, 0)$ in the parameter space, i.e., $(\mathcal{H}_x, \mathcal{H}_y)$-plane. In such a plane, the origin represents zero-Hamiltonian and therefore is singular. Rigorously, the Berry flux is calculated to be π if this circle surrounds origin ($t_1 > t_2$) and 0 otherwise ($t_1 < t_2$). Therefore it seems there exists a "magnetic monopole" at the origin of $(\mathcal{H}_x, \mathcal{H}_y)$-plane. In general, the Berry flux could be an integer multiple of π. And whenever such a multiple is nonzero, the system is topological.

4.2.1.2 Twisting of ground state

In this part, we will use twisting due to Berry phase to show that the overlap of two topologically distinct ground states must be 0 at some momentum.

Define $\theta_k \in [0, \pi]$ and $\phi_k \in [0, 2\pi)$ such that

$$\cos\left(\frac{\theta_k}{2}\right) e^{i\phi_k} = \langle v(k)|u(k)\rangle\,, \tag{4.7}$$

where $|u(k)\rangle\,, |v(k)\rangle$ are two topologically distinct ground states. Here θ is always well-defined since the absolute value of the overlap is always in the region $[0, 1]$. If ϕ is not well-defined, meaning that no single-valued ϕ could be specified from the above relation, then the overlap must be 0. So we are done with our argument. So without loss of generality, we should assume that there is no singular point where either θ or ϕ is not well-defined. Then we could prove by contradiction that there

exists at least one momentum point such that the overlap above is zero. Notice that the 1BZ of SSH model is topologically a circle and going around this circle would give rise to an extra Berry flux π to the topological band ($t_1 > t_2$ case) and Berry flux 0 to the trivial band ($t_1 < t_2$ case). On the one hand, since $|u(k)\rangle, |v(k)\rangle$ belongs to two topologically different bands, the overlap would get an extra phase $\pm\pi$ (signature determined by which band is topological); On the other hand, the overlap before and after winding arround the 1BZ should be the same (by periodicity of the 1D Brillouin zone).

$$\begin{aligned} &\langle v(k)|u(k)\rangle = \langle v(k+T)|u(k+T)\rangle \\ \Rightarrow &\cos\left(\frac{\theta_k}{2}\right) e^{i\phi_k} = \cos\left(\frac{\theta_k}{2}\right) e^{i\phi_k} e^{\pm\pi i} \\ \Rightarrow &\cos\left(\frac{\theta_k}{2}\right) = 0 \\ \Rightarrow &\langle v(k)|u(k)\rangle = 0. \end{aligned} \tag{4.8}$$

So there must be one point in the 1BZ where the overlap vanishes.

4.2.2 Chern number and Chern insulators

In this part, we will review the Chern insulators (also dubbed as quantum Hall insulators) and then study the overlap between two topologically different Chern insulators.

4.2.2.1 Quantum Hall insulator: Haldane's model

Here we utilize the model of Haldane [14] to demonstrate the physics. As pointed out by Haldane, for a honeycomb lattice, the Dirac band-touching point can be gapped by two different methods: (1) introducing a magnetic flux pattern, which breaks the time-reversal symmetry or (2) introducing a staggered potential, which breaks the degeneracy between the two sublattices. At half-filling, these two approaches

result in two different insulators with different topology, a topologically nontrivial Chern insulator and a topologically trivial conventional insulator. Haldane's model on honeycomb lattice [14] is a simple 2D model for Chern insulators exhibiting quantum Hall effect without Landau levels. The Hamiltonian is given by

$$H = -t_1 \sum_{\langle i,j \rangle} a_i^\dagger b_j - t_2 \sum_{\langle\langle i,j \rangle\rangle} (a_i^\dagger a_j e^{i\phi} + b_i^\dagger b_j e^{-i\phi}) + h.c. \tag{4.9}$$

where t_1, t_2 are the nearest-neighbor and next-nearest-neighbor hopping strength respectively. After Fourier transform, one can show that the Hamiltonian kernel is a 2×2-matrix:

$$\mathcal{H}_{\text{Haldane}} = \boldsymbol{h} \cdot \boldsymbol{\sigma} \tag{4.10}$$

where

$$h_1 = -t_1 \left[\cos(k_y a) + 2\cos\left(\frac{\sqrt{3}}{2} k_x a\right) \cos\left(\frac{k_y a}{2}\right) \right], \tag{4.11}$$

$$h_2 = t_1 \left[\sin(k_y a) - 2\cos\left(\frac{\sqrt{3}}{2} k_x a\right) \sin\left(\frac{k_y a}{2}\right) \right], \tag{4.12}$$

$$h_3 = \mu - 2t_2 \sin(\phi) \left[\sin(\sqrt{3} k_x a) - \sin\left(\frac{\sqrt{3}}{2} k_x a\right) \cos\left(\frac{3}{2} k_y a\right) \right] \tag{4.13}$$

Then based on Berry connection mentioned in the last section, one can calculate the Abelian Berry curvature:

$$\Omega_{\mu\nu} = (d\mathcal{A})_{\mu\nu} = \partial_\mu \mathcal{A}_\nu - \partial_\nu \mathcal{A}_\mu. \tag{4.14}$$

Finally, the integral of Ω over the whole 1BZ gives the Chern number 1 for this specific model when $\mu < 3\sqrt{3} t_2 \sin(\phi)$ and this shows that Haldane's model is a topological insulator and chiral edge states exist.

4.2.2.2 General consideration for Chern insulators

In general, the minimal Hamiltonian for a Chern insulator is given by a 2×2 matrix $\mathcal{H} = \boldsymbol{h} \cdot \boldsymbol{\sigma}$ ($\boldsymbol{h}$ being normalized). Suppose $|u^I(\boldsymbol{k})\rangle, |u^{II}(\boldsymbol{k})\rangle$ are ground states of this Hamiltonian in different gauge and they are smooth in region I and II of Fig. 4.1 respectively. Under gauge transformation,

$$|u^{II}(\boldsymbol{k})\rangle = e^{i\phi(\boldsymbol{k})} |u^I(\boldsymbol{k})\rangle \Rightarrow \mathcal{A}^{II} = \mathcal{A}^I + d\phi(\boldsymbol{k}) \tag{4.15}$$

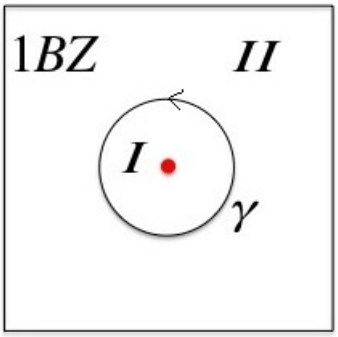

Figure 4.1: 1BZ of 2D systems: γ is a contour with counterclockwise orientation

Now we can calculate the Chern number as a winding number [127]:

$$\begin{aligned} \mathcal{C} =& \frac{1}{2\pi} \int_{1BZ} \Omega = \frac{1}{2\pi} \left(\int_{\mathrm{I}} \Omega + \int_{\mathrm{II}} \Omega \right) \\ \xrightarrow{\text{Stokes' Theorem}} & \frac{1}{2\pi} \left(\int_{\gamma} \mathcal{A}^{\mathrm{I}} + \int_{-\gamma} \mathcal{A}^{\mathrm{II}} \right) = -\frac{1}{2\pi} \int_{\gamma} d\phi(\boldsymbol{k}). \end{aligned} \tag{4.16}$$

We have known from the definition of Chern number ($\mathcal{C} = \frac{1}{2\pi} \int_{1BZ} \Omega - \frac{1}{2\pi} \int_{\partial(1BZ)} \mathcal{A}$) that Chern number is the obstruction of Stokes' theorem. Now notice here $\frac{1}{2\pi} \int_\gamma \mathcal{A}^{\mathrm{I}} = \frac{1}{2\pi} \int_\gamma \mathcal{A}^{\mathrm{II}} + \mathcal{C}$. We thus conclude that whenever $\mathcal{C} \neq 0$ there exists singularity for wave functions in both gauge in 1BZ. Similar argument will be of essential importance when we try to verify the overlap theorem for $\mathbb{Z}_2$ topological insulators in next section.

In fact, one can also calculate the Berry curvature directly using the ground state

(lower-energy eigenstate of $\mathcal{H}$)

$$|u\rangle = \frac{1}{2|\boldsymbol{h}|(|\boldsymbol{h}|-h_3)}\begin{pmatrix} h_3-|\boldsymbol{h}| \\ h_1+ih_2 \end{pmatrix} = \frac{1}{2(1-h_3)}\begin{pmatrix} h_3-1 \\ h_1+ih_2 \end{pmatrix} \tag{4.17}$$
$$\Omega_{\mu\nu} = \frac{1}{2}\epsilon^{ijk}\partial_\mu h_i \partial_\nu h_j h_k.$$

So the Chern number can also be written as

$$\mathcal{C} = \frac{1}{2\pi}\int_{1BZ}\Omega = \frac{1}{4\pi}\int_{1BZ} dk^2(\partial_{k_x}\boldsymbol{h}\times\partial_{k_y}\boldsymbol{h})\cdot\boldsymbol{h}. \tag{4.18}$$

This is exactly the degree of the map $\boldsymbol{h}: 1BZ \to S^2$. So Chern number is just the number of times that the unit vector $\boldsymbol{h}$ wraps the 2-sphere. With this interpretation, we will be able to analyze Chern insulators in general in the next section.

4.2.2.3 0-overlap of topologically different ground states

As discussed in Yang's paper [124], the existence of vanishing overlap in 1BZ is only due to topology and breaking discrete rotational symmetry would not give rise to a different conclusion. To obtain a clear intuition and rigorous proof, we define an explicit map from 1BZ (a torus T^2) to a sphere (S^2) parameterized by polar angle $\theta_{\boldsymbol{k}}$ and azimuth angle $\phi_{\boldsymbol{k}}$. $\theta_{\boldsymbol{k}} \in [0,\pi], \phi_{\boldsymbol{k}} \in [0,2\pi)$ are determined by:

$$\cos\left(\frac{\theta_{\boldsymbol{k}}}{2}\right)e^{i\phi_{\boldsymbol{k}}} = \langle v(\boldsymbol{k})|u(\boldsymbol{k})\rangle\,, \tag{4.19}$$

where $|u(\boldsymbol{k})\rangle$ and $|v(\boldsymbol{k})\rangle$ are in general two quantum states taken from two bands with different topology (In the situation of Ref. [124] they are the "to-be-hybridized" surface mode and bulk mode at the same momentum $\boldsymbol{k}$ in 1BZ). If these two bands are not orthogonal everywhere, then the degree of this map (how many times the

image wraps S^2) is exactly the Chern number difference $\Delta\mathcal{C}$ of these two bands.

$$\Delta\mathcal{C} = \frac{1}{4\pi}\int_{1BZ} dk_x dk_y (\partial_{k_x}\boldsymbol{n} \times \partial_{k_y}\boldsymbol{n})\cdot\boldsymbol{n} \tag{4.20}$$

where $\boldsymbol{n} = (\sin\theta_{\boldsymbol{k}}\cos\phi_{\boldsymbol{k}}, \sin\theta_{\boldsymbol{k}}\sin\phi_{\boldsymbol{k}}, \cos\theta_{\boldsymbol{k}})$.

Notice that the overlap vanishes if and only if $\theta_{\boldsymbol{k}} = \pi$, i.e. if and only if the image of this map contains the south pole of S^2. Therefore if the two bands have Chern number difference $\Delta\mathcal{C}$ the overlap vanishes $|\Delta\mathcal{C}|+2n$ times (where n is a non-negative integer). That is, there are $\Delta\mathcal{C}+2n$ surface modes protected from hybridizing with bulk states. This calculation also provides another way to calculate Chern number: if choosing $|v(\boldsymbol{k})\rangle$ to be independent of $\boldsymbol{k}$ (completely trivial), then degree of this map is just the Chern number of $|u(\boldsymbol{k})\rangle$.

Following our general argument above, the image wraps S^2 exactly $2n\pm 1$ times ($n > 0$) if one band is taken from Haldane's model [14] (Chern number ± 1) and the other band is trivial. To verify this numerically, we choose the parameters in Haldane's model as $a = 1, \phi = \pi/2, \mu = 0, t_1 = 3.5, t_2 = 1$ for the topologically non-trivial system, and $a = 1, \mu = 7.5, t_1 = 1, t_2 = 0$ for the trivial one. Utilizing these two topologically different insulators, we can compute the overlap between Bloch states in their valence bands, i.e., $\phi(\boldsymbol{k})$ defined above. As shown in Fig. 4.2, this overlap vanishes at the K point and reaches 1 at K' point, in agreement with our conclusions above. Also, the degree of the map defined above is calculated to be 1 up to 10^{-3} accuracy in our calculation. So in this specific model, K point and K' point are mapped to the south and north pole of S^2 respectively.

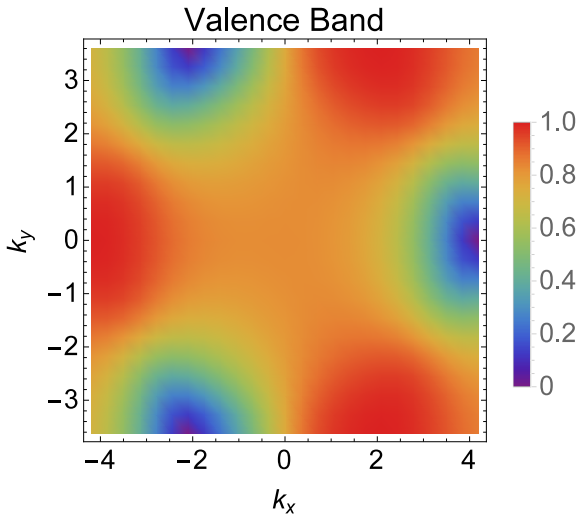

Figure 4.2: The absolute value of the Bloch-wave function overlap in Haldane's model. Here, we examined two insulating states in the model of Haldane with different Chern numbers (+1 and 0). Utlizing the Bloch waves of the valence bands in the two insulators, we computed the wave function overlap $\phi(\boldsymbol{k})$ and plotted its absolution value as a function of the crystal momentum k_x and k_y. As shown in the figure, the overlap vanishes at certain momentum point, which happens to be the K point for this model.

4.2.3 Time-reversal (TR) invariant topological insulators

In this part, we give an example for systems with multiple valence bands.

4.2.3.1 Quantum spin Hall insulator (QSHI): Kane-Mele model [24, 25]

We start by reviewing some of the features of Kane-Mele model based on the graphene honeycomb lattice. Without spin-mixing (Rashba coupling) terms, the Hamiltonian is just two copies of Haldane's model discussed in the last section and

thus gives rise to chiral edge states for spin up and down.

$$
\begin{aligned}
H_{KM} &= H_0 + H_R, \\
H_0 &= t_1 \sum_{\langle i,j\rangle,\sigma} a^\dagger_{i,\sigma} b_{j,\sigma} - t_2 \sum_{\langle\langle i,j\rangle\rangle,\sigma} (a^\dagger_{i,\sigma} a_{j,\sigma} e^{i\phi} + b^\dagger_{i,\sigma} b_{j,\sigma} e^{-i\phi}) + h.c. \\
&\xrightarrow{\text{Fourier Transform}} \mathcal{H}_0 = d_1 I_{2\times 2} \otimes \sigma_1 + d_{31} I_{2\times 2} \otimes \sigma_2 + \mu I_{2\times 2} \otimes \sigma_3 + d_{12} \sigma_3 \otimes \sigma_3 \\
&= \begin{pmatrix} \mathcal{H}^{\text{Haldane}}_{\uparrow} & 0 \\ 0 & \mathcal{H}^{\text{Haldane}}_{\downarrow} \end{pmatrix}, \\
H_R &= -i\lambda_R \sum_{\langle i,j\rangle} a^\dagger_{i,\sigma} (\boldsymbol{s} \times \boldsymbol{d}) b_{j,\sigma} + h.c. \\
&\xrightarrow{\text{Fourier Transform}} \mathcal{H}_R = d_{53} \sigma_1 \otimes \sigma_1 + d_{43} \sigma_2 \otimes \sigma_1 + d_5 \sigma_1 \otimes \sigma_2 + d_4 \sigma_2 \otimes \sigma_2
\end{aligned}
\tag{4.21}
$$

where H_R is the Rashba spin-mixing term and

$$d_1 = -t_1 \left[\cos(k_y a) + 2\cos\left(\frac{\sqrt{3}}{2} k_x a\right) \cos\left(\frac{k_y a}{2}\right) \right], \tag{4.22}$$

$$d_{31} = t_1 \left[\sin(k_y a) - 2\cos\left(\frac{\sqrt{3}}{2} k_x a\right) \sin\left(\frac{k_y a}{2}\right) \right], \tag{4.23}$$

$$d_{12} = -2t_2 \sin(\phi) \left[\sin(\sqrt{3} k_x a) - \sin\left(\frac{\sqrt{3}}{2} k_x a\right) \cos\left(\frac{3}{2} k_y a\right) \right], \tag{4.24}$$

$$d_{53} = -\lambda_R a \left[\sin(k_y a) + \sin\left(\frac{k_y a}{2}\right) \cos\left(\frac{\sqrt{3}}{2} k_x a\right) \right], \tag{4.25}$$

$$d_{43} = \sqrt{3} \lambda_R a \cos\left(\frac{k_y a}{2}\right) \sin\left(\frac{\sqrt{3}}{2} k_x a\right), \tag{4.26}$$

$$d_5 = -\lambda_R a \left[\cos(k_y a) - \cos\left(\frac{k_y a}{2}\right) \cos\left(\frac{\sqrt{3}}{2} k_x a\right) \right], \tag{4.27}$$

$$d_4 = \sqrt{3} \lambda_R a \sin\left(\frac{k_y a}{2}\right) \sin\left(\frac{\sqrt{3}}{2} k_x a\right). \tag{4.28}$$

Although Kane-Mele model with Rashba term breaks s_z conservation the TR symmetry is preserved: $[\Theta, \mathcal{H}] = 0$, where the TR operator $\Theta = e^{-i\pi s_y/\hbar} K = -\sigma_y K$

for spin-$\frac{1}{2}$ particle. So if $|u\rangle$ is an eigenstate of $\mathcal{H}$ with energy E, one can show $\Theta|u\rangle$ and $|u\rangle$ are two degenerate and orthogonal states (Kramer's theorem). By this theorem, one concludes that small Rashba coupling wouldn't split the degeneracy of the edge state pairs on the TR-invariant momenta. To understand this type of system, Kane and Mele defined a $\mathbb{Z}_2$ invariant using zeroes of $P(\boldsymbol{k}) = \mathrm{Pf}[\langle u_m(\boldsymbol{k})|\Theta|u_n(\boldsymbol{k})\rangle]$:

$$I = \frac{1}{2\pi i}\oint_C d\boldsymbol{k}\cdot\nabla_{\boldsymbol{k}}\log[P(\boldsymbol{k})+i\delta] \pmod 2 \tag{4.29}$$

where C is the contour surrounding half of 1BZ. By Poincare-Hopf theorem, the zeroes of vector field $P(\boldsymbol{k})$ must form "particle-antiparticle" pairs so that the indices of this vector field add up to 0 (Euler characteristic of 2-torus), that is, the pfaffian possess even number of zeroes with opposite phases that can annihilate each other when two of such zeroes meet. Due to TR-symmetry of the system, at least one pair of such zeroes must meet at TR-invariant point if I is odd. But it could be shown that pfaffian at these points can never be 0 [108]. Thus odd I corresponds to topologically nontrivial insulators.

Another equivalent definition of $\mathbb{Z}_2$ index was provided by Fu and Kane [128] using the TR polarization $P_\theta = P^{\mathrm{I}} - P^{\mathrm{II}}$ where $P^s = \frac{1}{2\pi}\int_{-\pi}^{\pi} dk\mathcal{A}^s(k)$ for $s = \mathrm{I}, \mathrm{II}$. There they defined it to be

$$\begin{aligned} &\nu = P_\theta(T/2) - P_\theta(0) \pmod 2, \text{ or} \\ &(-1)^\nu = \prod_{i=1}^{4}\frac{\sqrt{\det[w(\Gamma_i)]}}{\mathrm{Pf}[w(\Gamma_i)]}, \end{aligned} \tag{4.30}$$

where the unitary matrix $w(\boldsymbol{k}) = \langle u_m(-\boldsymbol{k})|\Theta|u_n(\boldsymbol{k})\rangle$ and Γ_i's are the TR-invariant momenta in 1BZ. This second expresion can be easily generalized to 3D case, which will be considered in the end of this subsection.

4.2.3.2 Numerical verification for explicit QSHI models

TR-invariant topological insulators are characterized by $\mathbb{Z}_2$ invariant as defined in Ref. [24] and [27]. In such a system, quantum states at $\boldsymbol{k}$ and $-\boldsymbol{k}$ are actually related by TR symmetry [24]: $|u_i(-\boldsymbol{k})\rangle = \Theta\,|u_i(\boldsymbol{k})\rangle$ (i is the label of bands). In this part, we calculate the overlaps for ground states with two famous models for QSHI, Bernevig-Hughes-Zhang (BHZ) model for HgTe quantum well [31] and Kane-Mele (KM) model based on graphene [24, 25]. In both models, two bands are degenerate in general due to TR symmetry. So by the analysis above, our overlap matrix becomes:

$$\begin{pmatrix} \langle v_1(\boldsymbol{k})|u_1(\boldsymbol{k})\rangle & \langle v_1(\boldsymbol{k})|u_2(\boldsymbol{k})\rangle \\ \langle v_2(\boldsymbol{k})|u_1(\boldsymbol{k})\rangle & \langle v_2(\boldsymbol{k})|u_2(\boldsymbol{k})\rangle \end{pmatrix}, \tag{4.31}$$

where u, v represents topologically non-trivial and topologically trivial bands respectively as usual.

BHZ model and KM model without Rashba term are just two copies of Chern insulators. In this case, spin Chern number is well-defined. The overlap matrix is diagonal and diagonal entries give us ± 1 as the Chern number difference similar to the case in the last section. So following the argument for Chern insulators we would get overlap 0 at some momentum in 1BZ, as verified by numerical results in Fig. 4.3. In our calculation, we used the Hamiltonians for BHZ model as the following,

$$\mathcal{H}_{BHZ} = \sin(k_x)\sigma_3\otimes\sigma_1 + \sin(k_y)I_{2\times 2}\otimes\sigma_1 + [2+m-\cos(k_x)-\cos(k_y)]I_{2\times 2}\otimes\sigma_3, \tag{4.32}$$

where σ_i's are the Pauli matrices and we used the parameter $m = \pm 1$ to obtain the two topologically distinct systems. And the parameters for KM model is chosen to be $a = 1, t_1 = 3, t_2 = 1, \mu = 0, \lambda_R = 0$ for topologically nontrivial system and $a = 1, t_1 = 1, t_2 = 0.2, \mu = 7.5, \lambda_R = 0$ for the topologically trivial one.

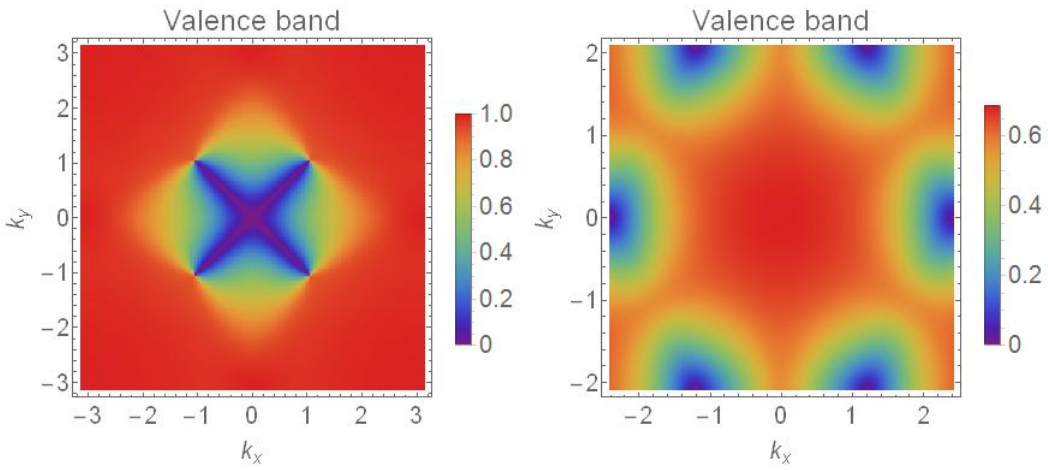

(a) BHZ model (b) KM model

Figure 4.3: Two copies of Chern insulators: absolute value for determinant

By changing the numerical value of λ_R to 0.1 for both systems, we introduce the Rashba term to destroy spin Chern number. Now spin Chern number is ill-defined and we only have $\mathbb{Z}_2$ invariant to classify these insulators. However, our determinant calculation still gives similar results as the model without Rashba term (see Fig. 4.4). Further calculation with broken C_3 symmetry also shows 0 determinant as long as the two systems are topologically distinct. In the next section we will show analytically that this is again due to the topological difference between the two ground-state band pairs.

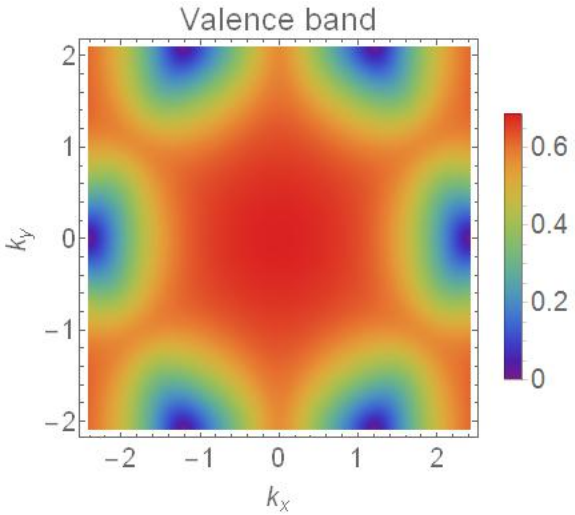

Figure 4.4: Adding Rashba term for KM model: absolute value for determinant

4.2.3.3 Analytical consideration

$\mathbb{Z}_2$ invariant in TR-invariant topological insulators could be understood as an obstruction for Stokes' Theorem [128]. In Ref. [128] Fu and Kane enforced the "time reversal constraint" in 2D TR invariant system

$$\begin{aligned} |u_2(-k_x,-k_y)\rangle &= \Theta\,|u_1(k_x,k_y)\rangle \\ |u_1(-k_x,-k_y\rangle &= -\Theta\,|u_2(k_x,k_y)\rangle\,. \end{aligned} \tag{4.33}$$

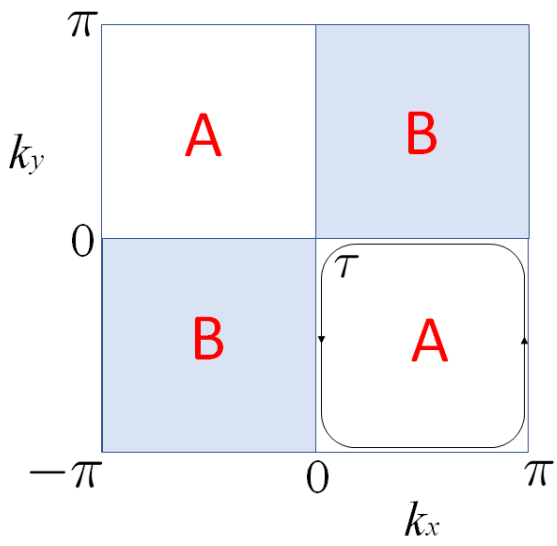

Figure 4.5: Figure for 1BZ, horizontal and vertical axes are k_x, k_y

On patches A and B, $|u_1(k_x,k_y)\rangle_A$ and $|u_2(k_x,k_y)\rangle_B$ are wave functions satisfying these conditions. But $|u_1(k_x,k_y)\rangle_B$ is not smooth in A due to the non-trivial $\mathbb{Z}_2$ invariant. On the common boundary of region A and B they are related by a U(2) transition matrix T

$$|u_m(k_x,k_y)\rangle_B = T_{mn}\,|u_n(k_x,k_y)\rangle_A \tag{4.34}$$

With this transition matrix, the authors defined a $\mathbb{Z}_2$ invariant (even for trivial insu-

lators and odd for non-trivial ones)

$$D = \frac{1}{2\pi i} \oint_{\partial\tau} d\boldsymbol{l} \cdot \mathrm{tr}(T^\dagger \boldsymbol{\nabla} T). \tag{4.35}$$

D is also the winding number of the map $\det(T) : \partial\tau \to S^1$ due to the following reason. In general we have $T = \exp(it^\mu \sigma_\mu)$ with $t^\mu \in \mathbb{R}$. The winding number of this map is

$$\begin{aligned}
w =& \frac{1}{2\pi i} \oint_{\partial\tau} d\boldsymbol{l} \cdot \det(T)^* \boldsymbol{\nabla} \det(T) \\
=& \frac{1}{2\pi i} \oint_{\partial\tau} d\boldsymbol{l} \cdot [\exp(\mathrm{tr} \ln T)]^* \boldsymbol{\nabla} \exp(\mathrm{tr} \ln T) \\
=& \frac{1}{2\pi i} \oint_{\partial\tau} d\boldsymbol{l} \cdot \boldsymbol{\nabla} \mathrm{tr}(\ln T) \\
=& \frac{1}{2\pi i} \oint_{\partial\tau} d\boldsymbol{l} \cdot \mathrm{tr}\, \boldsymbol{\nabla} (it^\mu \sigma_\mu) \\
=& \frac{1}{2\pi} \oint_{\partial\tau} d\boldsymbol{l} \cdot 2\boldsymbol{\nabla} t^0 \\
=& \frac{1}{2\pi i} \oint_{\partial\tau} d\boldsymbol{l} \cdot \mathrm{tr}(T^\dagger \boldsymbol{\nabla} T) \\
=& D.
\end{aligned} \tag{4.36}$$

Suppose a Kramer pair $|u_1(k_x, k_y)\rangle, |u_2(k_x, k_y)\rangle$ is the ground state of a topologically nontrivial TR-invariant system and another Kramer pair $|v_1(k_x, k_y)\rangle, |v_2(k_x, k_y)\rangle$ is the ground state of another trivial TR-invariant system. The overlap of ground

states on the boundary $\partial\tau$ is

$$\begin{aligned}
&\phi_B(k_x,k_y) = \det(\mathcal{F}) \\
:=&\det\begin{pmatrix} \langle v_1(k_x,k_y)|u_1(k_x,k_y)\rangle_B & \langle v_1(k_x,k_y)|u_2(k_x,k_y)\rangle_B \\ \langle v_2(k_x,k_y)|u_1(k_x,k_y)\rangle_B & \langle v_2(k_x,k_y)|u_2(k_x,k_y)\rangle_B \end{pmatrix} \\
=&\det\left[\begin{pmatrix} \langle v_1(k_x,k_y)|u_1(k_x,k_y)\rangle_A & \langle v_1(k_x,k_y)|u_2(k_x,k_y)\rangle_A \\ \langle v_2(k_x,k_y)|u_1(k_x,k_y)\rangle_A & \langle v_2(k_x,k_y)|u_2(k_x,k_y)\rangle_A \end{pmatrix}\begin{pmatrix} T_{11} & T_{21} \\ T_{12} & T_{22}\end{pmatrix}\right] \\
=&\phi_A(k_x,k_y)\det(T)
\end{aligned} \tag{4.37}$$

where we used equation 4.34 for the gauge transformation. We now show that the overlap $\phi(k_x,k_y)$ must vanish at some point in region τ. Suppose $\phi(k_x,k_y)\neq 0$ along $\partial\tau$ (otherwise we are done). Define a map $\mathcal{N}(k_x,k_y) = \phi(k_x,k_y)/|\phi(k_x,k_y)| : \partial\tau \to S^1$. Then the winding number for this map is given as

$$W = \frac{1}{2\pi}\oint_{\partial\tau} d\boldsymbol{l}\cdot\mathcal{N}^*(k_x,k_y)\boldsymbol{\nabla}\mathcal{N}(k_x,k_y). \tag{4.38}$$

So using equation (4) and the fact $T\in U(2)$,

$$\begin{aligned}
W_B =&\frac{1}{2\pi}\oint_{\partial\tau} d\boldsymbol{l}\cdot\mathcal{N}_B^*(k_x,k_y)\boldsymbol{\nabla}\mathcal{N}_B(k_x,k_y) \\
=&\frac{1}{2\pi}\oint_{\partial\tau} d\boldsymbol{l}\cdot\left[\mathcal{N}_A(k_x,k_y)\det(T)\right]^*\boldsymbol{\nabla}\left[\mathcal{N}_A(k_x,k_y)\det(T)\right] \\
=&\frac{1}{2\pi}\oint_{\partial\tau} d\boldsymbol{l}\cdot\left[\det(T)^*\det(T)\right]\left[\mathcal{N}_A^*(k_x,k_y)\boldsymbol{\nabla}\mathcal{N}_A(k_x,k_y)\right] + \\
&\frac{1}{2\pi}\oint_{\partial\tau} d\boldsymbol{l}\cdot\left[\mathcal{N}_A^*(k_x,k_y)\mathcal{N}_A(k_x,k_y)\right]\left[\det(T)^*\boldsymbol{\nabla}\det(T)\right] \\
=&\frac{1}{2\pi}\oint_{\partial\tau} d\boldsymbol{l}\cdot\mathcal{N}_A^*(k_x,k_y)\boldsymbol{\nabla}\mathcal{N}_A(k_x,k_y) + \frac{1}{2\pi}\oint_{\partial\tau} d\boldsymbol{l}\cdot\det(T)^*\boldsymbol{\nabla}\det(T) \\
=&W_A + D
\end{aligned} \tag{4.39}$$

Here $W_B - W_A = D$ is an odd integer and can not be gauged away as mentioned in Ref. [128]. So there must be a singularity ($|\phi(k_x, k_y)| = 0$) inside τ.

The argument above is easily generalized to 3D case. In 3D TR-invariant topological insulators, there are 8 TR-invariant momenta, denoted by $\Gamma_{i=(n_1 n_2 n_3)} = (n_1 \boldsymbol{b}_1 + n_2 \boldsymbol{b}_2 + n_3 \boldsymbol{b}_3)/2$ with $n_j = 0, 1$. The 16 phases of 3D TR-invariant topological insulators are characterized by 4 $\mathbb{Z}_2$ indices $\nu_0; (\nu_1, \nu_2, \nu_3)$ [26], where (ν_1, ν_2, ν_3) can be regarded as Miller indices for the 8 elements mod 2 reciprocal lattice $\boldsymbol{G}_\nu = \sum_i \nu_i \boldsymbol{b}_i$. Clearly, these indices are equivalent to the 6 2D $\mathbb{Z}_2$ indices $\begin{pmatrix} \nu_0 + \nu_1 & \nu_0 + \nu_2 & \nu_0 + \nu_3 \\ \nu_1 & \nu_2 & \nu_3 \end{pmatrix}$ (mod 2), where the first row represents $\mathbb{Z}_2$ indices for planes $k_x = 0, k_y = 0, k_z = 0$ respectively while the second row for planes $k_x = \pi, k_y = \pi, k_z = \pi$. Under this construction, we can easily see that if two Kramer pairs (bands in 3D) are topologically different, then at least one correspondent ν_μ differs. Consequently, at least 2 out of the 6 planes have different 2D topological indices for these Kramer pairs. Now the argument for 2D case applies to these planes in k-space.

4.3 Overlap of bands with different symmetries

In this section, we provide an example to show that the generic zero overlap is indeed due to different topology instead of different symmetries. We take the same Hamiltonian for Kane-Mele model as in Ref. [124]

$$\begin{aligned} H_{\mathrm{KM}} &= d_1 I_{2\times 2} \otimes \tau_1 + d_2 I_{2\times 2} \otimes \tau_2 + d_3 \sigma_3 \otimes \tau_3; \\ d_1 &= -t_1[1 + \cos(k_1) + \cos(k_2)]; \\ d_2 &= -t_1[\sin(k_1) + \sin(k_2)]; \\ d_3 &= -2t_2 \sin(\phi)[\sin(k_1) - \sin(k_2) - \sin(k_1 - k_2)]; \end{aligned} \tag{4.40}$$

where $k_1 = \frac{1}{2}k_x + \frac{\sqrt{3}}{2}k_y, k_2 = -\frac{1}{2}k_x + \frac{\sqrt{3}}{2}k_y$, σ_i and τ_i represent spin and valley respectively and t_1, t_2 are nearest neighbor and next nearest neighbor hopping strengh, ϕ is the phase change along with next nearest neighbor hopping. The first Brillouin zone can be chosen to be a rhombus formed by reciprocal lattice vectors $\frac{4\pi}{\sqrt{3}}(\frac{\sqrt{3}}{2}, \pm\frac{1}{2})$.

The Bernevig-Hughes-Zhang model [31] we used is given by

$$H_{\text{BHZ}} = \sin(k_x)\sigma_3 \otimes \tau_1 + \sin(k_y) I_{2\times 2} \otimes \tau_2 + [2 - m - \cos(k_x) - \cos(k_y)] I_{2\times 2} \otimes \tau_3. \quad (4.41)$$

And the first Brillouin zone is a square region $(-\pi, \pi] \times (-\pi, \pi]$.

We choose $t_1 = 3, t_2 = 1, \phi = \pi/2$ for KM model and $m = 1$ for BHZ model so that their ground states share the same spin Chern number. Then the overlap (determinant) can be calculated pointwise through a map KM $\to$ BHZ : $(x, y) \mapsto (-\pi + \frac{1}{2}x + \frac{\sqrt{3}}{2}y, -\pi + \frac{1}{2}x - \frac{\sqrt{3}}{2}y)$. The final density plot in the first Brillouin zone of BHZ model is shown below, from which we clearly see no vanishing determinant (despite different lattice symmetries of these two models).

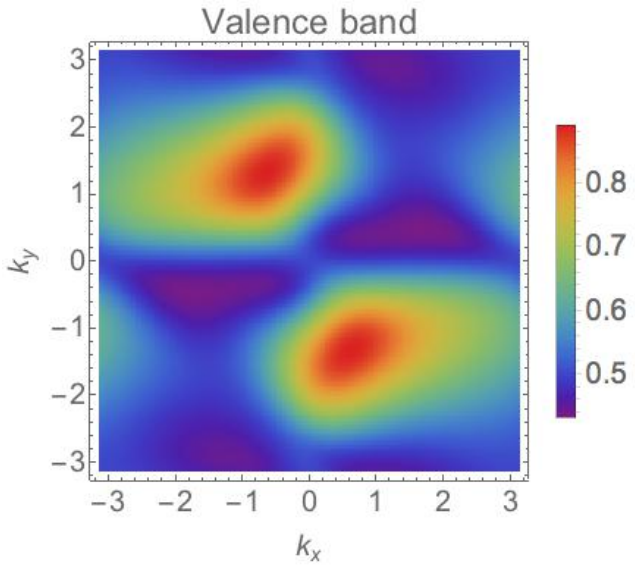

Figure 4.6: Absolute value of determinant for the two ground states of KM and BHZ models

4.4 Application to interacting systems

To show that our theorem applies for interacting systems despite Anderson's orthogonality catastrophe, here we provide two examples.

4.4.1 Quantum Hall and Chern insulators

For certain topological states, the topological structure is well defined for both finite and infinite systems. The most well-known example of this type is the integer and fractional quantum Hall systems, as well as the integer and fraction Chern insulators, where the topological index can be computed using twisted boundary conditions for both finite-size and infinite systems [125].

4.4.1.1 Definition of topological indices for a finite-size system

Consider a finite-size two-dimensional many-body systems with size $L_x \times L_y$. We enforce a twisted boundary condition for the many body wave function

$$\psi(\ldots, x_i + L_x, y_i, \ldots) = e^{i\varphi_x}\psi(\ldots, x_i, y_i, \ldots) \tag{4.42}$$

$$\psi(\ldots, x_i, y_i + L_y, \ldots) = e^{i\varphi_y}\psi(\ldots, x_i, y_i, \ldots) \tag{4.43}$$

where ψ is the many-body wave function, while x_i and y_i are the x and y cooridnates of the ith particle. φ_x and φ_y are two phase factors. For $\varphi_x = \varphi_y = 0$ ($\varphi_x = \varphi_y = \pi$), it recovers the periodic (antiperiodic) boundary conditions. For other values of φ_x and φ_y, it is known as the twisted boundary conditions.

We can find the ground state of a quantum system under twisted boundary conductions $|\psi(\varphi_x, \varphi_y)\rangle$. In general, the ground-state wave function depends on the

values of φ_x and φ_y. For a gapped system, we can define the following integral

$$C = \int_0^{2\pi} d\varphi_x \int_0^{2\pi} d\varphi_y \frac{\langle \partial_{\varphi_x}\psi|\partial_{\varphi_y}\psi\rangle - \langle \partial_{\varphi_y}\psi|\partial_{\varphi_x}\psi\rangle}{2\pi i} \tag{4.44}$$

As pointed out in Ref. [125], this integral is a topological invariant, i.e. the first Chern number, regardless of the size of the system. In the thermodynamic limit, this topological index coincides with the Hall conductivity [125]. Because the definition utilizes many-body wave functions (without using single-particle Bloch waves), it is applicable for both interacting and non-interacting systems. In the non-interacting limit, it recovers the Chern number computed using single-particle Bloch waves [13].

It is also worthwhile to mention that it is straightforward to generalize this definition to fractional quantum Hall systems (fractional Chern insulators). Once topological degeneracy is taken into account, the integral shown above produces fractional values, i.e. the fractional Hall conductivity [129].

4.4.1.2 Wave function overlap and topological index

Consider a 2D finite-size system with Hamiltonian H_1 and another 2D system with the same size but a different Hamiltonian H_2. Here, we allow the Hamiltonians to contain interactions, and we assume that the ground states are gapped for both Hamiltonians (for any twisted boundary conditions). We can find the many-body ground states for the two Hamiltonians under twisted boundary condition $|\psi_1(\varphi_x, \varphi_y)\rangle$ and $|\psi_2(\varphi_x, \varphi_y)\rangle$ respectively. Using Eq. (4.44), one can compute the Chern number for the ground states of both Hamiltonians.

Here, we ask the following question: *if the ground states of the two Hamiltonians have different Chern numbers, what is the wave function overlap between the two insulators,* $\langle \psi_1(\varphi_x, \varphi_y)|\psi_2(\varphi_x, \varphi_y)\rangle$. Because we have set the system-size to be finite, the wave function overlap *does not* suffer from the orthogonality catastrophe, and

thus we can directly apply the theorem proved above.

Because the two ground states have different topological index, it is impossible to adiabatically deform one state into the other without closing the excitation gap (between the ground state and the first excited state). This implies that no matter how we tries to deform H_1 into H_2, adiabatically, the excitation gap must close for at least one set of φ_x and φ_y. Utilizing the theorem proved above, this implies that we can find at least one set of φ_x and φ_y, the wave function overlap vanishes $\langle\psi_1(\varphi_x,\varphi_y)|\psi_2(\varphi_x,\varphi_y)\rangle = 0$. Otherwise, an adiabatic path will exist, which is in contradiction to the assumption that the two states have different Chern numbers.

Now we consider the opposite situation, where $\langle\psi_1(\varphi_x,\varphi_y)|\psi_2(\varphi_x,\varphi_y)\rangle \neq 0$ for all possible values of φ_x and φ_y. Utilizing the theorem shown above, for any twisted boundary condition, we can construct an adiabatic path between these two quantum states without closing the gap. As a result, the two states must have the same Chern number.

4.4.1.3 Topological phase transitions in interacting systems

Now we study a topological phase transitions in a 2D interacting system. Considering a Hamiltonian $H(\alpha)$, where α is a control parameter. We assume that by tuning the control parameter α, the system undergoes a topological phase transition, where the Chern number changes its value, i.e., the Hamiltonian has a gapped ground state for both $\alpha > \alpha_C$ and $\alpha < \alpha_C$, but the ground state has different Chern numbers for $\alpha > \alpha_C$ and $\alpha < \alpha_C$. Here again, we consider a finite-size system, although one can take the thermodynamic limit later via finite size scaling. As shown above and pointed out in Ref. [130], even for finite size systems, the Chern number and the topological phase transition is well-defined.

The ground-state wave function of this Hamiltonian, $|\psi_\alpha(\varphi_x,\varphi_y)\rangle$ depends on the value of the control parameter α, as well as the phases of the twisted boundary

conditions φ_x and φ_y. We can compute the wave function overlap for the ground state at different values of α,

$$\phi_{\alpha_1,\alpha_2}(\varphi_x,\varphi_y) = \langle \psi_{\alpha_1}(\varphi_x,\varphi_y)|\psi_{\alpha_2}(\varphi_x,\varphi_y)\rangle \tag{4.45}$$

The conclusions that we proved above indicate immediately that if this overlap never vanishes for any φ_x and φ_y, $H(\alpha_1)$ and $H(\alpha_2)$ describe states in the same quantum phase, i.e. $\alpha_1 > \alpha_C$ and $\alpha_2 > \alpha_C$, or $\alpha_1 < \alpha_C$ and $\alpha_2 < \alpha_C$.

Similarly, if we compute the overlap for two wave functions from two different topological phases, (e.g., $\alpha_1 > \alpha_C$ and $\alpha_2 < \alpha_C$), then this overlap must vanish for some values of φ_x and φ_y. A special case of this type has been shown in Ref. [131], where α_1 and α_2 are very close to the transition point, i.e. $\alpha_1 = \alpha_C + \epsilon$ and $\alpha_2 = \alpha_C - \epsilon$ where ϵ is a very small positive number. There, the vanishing wave function overlap results in a singularity (i.e. an Dirac δ-function) in the fidelity matrix [132–134], which can be used to pin-point the topological phase transition in a finite-size interacting system. The results shown above generalize the same conclusion for any values of $\alpha_1 > \alpha_C$ and $\alpha_2 < \alpha_C$, close or far away from the topological transition point.

4.4.2 Factorized wave function overlap in certain interacting systems

In general, a many-body ground-state wave function of an interacting system cannot be factorized as the product of single-particle (or few-particle) wave functions, in contrast to non-interacting systems discussed in Sec. 3.2. However, for certain interacting systems, such a factorization could happen, which offers us another way to avoid the orthogonality catastrophe in the study of wave function overlap.

Here we consider a (AA-stacked) bilayer Kane-Mele model as studied in Ref. [135]. For each layer, we have a non-interacting Kane-Mele model (on a honeycomb lattice), which describes a $\mathbb{Z}_2$ topological insulator. Between the layers, an interlayer antifer-

romagnetic spin-spin interaction is introduced between interlayer nearest neighbors.

In this model, because the z-component of the spin is conserved, the insulating ground state is characterized by an integer-valued topological index, known as the spin Chern number. In the non-interacting limit, the topological index is +2, i.e., the system is topologically nontrivial. Because there is no interaction, the ground state factorizes as the antisymmetrized product of Bloch states

$$|\psi_I\rangle = \prod_{\boldsymbol{k}} c^\dagger_{\mathrm{t},\boldsymbol{k}} d^\dagger_{\mathrm{t},\boldsymbol{k}} c^\dagger_{\mathrm{b},\boldsymbol{k}} d^\dagger_{\mathrm{b},\boldsymbol{k}} |0\rangle \tag{4.46}$$

where $c^\dagger_{\mathrm{t},\boldsymbol{k}}$ and $d^\dagger_{\mathrm{t},\boldsymbol{k}}$ are the creation operators for the two valence band in the top layer. Here, the top layer is a non-interacting Kane-Mele model, which has two valence bands (taking into account the spin degrees of freedom). The other two creation operators $c^\dagger_{\mathrm{b},\boldsymbol{k}}$ and $d^\dagger_{\mathrm{b},\boldsymbol{k}}$ are for the bottom layer, which is identical to the top layer.

When the interlayer antiferromagnetic coupling is infinitely strong, electrons between the two layers form singlet pairs (i.e., dimers). At half-filling, the dimers fill up the whole system, and electrons can no longer move, i.e. the system becomes a topologically trivial insulator with spin Chern number 0. Here, the ground-state wave function is

$$|\psi_{II}\rangle = \prod_i (a^\dagger_{\mathrm{t},i,\uparrow} a^\dagger_{\mathrm{b},i,\downarrow} - a^\dagger_{\mathrm{t},i,\downarrow} a^\dagger_{\mathrm{b},i,\uparrow})(b^\dagger_{\mathrm{t},i,\uparrow} b^\dagger_{\mathrm{b},i,\downarrow} - b^\dagger_{\mathrm{t},i,\downarrow} b^\dagger_{\mathrm{b},i,\uparrow}) |0\rangle$$

Here, $a^\dagger$ and $b^\dagger$ are the creation operator for the A and B sublattices of the honeycomb lattice respectively. The subindices t and b represent the top and bottom layers, and i is the index for unit cells. $\uparrow$ and $\downarrow$ are spin indices (spin up and down). Here, $a^\dagger_{\mathrm{t},i,\uparrow} a^\dagger_{\mathrm{b},i,\downarrow} - a^\dagger_{\mathrm{t},i,\downarrow} a^\dagger_{\mathrm{b},i,\uparrow}$ and $b^\dagger_{\mathrm{t},i,\uparrow} b^\dagger_{\mathrm{b},i,\downarrow} - b^\dagger_{\mathrm{t},i,\downarrow} b^\dagger_{\mathrm{b},i,\uparrow}$ create spin singlets (dimers) in the A and B sites of the ith unit cell.

Because the non-interacting limit and the strong-coupling limit have different topological indices (+2 and 0), a topological phase transition must arise as the anti-

ferromagnetic coupling strength increases. This transition was observed and studied using quantum Monte Carlo simulations [135].

Here, we focus on the non-interacting limit and the infinite-coupling limit. As shown above, in both cases, the ground states are product states. With periodic boundary conditions, the number of momentum points in a Brillouin zone coincides with the number of unit cells in the real space. Thus, we can define a one-to-one mapping between the unit cell index i and crystal momentum $\boldsymbol{k}$

$$i \to \boldsymbol{k} = \boldsymbol{k}_i \tag{4.47}$$

Utilizing this mapping, the wave function overlap between $|\psi_I\rangle$ and $|\psi_{II}\rangle$ can be factorized

$$|\phi| = |\langle\psi_I|\psi_{II}\rangle| = \prod_i |\phi_i| \tag{4.48}$$

where

$$\begin{aligned}\phi_i = \langle 0| d_{\mathrm{b},\boldsymbol{k}_i} c_{\mathrm{b},\boldsymbol{k}_i} d_{t,\boldsymbol{k}_i} c_{\mathrm{t},\boldsymbol{k}_i} (a^\dagger_{\mathrm{t},i,\uparrow} a^\dagger_{\mathrm{b},i,\downarrow} - a^\dagger_{\mathrm{t},i,\downarrow} a^\dagger_{\mathrm{b},i,\uparrow}) \\ (b^\dagger_{\mathrm{t},i,\uparrow} b^\dagger_{\mathrm{b},i,\downarrow} - b^\dagger_{\mathrm{t},i,\downarrow} b^\dagger_{\mathrm{b},i,\uparrow}) |0\rangle\end{aligned} \tag{4.49}$$

Here, for each i, this overlap only involves four creation (annihilation) operators, and thus ϕ_i doesn't suffer from the orthogonality catastrophe. Because the two regimes (non-interacting and infinite-interaction) have ground states with different topology, we expect at least one i, at which ϕ_i vanishes. This is indeed the case for the model considered here.

4.5 Conclusion

In this chapter, we explored a variety of models to verify our overlap theorem. These models range from 1D to 3D, from band insulators to certain interacting systems, from systems with the same lattice symmetry to those with distinct symmetries. Specifically, we show that although Anderson orthogonality catastrophe prohibits overlaps to give more information to topological phase transitions in infinite systems, there are certain interacting systems in which the overlap theorem still works. In next chapter, we will try to attack generic interacting systems by showing that more information could be extracted from finite-size scaling.

CHAPTER V

Anderson orthogonality catastrophe in $2+1$-D topological systems

5.1 Introduction

Ground states of condensed matter systems encode the information of quantum phases. Topological insulators, for example, are defined through the calculation of certain topological invariants [14, 24–27, 31, 128] based on ground states. There has been many efforts trying to understand such information in the ground-state wave functions. In particular, the ground-state overlaps have been utilized to investigate geometric entanglement [136–138] and (topological) quantum phase transitions [131, 132, 139–142]. Among those efforts, our previous work [139] has proven that two insulators lie in the same topological phase if their single-particle ground-state overlap does not vanish in the first Brillouin zone.

However, many-body ground-state overlaps in the thermodynamic limit are always 0 due to Anderson orthogonality catastrophe [112]. At first glance, it seems no information could be extracted from the wave-function overlap. But we learned in first-year calculus that functions could approach 0 in different order under certain limit condition. Thus, it is expected that more information could be generated from the finite-size scaling of overlaps. For the impurity problem, Anderson first showed a

power law decay for the overlap,

$$\langle \Psi | \Psi' \rangle \sim N^{-\epsilon}, \tag{5.1}$$

where N is the number of electrons and $\epsilon > 0$. For two generic wave functions, if the overlap on each lattice site differs by a finite amount then one would naively expect the many-body wave-function overlap exhibit an exponential decay.

In this chapter, we focus on the study of $(2+1)$-D topological states which includes both symmetry-protected topological (SPT) states and intrinsic topological states. SPT systems are adiabatically connected with trivial product states under local unitary transformation [18, 39]. However, there is no such a smooth path connecting nontrivial SPT states and product states if the symmetries are preserved. Such systems in $(2+1)$-D must have gapless surface/edge modes [18, 39]. In higher dimensions, these boundary modes could also be gapped. But the ground state on the boundary must be degenerate if the essential symmetries are spontaneously broken there [18, 39]. In the following, we will exploit the ideal ground-state wave function for $(2+1)$-D fixed-point SPT systems (in renormalization-group sense) to prove the existence of a topological response term in ground-state overlaps. Then we will verify it with the example of $\mathbb{Z}_2$-protected Ising paramagnetic topological systems [143]. We show that the overlap of generic fixed-point SPT states has a universal sub-leading terms depending on the Euler characteristic of the manifold the systems live on. Such a topological response term is an analogue of the corrections of entanglement entropy and free energy in $(1+1)$-D critical systems. Indeed, we find the coefficient of the topological response term is related to the central charge of an underlying CFT. Similar behavior is seen in systems with intrinsic topological order. More surprisingly, we find an overlap decaying faster than exponential in the case of fractional quantum Hall (FQH) systems. We will end with some open questions.

5.2 Physical Intuition

In this section, we will provide an intuitive argument that will serve as a basic physical picture for the rigorous calculations in later sections.

The imaginary time evolution of an arbitrary state could be written as

$$|\text{final}\rangle = \mathcal{T}\left(e^{-\int_0^\beta H(\tau)d\tau}\right)|\text{initial}\rangle \tag{5.2}$$

up to a normalization factor. Here $\mathcal{T}$ is the time-ordering operator, the initial state is an arbitrary state at time 0 and it evolves within time β to the final state. Denote the eigenvalues and eigenstates of such a system as E_i and $|i\rangle$ respectively. $|i\rangle$'s form a complete set of basis vectors in the wave-function space. So any initial state could be written as a linear combination of $|i\rangle$'s,

$$|\text{initial}\rangle = \sum_i \alpha_i |i\rangle\,, \tag{5.3}$$

where α_i's are finite constants. Insert this equation to Eq. (5.2), we get

$$|\text{final}\rangle = \sum_i \alpha_i e^{-\int_0^\beta E_i d\tau}|i\rangle \tag{5.4}$$

It becomes obvious that in the infinite-time/zero-temperature limit $\beta \to \infty$, coefficients of all excited states are suppressed exponentially to 0. In other words, if the initial state contains some component from the ground states, then the final state must be a linear combination of degenerate ground states under long-time evolution. In the case the ground state is non-degenerate, we have reached the unique ground state in this calculation. This is consistent with the fact that when the temperature is 0, quantum systems reside in their ground states.

Once the ground states are obtained, we could calculate the ground-state overlaps. Similar to the argument by You et al. [123], here we only give an intuitive argument.

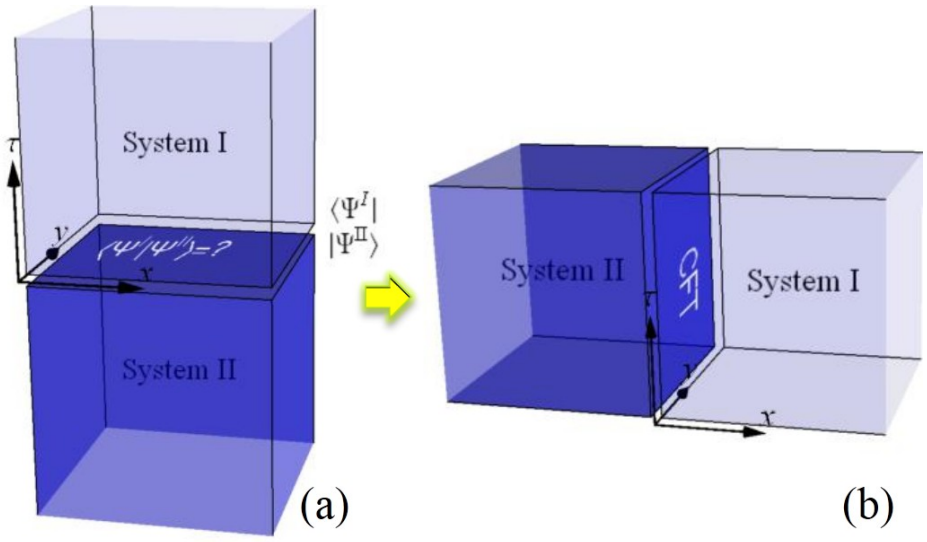

Figure 5.1: (a) $|\Psi^{\mathrm{I}}\rangle, |\Psi^{\mathrm{II}}\rangle$ are obtained from the infinite-time evolution of arbitrary states from $+\infty$ and $-\infty$ under the path integral of system I and II respectively. The overlap describes the interface $\tau = 0$. (b) Rotate the combined system by 90°. The interface becomes $x = 0$ which is a CFT.

In the following sections, we will prove it through rigorous formulation for a large variety of fixed-point topological systems. Consider two (almost) arbitrary states evolving under the Hamiltonian of systems I and II from $\tau = +\infty$ and $\tau = -\infty$ to $\tau = 0$ respectively. Since the components of excited states in the two initial states are exponentially suppressed during the evolution, the final states at $\tau = 0^+$ and $\tau = 0^-$ are the ground states $\langle\Psi^{\mathrm{I}}|, |\Psi^{\mathrm{II}}\rangle$ of system I and system II respectively (Fig. 5.1(a)). So the overlap $\langle\Psi^{\mathrm{I}}|\Psi^{\mathrm{II}}\rangle$ describes the theory on the interface $\tau = 0$. Rotating such a system by 90°, the imaginary-time interface at $\tau = 0$ becomes a spatial interface at $x = 0$ (Fig. 5.1(b)). So as long as the interface at $x = 0$ is gapless (which is true for any $(2+1)$-D SPT systems) and described by some CFT, the corresponding wave function overlap would be related to a critical theory.

Indeed, we will show later case by case that the overlaps can be interpreted as partition function Z of certain CFT. For a generic CFT, Cardy [144] shows that the

free energy scales as

$$F = -\ln(Z) = \alpha N + \beta\sqrt{N} - \frac{\chi c}{12}\ln(N) + O(1). \tag{5.5}$$

In this expression, the N term comes from the contribution of bulk, the $\sqrt{N}$ term from the boundary contribution. The coefficient of $\ln(N)$ correction depends on the Euler characteristic χ of the manifold M where the system lives on and the central charge c of the underlying CFT. Following this key expression for scaling, we conclude that $\ln(\langle\Psi^{\mathrm{I}}|\Psi^{\mathrm{II}}\rangle)$ contains the topological response term $\frac{\chi c}{12}\ln(N)$ as we expected.

5.3 Bosonic SPT

In this section, we will give a more rigorous derivation for $(2+1)$-D fixed-point bosonic SPT systems. It was shown that a large number of $(2+1)$-D SPT states could be described by *continuous* nonlinear σ models with topological θ terms [145]. For example, in spin systems with $SO(3)$ rotational symmetry, the action is given by

$$S = \int d\tau d^2x \left(\frac{1}{2\rho}\,\mathrm{tr}(\partial_\mu g^\dagger \partial_\mu g) + i\frac{\theta}{2\pi^2}\frac{\epsilon^{\mu\nu\lambda}}{6}\frac{1}{8}\,\mathrm{tr}[(g^{-1}\partial_\mu g)(g^{-1}\partial_\nu g)(g^{-1}\partial_\lambda g)] \right) \tag{5.6}$$

where $g(\boldsymbol{x}, t)$ is a group element in $SO(3)$ and $\theta = 2\pi k$ with $k \in \mathbb{Z}$. A more complete classification of bosonic SPT can be achieved through group cohomology [18, 146], which could be loosely considered as a discrete version for the topological field theories mentioned above. In the group cohomology construction, the partition function for fixed-point systems are required to be 1. This will be one of the essential requirements when we work with the discrete space-time path integrals in the following.

5.3.1 Warm-up: Ground States of $(1+1)$-D Fixed Points

As we have seen in Section 5.2, theories in continuous space-time can find their ground-state wave function by infinite-time evolution of (almost) arbitrary states. Similarly, after we discretize the space-time, the fixed-point ground states of different SPT phases could be represented through discretized version of space-time evolution of states. For the sake of simplicity, we give an example of a $(1+1)$-D bosonic SPT sytem with onsite symmetry G (see Fig. 5.2). In the discrete space-time or triangulation of space-time, group cohomology theory assigns one group element $g \in G$ to each vertex and a phase factor ν (dubbed cocycle) to the simplex (a triangle in $(1+1)$-D and a tetrahedron in $(2+1)$-D).

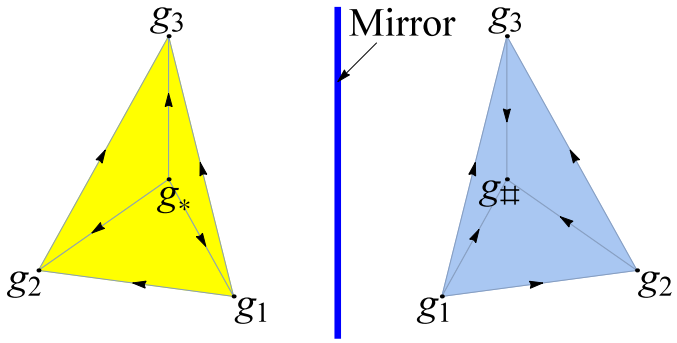

Figure 5.2: For simplicity, we only illustrate the graphic representation of the fixed point wave function in (1+1)-D where M is topologically a circle instead of a sphere in the main text. (Left) The time evolution of an arbitrary state from the point $*$ to the boundary $\partial\Sigma = M$ would produce the ground state $|\Psi\rangle$ of the corresponding theory. (Right) The Hermitian conjugate $\langle\Psi|$ can be obtained through a mirror reflection of the state $|\Psi\rangle$ except the orientation of each simplex is reversed. And such a state could be considered as some arbitrary wave function evolves from the point # backward in time to the boundary M.

Intuitively, the fixed-point ground state of such a system is given by the time evolution of an arbitrary state from vertex $*$ to the boundary (123). Mathematically, the combinations of $\{g_1, g_2, g_3\}$ on the boundary forms an orthogonal set of basis vectors in the wave-function space. The ground-state amplitude over the basis vector

$|\{g_1, g_2, g_3\}\rangle$ is given by

$$\Psi(\{g_1, g_2, g_3\}) = \frac{1}{|G|} \sum_{g_* \in G} \nu_2^{-1}(g_*, g_1, g_2)\nu_2^{-1}(g_*, g_2, g_3)\nu_2(g_*, g_1, g_3), \tag{5.7}$$

where $|G|$ is the order of group G, $\nu_2(g_i, g_j, g_k)$ is the 2-cocycle associated with triangle (ijk) and its exponent ± 1 is determined through the orientation of the triangle (ijk). Each ν could be considered as the discrete version of the action amplitude e^{-S} where S is the fixed-point action of the topological system. The Hermitian conjugate of this state is represented as the mirror image of the triangulation on the left panel in Fig. 5.2 except the time-evolution arrows reversed. Its wave-function amplitude over the basis $|\{g_1, g_2, g_3\}\rangle$ is

$$\Psi^\dagger(\{g_1, g_2, g_3\}) = \frac{1}{|G|} \sum_{g_\# \in G} \nu_2(g_1, g_2, g_\#)\nu_2(g_2, g_3, g_\#)\nu_2^{-1}(g_1, g_3, g_\#). \tag{5.8}$$

Pictorially, the overlap $\langle\Psi|\Psi\rangle = \mathrm{tr}(\Psi\Psi^\dagger)$ is the gluing of two $(1+1)$-D manifolds [39] sharing the same boundary (123). This is mathematically represented as

$$\langle\Psi|\Psi\rangle = \frac{1}{|G|^3} \sum_{g1,g2,g3} \Psi(\{g_1, g_2, g_3\})\Psi^\dagger(\{g_1, g_2, g_3\}) \tag{5.9}$$

where the third power of $|G|$ is due to the fact that there are in total 3 vertices on the gluing boundary. For this specific $(1+1)$-D case, the resulting manifold is a sphere with the vertex g_* representing negative infinite time and $g_\#$ representing positive infinite time. Plugging in the expressions of Ψ and $\Psi^\dagger$, we immediately realize that $\langle\Psi|\Psi\rangle$ is exactly the discrete version of a path integral. Since the path integral of fixed-point topological field theories over closed manifolds [18] are required to be 1, we obtain $\langle\Psi|\Psi\rangle = 1$, consistent with the normality of quantum states. In fact, this result could also be trivially derived from the more basic branching rules [18], which we omit here.

5.3.2 Ground-state Overlaps of $(2+1)$-D Fixed Points

Now consider a bosonic SPT system with on-site symmetry G defined on 2-dimensional closed manifold M. Including the time direction, the ground state would be defined on a $(2+1)$-D manifold Σ with boundary $\partial\Sigma = M$. Pick an arbitrary point $*$ inside Σ and connect it with all the vertices on M. In this way we have built a triangulation of the $(2+1)$-D manifold (see Fig. 5.3). One example for such a manifold Σ is a solid 2-sphere and its boundary M is a hollow 2-sphere. But it could be much more general. The ground-state wave function could be considered as the time evolution of an arbitrary state from any point $*$ inside of Σ to its boundary M. Explicitly, the fixed-point wave-function amplitude is given by

$$\Psi(\{g_i\}_M) = \frac{1}{|G|}\sum_{g_*\in G}\prod_{(*ijk)\in\Sigma}\nu_3^{s_{*ijk}}(g_*, g_i, g_j, g_k). \tag{5.10}$$

Here $\nu_3^{s_{*ijk}}(g_*, g_i, g_j, g_k)$ corresponds to the action amplitude $e^{-\int_{(*ijk)} d^2x d\tau \mathcal{L}[g(\boldsymbol{x},\tau)]}$ on a single simplex $(*ijk)$ and $s_{*ijk} = \pm 1$ depends on the orientation of the simplex. The summation $|G|^{-1}\sum_{g_*\in G}$ is understood as $\int dg_i$ over the group manifold if G is a continuous group. We also denoted Σ as the discrete $(2+1)$-D complex whose boundary is M and inside of Σ there is only one more vertex $*$. In order for the action S to exhibit a quantized topological θ-term, one essential constraint on the three-cocycle $\nu_3(g_i, g_j, g_k, g_l) \in \mathcal{H}^3[G, U_T(1)]$ is that on closed $(2+1)$-D manifolds,

$$e^{-S(\{g_i\})} = \prod_{(ijkl)}\nu_3^{s_{ijkl}}(g_i, g_j, g_k, g_l) = 1. \tag{5.11}$$

The above wave function can be considered as a state on M evolved from $*$. All excited states are exponentially suppressed. So such a wave function is the ground state. And its Hermitian conjugate is the state defined on the mirror reflection $\widetilde{\Sigma}$ (similar to the $(1+1)$-D case in Fig. 5.2). Therefore calculating the inner product

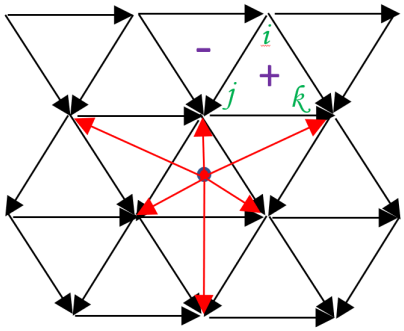

Figure 5.3: One part of a triangulation of $(2+1)$-D manifold. The red arrows point from a point inside of Σ to points on the boundary M and the black arrows form a triangulation of M. Together they form a triangulation of the $(2+1)$-D manifold Σ. Associated with vertices are group elements g. Triangle $[ijk]$ has positive orientation while its adjacent triangles have negative orientation. The orientation of other triangles could be derived easily from this convention.

of these two states is equivalent to gluing Σ and $\widetilde{\Sigma}$ together along M [39]. Similarly, the overlap of two distinct SPT states $|\Psi^{\mathrm{I}}\rangle, |\Psi^{\mathrm{II}}\rangle$ is a gluing with mismatches of the 3-cocycle ν_3,

$$\begin{aligned}\langle \Psi^{\mathrm{I}}_M | \Psi^{\mathrm{II}}_M \rangle =& \frac{1}{|G|^{N+2}} \sum_{\{\text{all } g \text{ on } \widetilde{\Sigma}\cup\Sigma\}} \\ & \prod_{(*ijk)} (\nu_3^{\mathrm{I}})^{-s_{*ijk}}(g_*, g_i, g_j, g_k) \prod_{(ijk\#)} (\nu_3^{\mathrm{II}})^{s_{ijk\#}}(g_i, g_j, g_k, g_\#)\end{aligned} \tag{5.12}$$

where N is the number of vertices on M and thus $N+2$ is the total number of vertices including $*$ and $\#$. $\widetilde{\Sigma}\cup\Sigma$ becomes a $(2+1)$-D closed manifold after the gluing and the orientation has been taken care of by the sign-flip of s_{*ijk}. Those 3-cocycles satisfying Eq. (5.11) cancel out. Finally one side of the mirror is occupied by trivial cocycles $\nu_3(g_*, g_i, g_j, g_k) = 1$ and the other side is occupied by the difference of the topological θ-terms for system I and II. On the boundary M the discrete version of the topological θ-term reduces to the Wess-Zumino-Witten (WZW) theory [147–150]. So the final expression for the overlap calculation is identical to a partition function Z of a conformal field theory (CFT) described by WZW action.

As mentioned above, the scaling behavior of generic $(1+1)$-D CFT is known to

follow Eq. (5.5). In our case the contribution from the $\sqrt{N}$ boundary term is 0 since M is a closed manifold without boundary. Therefore the finite-size scaling of the overlap follows

$$\ln \langle \Psi^{\mathrm{I}} | \Psi^{\mathrm{II}} \rangle = -\alpha N + \frac{\chi c}{12} \ln N + O(1). \tag{5.13}$$

The ground states are derived for generic $(2+1)$-D fixed-point bosonic SPT systems. So this result is also generic in the same realm. In $(2+1)$-D, SPT systems are guaranteed to have gapless modes in the space-direction interface and the edge modes are described by some CFT. This is consistent with our argument in the physical intuition section.

5.3.3 An Example on Bosonic SPT

As an example for our result above, we consider the two Ising-paramagnetic systems I and II as described by Levin and Gu [143]. The ground state of system I is the superposition of all states with different spin configurations. Each spin configuration corresponds to one domain wall (DW) configuration. So we could represent the ground state by the superposition of DW configurations,

$$|\Psi^{\mathrm{I}}\rangle = \frac{1}{\sqrt{\mathcal{N}}} \sum_{\{s_1,\ldots,s_N\}} |l \text{ DW's}\rangle \tag{5.14}$$

where the normalization factor $\mathcal{N} = \sum_{\{s_1,\ldots,s_N\}} 1^l = 2^N$ is the total number of spin configurations. This wave function is clearly topologically trivial since it can be rewritten as direct product of the spin triplet state $(|\downarrow_i\rangle + |\uparrow_i\rangle)/\sqrt{2}$ on each lattice site i. And system II is a $\mathbb{Z}_2$ SPT system. The ground-state wave function is the same superposition as system I except a factor $(-1)^l$ in front of each spin configuration where l is the number of DW's

$$|\Psi^{\mathrm{II}}\rangle = \frac{1}{\sqrt{\mathcal{N}}} \sum_{\{s_1,\ldots,s_N\}} (-1)^l |l \text{ DW's}\rangle \tag{5.15}$$

Since states with different spin configurations are mutually orthogonal, the overlap of the normalized wave functions $|\Psi^{\mathrm{I}}\rangle, |\Psi^{\mathrm{II}}\rangle$ is

$$\begin{aligned} \langle\Psi^{\mathrm{I}}|\Psi^{\mathrm{II}}\rangle =& \frac{\sum_{\{s_1,\ldots,s_N\}}(-1)^l}{\mathcal{N}} = \frac{Z_{O(n)}|_{x=1,n=-1}}{\mathcal{N}/2} \\ Z_{O(n)} =& \sum_{\text{DW config.}} x^L n^l \end{aligned} \tag{5.16}$$

where the factor 2 in the denominator is due to the fact that each domain wall configuration corresponds to two different spin configurations. We recognize that the numerator $Z_{O(n)}$ is the partition function of the classical $O(n)$-loop model and $x = 1, n = -1$ lies in the critical region [151] with central charge $c = -7$ [151–153] (see Appendix B.1). So the finite-size scaling of the numerator follows from Eq. (5.5) with $c = -7$. The denominator $\mathcal{N}/2$ in Eq. (5.16) only modifies the non-universal coefficient α. Therefore the scaling of $-\ln\langle\Psi^{\mathrm{I}}|\Psi^{\mathrm{II}}\rangle$ is the same as Eq. (5.13).

5.4 Fermionic SPT

Similar to bosonic SPT, a large class of fermionic SPT phases could be classified using a (special) group supercohomology theory [39]. In this chapter, we only focus on $(2+1)$-D systems where gapless edge states exist.

5.4.1 Ground-state Wave Functions

The fermionic SPT ground-state wave functions could be constructed in the same way as the bosonic SPT. Suppose the fermionic system with full symmetry G_f is defined on a closed 2-dimensional manifold M. The bosonic part of the symmetry is $G_f = G/\mathbb{Z}_2^f$ where $\mathbb{Z}_2^f$ is the fermion-number-parity symmetry. We can extend the hollow 2-dimensional manifold M to solid $(2+1)$-D manifold Σ with boundary $\partial\Sigma = M$. Triangulate M and assign a group element $g \in G_b$ to each vertex (see Fig. 5.3). Following the same physical intuition as the bosonic case, we can then write

down the ground state as the time evolution of arbitrary state from the point $*$ inside Σ to the boundary M.

In the bosonic SPT systems, a single tetrahedron with vertices 0, 1, 2, 3 is denoted as (0123). We assigned a pure phase (3-cocycle) $\nu_3^{s_{0123}}(g_0, g_1, g_2, g_3)$ where s_{0123} depends the orientation of the tetrahedron (0123). Here, each tetrahedron is associated with a Grassmann tensor. Comparing with the $(d+1)$-D bosonic SPT, the new ingredient is to multiply a Grassmann number for each d-simplex. In our interested case of $(2+1)$-D, this means adding a Grassmann number on each triangular face of the tetrahedron. Such a Grassmann tensor in positive oriented tetrahedron is given by

$$\begin{aligned}\mathcal{V}_3^{+}(g_0, g_1, g_2, g_3) =& \nu_3^{+}(g_0, g_1, g_2, g_3)\theta_{123}^{n_2(g_1,g_2,g_3)} \\ & \theta_{013}^{n_2(g_0,g_1,g_3)}\bar{\theta}_{023}^{n_2(g_0,g_2,g_3)}\bar{\theta}_{012}^{n_2(g_0,g_1,g_2)}\end{aligned} \tag{5.17}$$

where $\nu_3^{+}(g_0, g_1, g_2, g_3) = (-1)^{m_1(g_0,g_2)}\nu_3(g_0, g_1, g_2, g_3)$ with $m_1(g_0, g_2) = 0, 1$. The ordering of Grassmann number θ is naturally inherited from the ordering of the missing indices $0, 2, 4, \ldots$ and the ordering of $\bar{\theta}$ is from the missing indices $1, 3, 5, \ldots$. The exponent $n_2(g_i, g_j, g_k) = 0, 1$ satisfies

$$\sum_{i=0}^{3} n_2(g_0, \ldots, \hat{g}_i, \ldots, g_3) = \text{even}, \tag{5.18}$$

so that the total Grassmann number is even. There is also a relation between n_2's and m_1's,

$$n_2(g_1, g_2, g_3) = m_1(g_2, g_3) + m_1(g_1, g_3) + m_1(g_1, g_2) \bmod 2. \tag{5.19}$$

Such a construction of the sign conventions will be essential in calculating the fermionic path integral in the following.

For a corresponding negatively oriented tetrahedron [see Fig. 5.4(b)], the general rule to write down the Grassmann tensor is to reverse the order of θ's and $\bar{\theta}$'s, and

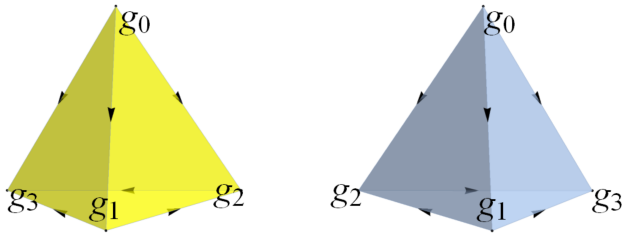

Figure 5.4: Two branched simplexes with opposite orientations. (Left) A simplex with positive orientation; (Right) A simplex with negative orientation.

then switch θ with $\bar{\theta}$ so that θ's are in front of $\bar{\theta}$'s. As an example, the Grassmann tensor after reversing the orientation of the above tetrahedron (0123) would be

$$\begin{aligned}\mathcal{V}_3^-(g_0,g_1,g_2,g_3) =& \nu_3^-(g_0,g_1,g_2,g_3)\theta_{012}^{n_2(g_0,g_1,g_2)} \\ & \theta_{023}^{n_2(g_0,g_2,g_3)}\bar{\theta}_{013}^{n_2(g_0,g_1,g_3)}\bar{\theta}_{123}^{n_2(g_1,g_2,g_3)},\end{aligned} \tag{5.20}$$

where $\nu_3^-(g_0,g_1,g_2,g_3) = (-1)^{m_1(g_1,g_3)}/\nu_3(g_0,g_1,g_2,g_3)$.

With each tetrahedron assigned with a Grassmann tensor defined above, we can write down the partition function in terms of fermionic path integral as

$$Z = \frac{1}{|G_b|}\sum_{g_*}\int_{\text{in}(\Sigma)}\prod_{(*ijk)}\mathcal{V}_3^{s_{ijk}}(g_*,g_i,g_j,g_k) \tag{5.21}$$

where $*$ is the vertex inside the manifold Σ and $(*ijk)$ is the 3-simplexes (tetrahedrons) in the triangulation of Σ. in(Σ) means inside Σ but not on the boundary M, i.e., $\int_{\text{in}(\Sigma)}$ is a shorthand notation for integral over all Grassmann variables inside Σ (up to a sign factor). Explicitly,

$$\int_{\text{in}(\Sigma)} = \int\prod_{[*ij]}d\theta_{*ij}^{n_2(g_*,g_i,g_j)}d\bar{\theta}_{*ij}^{n_2(g_*,g_i,g_j)}\prod_{\{*i\}}(-1)^{m_1(g_*,g_i)} \tag{5.22}$$

where the product $\prod_{\{*i\}}$ is over all the edges $\{*i\}$ connecting the inside vertex $*$ and vertices i on the boundary M. Similar to the bosonic case, the fixed-point ground

state for the fermionic SPT system is

$$
\begin{aligned}
&\Psi(\{g_i\},\{\theta_{ijk}\},\{\bar{\theta}_{ijk}\}) \\
=&\frac{1}{|G_b|}\sum_{g_*}\int_{\mathrm{in}(\Sigma)}\prod_{(*ijk)}\mathcal{V}_3^{s_{ijk}}(g_*,g_i,g_j,g_k) \\
=&\int\prod_{[*ij]}d\theta_{*ij}^{n_2(g_*,g_i,g_j)}d\bar{\theta}_{*ij}^{n_2(g_*,g_i,g_j)}\prod_{\bigtriangledown}\nu_3^{-1}(g_*,g_i,g_j,g_k)\prod_{\bigtriangleup}\nu_3(g_*,g_i,g_j,g_k) \\
&\prod_{\bigtriangledown}\theta_{*ij}^{n_2(g_*,g_i,g_j)}\theta_{*jk}^{n_2(g_*,g_j,g_k)}\bar{\theta}_{*ik}^{n_2(g_*,g_i,g_k)}\bar{\theta}_{ijk}^{n_2(g_i,g_j,g_k)} \\
&\prod_{\bigtriangleup}\theta_{ijk}^{n_2(g_i,g_j,g_k)}\theta_{*ik}^{n_2(g_*,g_i,g_k)}\bar{\theta}_{*jk}^{n_2(g_*,g_j,g_k)}\bar{\theta}_{*ij}^{n_2(g_*,g_i,g_j)}
\end{aligned}
\tag{5.23}
$$

where in the second line we omitted a sign factor [39] which does not influence the overlap calculation. $\prod_{[*ij]}$ is the product over all the edges on the triangulation of M, $\bigtriangleup$ represents positively oriented triangles and $\bigtriangledown$ represents negatively oriented triangles.

To write down the Hermitian conjugate of the ground-state wave function described above, we need to first understand its triangulation and configuration. Similar to the bosonic case, we could take the mirror image of the triangulation for the original system. Denote the mirror image of Σ as $\widetilde{\Sigma}$ and the point inside $\widetilde{\Sigma}$ as #. Then reverse the arrow between the point # and all of the vertices on $\widetilde{M}$ so that all arrows point to #. This new configuration has the same interpretation as time evolution of arbitrary initial state from $+\infty$ to 0. The resulting wave function corresponds to the

Hermitian conjugate of Ψ. Mathematically,

$$\begin{aligned}
&\Psi^\dagger(\{g_i\},\{\theta_{ijk}\},\{\bar{\theta}_{ijk}\}) \\
=&\int \prod_{[ij\#]} d\theta_{ij\#}^{n_2(g_i,g_j,g_\#)} d\bar{\theta}_{ij\#}^{n_2(g_i,g_j,g_\#)} \prod_{\triangle} \nu_3^{-1}(g_i,g_j,g_k,g_\#) \prod_{\triangledown} \nu_3(g_i,g_j,g_k,g_\#) \\
&\prod_{\triangle} \theta_{ij\#}^{n_2(g_i,g_j,g_\#)} \theta_{jk\#}^{n_2(g_j,g_k,g_\#)} \bar{\theta}_{ik\#}^{n_2(g_i,g_k,g_\#)} \bar{\theta}_{ijk}^{n_2(g_i,g_j,g_k)} \\
&\prod_{\triangledown} \theta_{ijk}^{n_2(g_i,g_j,g_k)} \theta_{ik\#}^{n_2(g_i,g_k,g_\#)} \bar{\theta}_{jk\#}^{n_2(g_j,g_k,g_\#)} \bar{\theta}_{ij\#}^{n_2(g_i,g_j,g_\#)}.
\end{aligned} \tag{5.24}$$

Here $\triangle, \triangledown$ represent negatively and positively oriented triangles in the mirror image $\widetilde{M}$ respectively, exactly opposite to the formula in the Ψ configuration.

5.4.2 Overlaps between Fermionic SPT Ground States

Calculating the overlap of Ψ and its Hermitian conjugate is equivalent to gluing the $(2+1)$-D complexes Σ and $\widetilde{\Sigma}$ over their common boundary M (or the mirror image $\widetilde{M}$)[39]. In general, the overlap of two ground states $|\Psi^{\mathrm{I}}\rangle, |\Psi^{\mathrm{II}}\rangle$ is defined as

$$\begin{aligned}
&\langle\Psi^{\mathrm{I}}|\Psi^{\mathrm{II}}\rangle = \mathrm{tr}\left(\Psi^{\mathrm{II}}(\Psi^{\mathrm{I}})^\dagger\right) \\
=&\frac{1}{|G_b|^{N+2}} \sum_{\{\text{all } g \text{ on } \Sigma\cup\widetilde{\Sigma}\}} \int_M \left(\int_{\mathrm{in}(\widetilde{\Sigma})} \prod_{[ijk]} (\mathcal{V}_3^{\mathrm{II}})^{s_{ijk}} \int_{\mathrm{in}(\Sigma)} \prod_{[ijk]} (\mathcal{V}_3^{\mathrm{I}})^{s_{ijk}} \right)
\end{aligned} \tag{5.25}$$

where N is the number of lattice sites on the manifold M, $|G_b|$ is the order of group G_b, and $M = \Sigma \cap \widetilde{\Sigma}$ is the common boundary of Σ and $\widetilde{\Sigma}$. In this equation, we follow the shorthand notation defined in Eq. (5.22).

Similar to the bosonic case, the overlap of Ψ with its Hermitian conjugate is a fermionic path integral over a closed manifold $\Sigma \cup \widetilde{\Sigma}$ and expected to be 1. Indeed, it was explicitly shown by Gu and Wen [39] that on any $(2+1)$-D closed manifold the

partition function reduces to

$$\int \mathcal{V}_3^+(g_0,g_1,g_2,g_3)\mathcal{V}_3^-(g_0,g_1,g_2,g_3)=1 \tag{5.26}$$

where $\int$ represents the integration over all Grassmann variables up to a sign factor. This result naturally leads to $\langle\Psi|\Psi\rangle = 1$, consistent with the normality of quantum states.

From the construction of Grassmann tensors we clearly see that the sign factors n_2's and m_1's only depend on the symmetry G_f and triangulation. The only factor encoding the topological theory is the cocycles ν_3. So if we have two different SPT phases defined on the same manifold M, the Grassmann integral part of the overlap $\langle\Psi^{\mathrm{I}}|\Psi^{\mathrm{II}}\rangle$ would be the same as calculating $\langle\Psi^{\mathrm{I}}|\Psi^{\mathrm{I}}\rangle$ or $\langle\Psi^{\mathrm{II}}|\Psi^{\mathrm{II}}\rangle$, and thus contributes 1 to the path integral. This was also pointed out by Gu and Wen [39]. They found that on the closed manifolds the integrals over Grassmann tensor give rise to complex numbers e^{-S}. So according to their results all the integrals over Grassmann numbers should also contribute 1, consistent with our analysis. After canceling out all the Grassmann numbers, the fermionic path integral $\langle\Psi^{\mathrm{I}}|\Psi^{\mathrm{II}}\rangle$ leads to the same bosonic path integral expression as in the Bosonic case [Eq. (5.12)]. Therefore the same argument leads to a WZW theory defined on the boundary M. So the amplitude of the overlap is again of the form

$$\ln\langle\Psi^{\mathrm{I}}|\Psi^{\mathrm{II}}\rangle = -\alpha N + \frac{\chi c}{12}\ln N + O(1). \tag{5.27}$$

5.5 Intrinsic Topological Orders

In this section, we use the famous FQH states to show that the term $\chi c/12\ln(N)$ still exists in the scaling of ground-state overlaps. Besides that, we also find a leading term decaying faster than exponential. This is quite surprising since traditional view

would expect exponential decay as leading term. In the following we will show the rigorous calculation.

5.5.1 FQH Wave Functions on Disks

FQH states have been well-known to exhibit intrinsic topological order [15]. Among these states, $1/m$ filling FQH states can be described by Laughlin wave functions [45], which are given on the disk as

$$\Psi_D^{\mathrm{II}} = \frac{1}{\sqrt{Z_d}} \prod_{i<j} (z_i - z_j)^m e^{-\sum_k \frac{|z_k|^2}{4}} \tag{5.28}$$

where Z_d is the normalization factor on the disk

$$Z_d = \int_0^R d^2 z_1 \cdots \int_0^R d^2 z_N e^{-\frac{1}{2}\sum_i |z_i|^2} \prod_{i<j} |z_i - z_j|^{2m}. \tag{5.29}$$

Due to rotational symmetry, the many-body angular momentum $J = mN(N-1)/2$ is a good quantum number and wave functions with different filling or particle number live in distinct Hilbert space. The meaningful overlaps should be calculated between Laughlin wave functions and topologically trivial wave functions with the same particle number, filling factor, and hence the same angular momentum (5.28). To find such a trivial wave function, we note that Laughlin wave functions can be expanded to a series of Slater determinants $\mathcal{D}_\lambda$ [154].

$$\begin{aligned} \Psi_D^{\mathrm{II}} &= \frac{1}{Z_d} \sum_\lambda a_\lambda \mathcal{D}_\lambda, \\ \mathcal{D}_\lambda &= \begin{vmatrix} z_1^{\lambda_1} & z_1^{\lambda_2} & \cdots & z_1^{\lambda_N} \\ z_2^{\lambda_1} & z_2^{\lambda_2} & \cdots & z_2^{\lambda_N} \\ \vdots & \vdots & \vdots & \vdots \\ z_N^{\lambda_1} & z_N^{\lambda_2} & \cdots & z_N^{\lambda_N} \end{vmatrix} \exp\left(-\sum_{i=1}^N \frac{|z_i|^2}{4} \right) \end{aligned} \tag{5.30}$$

where $\lambda = (\lambda_1, \lambda_2, \ldots, \lambda_N)$ is the partition of $J = mN(N-1)/2$. Each term $\mathcal{D}_\lambda$ in the expansion is a topologically trivial direct-product state with the same filling fraction and particle number as the original Laughlin wave function. And all of $\mathcal{D}_\lambda$'s constructed in this way are mutually orthogonal (see Appendix B.2). We choose the Slater determinant $\mathcal{D}_{\lambda^{(1)}}$ with $\lambda^{(1)} = (m(N-1), m(N-2), \ldots, 0)$ as the topologically trivial wave function since its coefficient $a_{\lambda^{(1)}} = 1$. So the normalized trivial wave function is

$$\begin{aligned} \Psi_D^{\mathrm{I}} =& \frac{1}{Z_d^{(1)}} \mathcal{D}_{\lambda^{(1)}}, \\ Z_d^{(1)} =& \int_0^R d^2 z_1 \cdots \int_0^R d^2 z_N e^{-\frac{1}{2}\sum_i |z_i|^2} \prod_{i<j} |z_i^m - z_j^m|^2. \end{aligned} \tag{5.31}$$

Then the overlap of Ψ_D^{I} and Ψ_D^{II} is

$$\langle \Psi_D^{\mathrm{I}} | \Psi_D^{\mathrm{II}} \rangle = \frac{\sum_\lambda a_\lambda \langle \mathcal{D}_{\lambda^{(1)}} | \mathcal{D}_\lambda \rangle}{\sqrt{Z_d^{(1)} Z_d}} = \sqrt{\frac{Z_d^{(1)}}{Z_d}} = \sqrt{\frac{A(N) Z_d^{(1)}}{Z_D}}. \tag{5.32}$$

where the denominator $Z_D = A(N) Z_d$ is the partition function of the one component plasma (OCP, see Appendix B.3). And the prefactor $A(N)$ (see Appendix B.3) comes from the ideal gas partition function, the background-background interaction and the constant part of particle-background interaction

$$A(N) = \frac{1}{N!} \left(\frac{\pi m M}{h^2} \right)^N L^{mN} e^{\frac{3mN^2}{4}} (2mN)^{-\frac{mN^2}{2}}. \tag{5.33}$$

where L is an arbitrary length scale, M is the mass of each charged particle and h is the Planck constant. Here we have also converted the disk radius R into the particle number N since the particle density is fixed at $n = N/(\pi R^2) \equiv 1/(2\pi m)$ in the plasma analogy [45].

The OCP can be considered as a critical system with central charge $c = -1$ [155–158]. So according to Eq. (5.5) the finite-size scaling of the partition function Z_D on

a disk is

$$\ln Z_D = -\alpha_D N - \beta_D \sqrt{N} - \frac{1}{12}\ln N + O(1) \tag{5.34}$$

where we used $\chi = 1$ for the disk. Following the method of Caillol [159], $Z_d^{(1)}$ in the numerator could be solved exactly by expanding the polynomial into a summation of monomials and then transforming the integral to polar coordinates. Integrating out the angular part of each coordinate we find that all terms with nonzero phases vanish.

$$\begin{aligned} Z_d^{(1)} =& (2\pi)^N N! \prod_{i=1}^{N} \int_0^R r_i dr_i \prod_{j=1}^{N} r_j^{m(j-1)} e^{-\frac{1}{2}\sum_k r_i^2} \\ =& (2\pi)^N 2^{\frac{m(N-1)N}{2}} \prod_{j=1}^{N} [m(j-1)]! N! Z_{\text{bdry}}^{(1)} \\ Z_{\text{bdry}}^{(1)} =& \prod_{i=1}^{N} \left(\frac{1}{[m(i-1)]!} \int_0^{mN} dx_i e^{-x_i} x_i^{m(i-1)} \right) \end{aligned} \tag{5.35}$$

where we made the coordinate transformation $x_i = r_i^2/2$. Those terms in $Z_{\text{bdry}}^{(1)}$ are close to 1 if i is small. So the only terms that contribute dramatically to $Z_{\text{bdry}}^{(1)}$ are those i's of order $\sqrt{N}$ or greater. Then the following asymptotic formula holds [160]

$$\begin{aligned} & \frac{1}{[m(i-1)]!} \int_0^{mN} dx_i e^{-x_i} x_i^{m(i-1)} \\ =& \frac{1}{2}\left[1 + \text{erf}\left(\frac{m(N-i+1)}{\sqrt{2mN}}\right)\right] + O\left(\frac{1}{\sqrt{N}}\right) \end{aligned} \tag{5.36}$$

where $\text{erf}(x) = \frac{2}{\sqrt{\pi}} \int_0^x e^{-t^2} dt$ is the error function. Replacing the summation over i by an integral over $y = m(N-i+1)/\sqrt{2mN}$, we find $\ln Z_{\text{bdry}}^{(1)}$ scales as $\sqrt{N}$

$$\ln Z_{\text{bdry}}^{(1)} = \sqrt{\frac{2N}{m}} \int_0^{\infty} dy \ln\left(\frac{1+\text{erf}(y)}{2}\right) + O(1). \tag{5.37}$$

The terms with factorials could be evaluated through converting the summations

into integrals using Euler-Maclaurin formula (see Appendix B.4). Putting every term together, the finite-size scaling for the overlap is

$$\ln \langle \Psi_D^{\mathrm{I}} | \Psi_D^{\mathrm{II}} \rangle = -aN \ln N - \alpha N - \beta \sqrt{N} + \gamma \ln N + O(1) \tag{5.38}$$

where $a = \frac{m-1}{4}, \alpha = \frac{1}{4}[(m-1)(\ln m - 1) + m \ln 2 - 3 \ln(2\pi) - 2 \ln(\frac{mM\pi}{h^2}) - 2\alpha_D], \beta = -\frac{1}{2}[\sqrt{\frac{2}{m}} \int_0^\infty dy \ln(\frac{1+\mathrm{erf}(y)}{2}) + \beta_D], \gamma = \frac{(m-1)^2}{24m}$.

5.5.2 FQH Wave Functions on 2-spheres

To show the effect of the topology, we also calculated the overlap on a sphere. Similar to the disk case, the N-particle Laughlin wave functions on the sphere can also be decomposed into Slater determinants $\mathcal{S}_\lambda$. And we choose the trivial wave function as the one with $\lambda^{(1)} = (m(N-1), m(N-2), \ldots, 0)$.

$$\begin{aligned}
\Psi_{S^2}^{\mathrm{II}} =& \frac{1}{Z_s} \prod_{i<j} (u_i v_j - u_j v_i)^m \\
=& \frac{1}{Z_s} \prod_{k=1}^{N} u_k^{m(N-1)} \prod_{i<j} \left(\frac{v_j}{u_j} - \frac{v_i}{u_i} \right)^m = \frac{1}{Z_s} \sum_\lambda b_\lambda \mathcal{S}_\lambda, \\
\Psi_{S^2}^{\mathrm{I}} =& \frac{1}{Z_s^{(1)}} \mathcal{S}_{\lambda^{(1)}} = \frac{1}{Z_s^{(1)}} \prod_{k=1}^{N} u_k^{m(N-1)} \prod_{i<j} \left[\left(\frac{v_j}{u_j} \right)^m - \left(\frac{v_i}{u_i} \right)^m \right],
\end{aligned} \tag{5.39}$$

where $u_i = \cos\left(\frac{\theta_i}{2}\right) e^{i\phi_i/2}, v_i = \sin\left(\frac{\theta_i}{2}\right) e^{-i\phi_i/2}$ are the spinor coordinates. And the normalization factors are

$$\begin{aligned}
Z_s =& \int d\Omega_1 \cdots d\Omega_N \prod_k |u_k|^{2m(N-1)} \prod_{i<j} \left| \frac{v_j}{u_j} - \frac{v_i}{u_i} \right|^{2m}, \\
Z_s^{(1)} =& \int d\Omega_1 \cdots d\Omega_N \prod_k |u_k|^{2m(N-1)} \\
& \prod_{i<j} \left| \left(\frac{v_j}{u_j} \right)^m - \left(\frac{v_i}{u_i} \right)^m \right|^2.
\end{aligned} \tag{5.40}$$

The same argument as in the disk case shows

$$\begin{aligned}\langle\Psi^{\mathrm{I}}_{S^2}|\Psi^{\mathrm{II}}_{S^2}\rangle =&\sqrt{\frac{Z_s^{(1)}}{Z_s}} = \sqrt{\frac{B(N)Z_s^{(1)}}{Z_{S^2}}},\\ Z_{S^2} =&B(N)Z_s,\\ B(N) =& \frac{1}{N!}\left(\frac{mM\pi}{h^2}\right)^N \left(\frac{L}{2}\right)^{mN} \left(\frac{mN}{2}\right)^{\frac{(2-m)N}{2}} e^{mN^2/2}\end{aligned} \tag{5.41}$$

where $B(N)$ (see Appendix B.5) comes from the partition function of N-particle ideal gas, background-background interaction, the constant part of particle-background interaction and the radius dependence of the integral in the partition function of the OCP.

As in the disk case, the denominator Z_{S^2} is the partition function of the OCP on a sphere and scales as

$$\ln Z_{S^2} = -\alpha_{S^2} N - \frac{1}{6}\ln N + O(1) \tag{5.42}$$

where we used $\chi = 2$ for spheres. And the $\sqrt{N}$ term vanishes because spheres do not have boundaries.

To evaluate $Z_s^{(1)}$ in the numerator, we follow Alastuey and Jancovici [161] to change variables $r_i = \tan\left(\frac{\theta_i}{2}\right)$ or $\sin\theta_i d\theta_i = \frac{4r_i dr_i}{(1+r_i^2)^2}$. Then the integral is over the plane (with no boundaries) defined by the polar coordinates (r_i, ϕ_i). Again, the only terms contributing to the integral are those terms with vanishing polar angles.

$$\begin{aligned}Z_s^{(1)} =&N!(2\pi)^N \prod_i \int \frac{4r_i^{2m(i-1)+1} dr_i}{(1+r_i^2)^{m(N-1)+2}}\\ =&N!(4\pi)^N \prod_i \frac{[m(i-1)]![m(N-i)]!}{[m(N-1)+1]!}\end{aligned} \tag{5.43}$$

Taking the logarithm of both sides and then using Euler-Maclaurin formula to convert the summation to integral (see Appendix B.6), we find the scaling of the overlap to

be

$$\ln \langle \Psi^{\mathrm{I}}_{S^2} | \Psi^{\mathrm{II}}_{S^2} \rangle = -aN \ln N - \alpha N + \gamma \ln N + O(1) \tag{5.44}$$

where $a = \frac{m-1}{4}, \alpha = \frac{1}{4}[(m-1)[\ln(2m) - 2] - 2m \ln L - 2 \ln(\frac{mM\pi}{h^2}) - 2\alpha_{S^2}], \gamma = \frac{(m-1)^2}{12m}$ and the boundary term $\sqrt{N}$ vanishes explicitly.

Comparing the results for disks and spheres, we find that the leading order coefficients for both cases are the same $a = (m-1)/4$. Such a term indicates a faster decay than typical Anderson orthogonality catastrophe. The coefficient of $\ln N$ is proportional to the Euler characteristic of the manifold where the system is defined. This term stems from the critical behavior of the classical OCP and thus is consistent with our physical intuition pictured in the introduction section.

5.6 Conclusion

In this chapter, we calculated the finite-size scaling of overlaps of topologically different states through mapping the overlaps to partition functions of critical systems. For generic $(2+1)$-D topologically different states, including both SPT states and intrinsic topological states, the fixed-point ground-state overlaps exhibit a universal sub-leading term $\frac{\chi c}{12} \ln N$ depending on the topology of the manifold on which the system lives. Such a universal topological response term relies on the gapless edge state on the interface of different topological systems, as described in Fig. 5.1. In $(2+1)$-D, SPT systems are known to have gapless edge modes described by some CFT. So we conclude that the topological response term always exists for $(2+1)$-D SPT systems at fixed-points.

In the case of intrinsic topological order, we calculate the overlaps between the famous Laughlin states and corresponding product states. We find that the same topological response term still exists and it is also related to a critical system, i.e., OCP system. In this overlap calculation, we also notice a leading-order scaling $-\frac{m-1}{4} N \ln N$

which decays faster than the expected exponential in typical Anderson orthogonality catastrophe. Its coefficient only depends on which Laughlin state participates in the overlap calculation. Such a behavior may be used as a signature for topological phase transitions between topologically ordered FQH states and trivial states.

CHAPTER VI

Conclusion and outlook

6.1 Conclusions

Landau theory of phase transition is quite successful and generic for many systems. But since the appearance of KT transition and quantum Hall effect, this paradigm is challenged. After decades' efforts of many experts, it has become clear that Landau paradigm accounts only symmetry part of physics. One more pillar for modern condensed matter physics is found to be topology.

In this thesis, I proposed a PDW system using Landau theory which could potentially be realized in experiments. There an infinite order KT transition appears and we are naturally led to the field of topology. Then I developed the overlap technique to investigate topological phase transitions. For generic topological band insulators, a theorem is formulated to make the connection among adiabatic continuity, ground-state overlaps and topological phase transitions. Based on the same technique, I explored generic fixed-point SPT systems and Laughlin states in $(2+1)$-D. There a generic topological response term related to certain CFT is discovered. For the overlaps between Laughlin wave functions and trivial product states, I also find a leading term decaying faster than exponential. These finite-size scaling behaviors could potentially become a signature for distinguishing different topological systems.

6.2 Outlook

There are several most accessible open questions that I would like to point out. These could serve as a guide for future directions.

SPT systems in $(2+1)$-D are shown to have gapless edge modes [18, 39]. More specifically, if the system is at its fixed point, the edge modes are described by some CFT. In the overlap calculation of Chapter V, the topological response term $\chi c/12$ exists for such systems. The central charge c indicates that there is another CFT associated with the two systems in the *time-direction* interface (see Fig. 5.1). And this CFT oftentimes appears to be non-unitary. It has been clear to us that this CFT from the overlap calculation is different from the CFT on the space-direction interface between the two systems. But it seems to appear when gapless edge modes exist on the space-direction interface of the two systems. We *conjecture* that the two CFT's are related in some way. Maybe the Wick rotation of a CFT in the time direction interface becomes the CFT on the interface of space direction.

Our calculation also assumes the SPT systems are at their fixed pints. Only in this way could we write down the exact wave functions. And such a constraint also guarantees that the gapless edge modes are described by some CFT. Our *conjecture* is that the topological response term still exists even if the SPT systems are not at fixed points. To verify this point, we need to understand how to write down the wave function (theoretically or numerically), and then prove that gapless edge modes are always described by some CFT.

In higher dimensions, the boundaries of SPT systems may also be gapped by symmetry breaking or due to intrinsic surface topological order [162–166]. In such systems, the overlap can not have $\ln N$ correction. But there might be other universal terms such as a constant term similar to the topological entanglement entropy [167, 168].

My calculation for the overlaps between Laughlin states and product state has

confirmed the existence of topological response term in intrinsic topological systems. we may *conjecture* that the topological response term persists for any intrinsic topological systems with gapless edge modes. But there is still another question. There would typically be ground state degeneracy in systems with intrinsic topological order. How should we construct the overlap between ground states?

We will leave these open questions as future work.

APPENDICES

APPENDIX A

Adiabatic continuity, wave-function overlap and topological phase transitions

A.1 Insulators with more than one valence bands

In this section, we present proofs for conclusions discussed in Sec. 3.2.2.

A.1.1 anticommutators for the c and d operators

We first prove the Eqs. (3.28) and (3.29). In general, creation operators $c_n^\dagger$ and $d_m^\dagger$ are connected by the following unitary transformation and the inverse tranformation is

$$d_{m,\boldsymbol{k}}^\dagger = \sum_{n=1}^{+\infty} \langle 0|c_{n,\boldsymbol{k}} d_{m,\boldsymbol{k}}^\dagger|0\rangle \, c_{n,\boldsymbol{k}}^\dagger \tag{A.1}$$

$$c_{n,\boldsymbol{k}}^\dagger = \sum_{m=1}^{+\infty} \langle 0|d_{m,\boldsymbol{k}} c_{n,\boldsymbol{k}}^\dagger|0\rangle \, d_{m,\boldsymbol{k}}^\dagger \tag{A.2}$$

We emphasize that in these two equatinos, the band indices n and m are summed over all bands (conduction and valence). Utilizing Eq. (A.1), it is straighforward to

verify that

$$\{c_{n,\boldsymbol{k}}, d^{\dagger}_{m,\boldsymbol{k}'}\} = \sum_{n'=1}^{+\infty} \langle 0|c_{n',\boldsymbol{k}'} d^{\dagger}_{m,\boldsymbol{k}'}|0\rangle \{c_{n,\boldsymbol{k}}, c^{\dagger}_{n',\boldsymbol{k}'}\}$$
$$= \sum_{n'=1}^{+\infty} \mathcal{F}_{n',m}\delta_{n,n'}\delta_{\boldsymbol{k},\boldsymbol{k}'} = \mathcal{F}_{n,m}\delta_{\boldsymbol{k},\boldsymbol{k}'} \tag{A.3}$$

Similarily, using Eq. (A.2), we have

$$\{d_{m,\boldsymbol{k}}, c^{\dagger}_{n,\boldsymbol{k}'}\} = \sum_{m'=1}^{+\infty} \langle 0|d_{m',\boldsymbol{k}'} c^{\dagger}_{n,\boldsymbol{k}'}|0\rangle \{d_{m,\boldsymbol{k}}, d^{\dagger}_{m',\boldsymbol{k}'}\}$$
$$= \sum_{m'=1}^{+\infty} \mathcal{F}^{*}_{nm'}\delta_{m,m'}\delta_{\boldsymbol{k},\boldsymbol{k}'} = \mathcal{F}^{*}_{n,m}\delta_{\boldsymbol{k},\boldsymbol{k}'} \tag{A.4}$$

A.1.2 the $\mathcal{F}$ and $\mathcal{U}$ matrices

In this section, we prove some properties for the $\mathcal{F}$ and $\mathcal{U}$ matrices.

A.1.2.1 the existence of the $\mathcal{U}$ matrix

First, we prove the existence of the $\mathcal{U}$ matrix. In the main text, we assumed that $\mathcal{U}$ is a unitary matrix, which diagonalizes the matrix $\mathcal{F}\mathcal{F}^{\dagger}$, i.e. $\mathcal{U}\mathcal{F}\mathcal{F}^{\dagger}\mathcal{U}^{\dagger}$ is a diagonal matrix. To prove that such a $\mathcal{U}$ indeed exists, we just need to show that $\mathcal{F}\mathcal{F}^{\dagger}$ is a hermitian matrix, because we know that any hermitian matrices can be diagonlized by some unitary matrices. Here, we compute directly the hermitian conjugate of $\mathcal{F}\mathcal{F}^{\dagger}$,

$$(\mathcal{F}\mathcal{F}^{\dagger})^{\dagger} = (\mathcal{F}^{\dagger})^{\dagger}\mathcal{F}^{\dagger} = \mathcal{F}\mathcal{F}^{\dagger} \tag{A.5}$$

which indeed recovers itself, i.e. it is a hermitian matrix. As a result, there must exist some unitary matrix $\mathcal{U}$, such that

$$\mathcal{U}_{l,n}\mathcal{F}_{n,m}\mathcal{F}^*_{n',m}\mathcal{U}^*_{l',n'} = \lambda_l \delta_{l,l'} \tag{A.6}$$

where λl are the eigenvalues of the matrix $\mathcal{F}\mathcal{F}^\dagger$.

A.1.2.2 $\lambda_l > 0$

Now, we will prove that the eigenvalues λ_l are positive, as long as $\det \mathcal{F} \neq 0$, which will be used later in Sec A.1.4 when we prove that the normalizaiton factor is singularity free. We first prove that $\mathcal{F}\mathcal{F}^\dagger$ is semi-postive definite (i.e. all eigenvalues are non-negative), regardless of the value of $\det \mathcal{F}$. Then, we will further prove that if $\det \mathcal{F} \neq 0$, the matrix $\mathcal{F}\mathcal{F}^\dagger$ is positive-definite (i.e. all eigenvalues are are positive).

Assuming that $\boldsymbol{w}$ is an arbitrary row vector composed by N complex numbers, and $\boldsymbol{w}^\dagger$ is the conjugate (column) vector composed by its complex conjugates.

$$\boldsymbol{w}\mathcal{F}\mathcal{F}^\dagger\boldsymbol{w}^\dagger = \boldsymbol{w}\mathcal{F}(\boldsymbol{w}\mathcal{F})^\dagger \geq 0 \tag{A.7}$$

Because this result holds for any $\boldsymbol{w}$, $\mathcal{F}\mathcal{F}^\dagger$ is semi-postive defiinte, and thus its eigenvalues are non-negative.

If $\det \mathcal{F} \neq 0$, $\det(\mathcal{F}\mathcal{F}^\dagger) = |\det \mathcal{F}|^2 \neq 0$. Because the determinant of a hermitian matrix equals to the product of all eigenvalues, this implies that none of the eigenvalues of the matrix $\mathcal{F}\mathcal{F}^\dagger$ is zero. Thus, this matrix is positive definite and all eigenvalues are positive.

A.1.2.3 $\frac{\mathcal{F}^*_{n,m}\mathcal{U}^*_{l,n}\mathcal{U}_{l,n'}\mathcal{F}_{n',m'}}{\mathcal{N}_l^2} = \delta_{m,m'}$

Now we prove that at $\alpha = 1$, $\frac{\mathcal{F}^*_{n,m}\mathcal{U}^*_{l,n}\mathcal{U}_{l,n'}\mathcal{F}_{n',m'}}{\mathcal{N}_l^2} = \delta_{m,m'}$, which was utilzed to simplify Eq. (3.37) in the main text. First, we rewrite Eq. (A.6) in a matrix form

$$\mathcal{U}\mathcal{F}\mathcal{F}^\dagger\mathcal{U}^\dagger = \mathcal{D} \tag{A.8}$$

where $\mathcal{D}$ is a diagonal matrix

$$\mathcal{D}_{l,l'} = \lambda_l \delta_{l,l'} \tag{A.9}$$

where λ_l's are the l-th eigenvalue of the $\mathcal{F}\mathcal{F}^\dagger$ matrix. We compute the matrix inverse for both sides of Eq. A.8. Because $\mathcal{U}$ is a unitary matrix, $\mathcal{U}^{-1} = \mathcal{U}^\dagger$ and thus

$$\mathcal{U}(\mathcal{F}^\dagger)^{-1}\mathcal{F}^{-1}\mathcal{U}^\dagger = \mathcal{D}^{-1} \tag{A.10}$$

And thus

$$\mathcal{F}^\dagger\mathcal{U}^\dagger[\mathcal{U}(\mathcal{F}^\dagger)^{-1}\mathcal{F}^{-1}\mathcal{U}^\dagger]\mathcal{U}\mathcal{F} = \mathcal{F}^\dagger\mathcal{U}^\dagger\mathcal{D}^{-1}\mathcal{U}\mathcal{F} \tag{A.11}$$

If we simplify this equation, we find that

$$\mathcal{I} = \mathcal{F}^\dagger\mathcal{U}^\dagger\mathcal{D}^{-1}\mathcal{U}\mathcal{F} \tag{A.12}$$

where $\mathcal{I}$ is the identity matrix. If we write down the components for these matrices, we get

$$\delta_{m,m'} = \mathcal{F}^*_{n,m}\mathcal{U}^*_{l,n}\mathcal{D}^{-1}_{l,l'}\mathcal{U}_{l',n'}\mathcal{F}_{n',m'} \tag{A.13}$$

Utilzing Eq. (A.9), it is easy to realize that the inverse of the diangonal matrix $\mathcal{D}$ is

$$\mathcal{D}^{-1}_{l,l'} = \lambda_l^{-1}\delta_{l,l'} \tag{A.14}$$

As shown in Eq. (A.19), at $\alpha = 1$, $\lambda_l^{-1} = 1/\mathcal{N}_l^2$, and thus we have

$$\delta_{m,m'} = \mathcal{F}^*_{n,m}\mathcal{U}^*_{l,n}\frac{\delta_{l,l'}}{\mathcal{N}_l^2}\mathcal{U}_{l',n'}\mathcal{F}_{n',m'} = \frac{\mathcal{F}^*_{n,m}\mathcal{U}^*_{l,n}\mathcal{U}_{l,n'}\mathcal{F}_{n',m'}}{\mathcal{N}_l^2}. \tag{A.15}$$

A.1.3 anticommutators

Now, we compute the anticommutators for a and $a^\dagger$,

$$\begin{aligned}
\{a_{l,\boldsymbol{k}}, a^\dagger_{l',\boldsymbol{k}'}\} =& \frac{(1-\alpha)^2}{|\mathcal{N}_l|^2}\mathcal{U}_{l,n}\mathcal{U}^*_{l',n'}\{c_{n,\boldsymbol{k}}, c^\dagger_{n',\boldsymbol{k}'}\} + \frac{(1-\alpha)\alpha}{|\mathcal{N}_l|^2}\mathcal{U}_{l,n}\mathcal{U}^*_{l',n'}\mathcal{F}^*_{n',m'}\{c_{n,\boldsymbol{k}}, d^\dagger_{m',\boldsymbol{k}'}\} \\
&+ \frac{(1-\alpha)\alpha}{|\mathcal{N}_l|^2}\mathcal{U}_{l,n}\mathcal{F}_{n,m}\mathcal{U}^*_{l',n'}\{d_{m,\boldsymbol{k}}, c^\dagger_{n',\boldsymbol{k}'}\} \\
&+ \frac{\alpha^2}{|\mathcal{N}_l|^2}\mathcal{U}_{l,n}\mathcal{F}_{n,m}\mathcal{U}^*_{l',n'}\mathcal{F}^*_{n',m'}\{d_{m,\boldsymbol{k}}, d^\dagger_{m',\boldsymbol{k}'}\}
\end{aligned} \tag{A.16}$$

$$\begin{aligned}
=& \frac{(1-\alpha)^2}{|\mathcal{N}_l|^2}\mathcal{U}_{l,n}\mathcal{U}^*_{l',n'}\delta_{n,n'}\delta_{\boldsymbol{k},\boldsymbol{k}'} + \frac{(1-\alpha)\alpha}{|\mathcal{N}_l|^2}\mathcal{U}_{l,n}\mathcal{U}^*_{l',n'}\mathcal{F}^*_{n',m'}\mathcal{F}_{n,m'}\delta_{\boldsymbol{k},\boldsymbol{k}'} \\
&+ \frac{(1-\alpha)\alpha}{|\mathcal{N}_l|^2}\mathcal{U}_{l,n}\mathcal{F}_{n,m}\mathcal{U}^*_{l',n'}\mathcal{F}^*_{n',m}\delta_{\boldsymbol{k},\boldsymbol{k}'} + \frac{\alpha^2}{|\mathcal{N}_l|^2}\mathcal{U}_{l,n}\mathcal{F}_{n,m}\mathcal{U}^*_{l',n'}\mathcal{F}^*_{n',m'}\delta_{m,m'}\delta_{\boldsymbol{k},\boldsymbol{k}'} \\
=& \frac{(1-\alpha)^2}{|\mathcal{N}_l|^2}\mathcal{U}_{l,n}\mathcal{U}^*_{l',n}\delta_{\boldsymbol{k},\boldsymbol{k}'} + \frac{\alpha(2-\alpha)}{|\mathcal{N}_l|^2}\mathcal{U}_{l,n}\mathcal{F}_{n,m}\mathcal{F}^*_{n',m}\mathcal{U}^*_{l',n'}\delta_{\boldsymbol{k},\boldsymbol{k}'}
\end{aligned} \tag{A.17}$$

Because $\mathcal{U}$ is a unitary matrix, $\mathcal{U}_{l,n}\mathcal{U}^*_{l',n} = \delta_{l,l'}$. For the second term, we have proved in Eq. (A.6) that $\mathcal{U}_{l,n}\mathcal{F}_{n,m}\mathcal{F}^*_{n',m}\mathcal{U}^*_{l',n'} = \lambda_l\delta_{l,l'}$, where λ_l is the lth eigenvalue of the matrix $\mathcal{F}\mathcal{F}^\dagger$. As a result,

$$\{a_{l,\boldsymbol{k}}, a^\dagger_{l',\boldsymbol{k}'}\} = \frac{(1-\alpha)^2 + \alpha(2-\alpha)\lambda_l}{|\mathcal{N}_l|^2}\delta_{l,l'}\delta_{\boldsymbol{k},\boldsymbol{k}'} \tag{A.18}$$

If we set the nomralizaiton factor

$$\mathcal{N}_l = \sqrt{(1-\alpha)^2 + \alpha(2-\alpha)\lambda_l} \tag{A.19}$$

the canonical anticommutation relation is proved

$$\{a_{l,\boldsymbol{k}}, a^\dagger_{l',\boldsymbol{k}'}\} = \delta_{l,l'}\delta_{\boldsymbol{k},\boldsymbol{k}'}. \tag{A.20}$$

A.1.4 singularity free normalization factor

In this section, we prove that the normalization factor defined in Eq. (A.19) is free of singularity.

As shown in Eq. (A.18), the key purpose of introducing the normalization factor is to set the prefactor in front of the Kronecker deltas to unity, i.e.

$$\frac{(1-\alpha)^2 + \alpha(2-\alpha)\lambda_l}{|\mathcal{N}_l|^2} = 1 \tag{A.21}$$

To achieve such an objective without singularity, it is important to show that the numerator $(1-\alpha)^2 + \alpha(2-\alpha)\lambda_l$ never reaches zero.

In Sec. A.1.2, we have proved that as long as the overlap function is nonzero, λ_l is postive. For a positive λ_l and $0 \leq \alpha \leq 1$, it is easy to verify that $(1-\alpha)^2+\alpha(2-\alpha)\lambda_l > 0$. Thus the normalization condition is singularity free.

A.2 Symmetry of the adiabatic path

In this section, we prove that for two quantum states with finite wave function overlap, the adiabatic path defined in the main text preserves all the symmetries of the two quantum states.

A.2.1 interacting systems

We start by examining the symmetry of the adiabatic path defined in Eq. (3.44). Here, we consider unitary symmetries, but all the conclusions can be easily generalized to antiunitary symmetries. In quantum mechanics, a symmetry of a quantum state implies that the wave function must remain invariant under certain transformation (e.g. translation, space inversion, etc) up to some possible $U(1)$ phase factor

$$|\psi\rangle \to e^{i\varphi} |\psi\rangle \tag{A.22}$$

$$|\psi'\rangle \to e^{i\varphi'} |\psi'\rangle \tag{A.23}$$

If these relations hold for $|\psi\rangle$ and $|\psi'\rangle$, it is straightforward to prove that under the same transformation, the wave function defined in Eq. (3.42) transforms as

$$|\Psi(\alpha)\rangle \to e^{i\varphi} |\Psi(\alpha)\rangle \tag{A.24}$$

the same as the state $|\psi\rangle$. The corresponding bra vector transforms as

$$\langle\Psi(\alpha)| \to e^{-i\varphi} \langle\Psi(\alpha)| \tag{A.25}$$

where the complex phase takes the opposite sign. As a result, the Hamiltonian defined in Eq. (3.44) is invariant under this transformation, because the phase factors from the bra and ket vectors cancel each other, i.e. the Hamiltonian preserves this symmetry.

A.2.2 band insulators with one valence band

Now we consider band insulators with one valence band, i.e. the Hamiltonian Eq. (3.12). Again, we consider unitary symmetries, but all the conclusions can be easily generalized to antiunitary symmetries. Assume that insulators I and II preserve some symmetry.

Under the symmetry transformation, we assume that the momentum points is transformed as

$$\boldsymbol{k} \to \boldsymbol{k}'. \tag{A.26}$$

and the Bloch waves transform according to certain unitary matrices. Because the insulator is invariant under the transformation, this unitary matrix will *not* mix conduction and valence bands. Since we have only a single valence band, the Bloch waves of the valence band can only change by a phase shift under this symmetry transformation

$$|\psi^{\mathrm{I}}(\boldsymbol{k})\rangle \to e^{i\varphi(\boldsymbol{k})}\,|\psi^{\mathrm{I}}(\boldsymbol{k})\rangle \tag{A.27}$$

Because the insulator is invariant under this transformation, we know that $e^{i\varphi(\boldsymbol{k})}\,|\psi^{\mathrm{I}}(\boldsymbol{k})\rangle$ must be identical to the Bloch wave of the valence band at $\boldsymbol{k'}$

$$|\psi^{\mathrm{I}}(\boldsymbol{k})\rangle \to |\psi^{\mathrm{I}}(\boldsymbol{k'})\rangle = e^{i\varphi(\boldsymbol{k})}\,|\psi^{\mathrm{I}}(\boldsymbol{k})\rangle \tag{A.28}$$

For insulator II, the wave function satisfies the same relation, but the phase factor could be different

$$|\psi^{\mathrm{II}}(\boldsymbol{k})\rangle \to |\psi^{\mathrm{II}}(\boldsymbol{k'})\rangle = e^{i\varphi'(\boldsymbol{k})}\,|\psi^{\mathrm{II}}(\boldsymbol{k})\rangle\,. \tag{A.29}$$

As a result, the overlap function must satisfy

$$\phi(\boldsymbol{k'}) = e^{i(\varphi'-\varphi)}\phi(\boldsymbol{k}) \tag{A.30}$$

It is easy to verify that for the Bloch state $|\Psi(\boldsymbol{k},\alpha)\rangle$ defined in Eq. (3.8), we have

$$|\Psi(\boldsymbol{k},\alpha)\rangle \to |\Psi(\boldsymbol{k}',\alpha)\rangle = e^{i\varphi(\boldsymbol{k})}\,|\Psi(\boldsymbol{k},\alpha)\rangle \tag{A.31}$$

the same as $|\psi^{\mathrm{I}}\rangle$. And thus the Hamiltonian that we defined for the adiabatic path [Eq. (3.12)] remains invariant, i.e., it preserves the symmetry

$$H(\alpha) \to H(\alpha) \tag{A.32}$$

A.2.3 band insulators with more than one valence bands

In this section, we consider more generic band insulators with multiple valence bands. Assume that insulators I and II preserve some unitary symmetry and under the symmetry transformation the momentum points transform as

$$\boldsymbol{k} \to \boldsymbol{k}'. \tag{A.33}$$

Because insulator I preserves the symmetry, under the symmetry transformation, Bloch waves of the valence bands must satisfy,

$$|\psi^{\mathrm{I}}_n(\boldsymbol{k})\rangle \to |\psi^{\mathrm{I}}_n(\boldsymbol{k}')\rangle = \mathcal{U}^{\mathrm{I}}_{n,n'}(\boldsymbol{k})\,|\psi^{\mathrm{I}}_{n'}(\boldsymbol{k})\rangle \tag{A.34}$$

where $\mathcal{U}^{\mathrm{I}}(\boldsymbol{k})$ is some unitary matrix that describe the transformation of the Bloch waves under the symmetry transformation. For insulator II, if the same symmetry is preserved, the wave function is transformed in a similar way, but the unitary matrix could be different

$$|\psi^{\mathrm{II}}_m(\boldsymbol{k})\rangle \to |\psi^{\mathrm{II}}_m(\boldsymbol{k}')\rangle = \mathcal{U}^{\mathrm{II}}_{m,m'}(\boldsymbol{k})\,|\psi^{\mathrm{II}}_{m'}(\boldsymbol{k})\rangle \tag{A.35}$$

As a result, the overlap matrix $\mathcal{F}_{n,m} = \langle \psi_n^{\mathrm{I}} | \psi_m^{\mathrm{II}} \rangle$ satisfies

$$\mathcal{F}_{\boldsymbol{k}'} = (\mathcal{U}_{\boldsymbol{k}}^{\mathrm{I}})^* \mathcal{F}_{\boldsymbol{k}} (\mathcal{U}_{\boldsymbol{k}}^{\mathrm{II}})^T \tag{A.36}$$

where $*$ and T stands for complex conjugate and transpose respectively. Here, we write the momentum as a subindex to simplify the formula (same below).

As a result, we know that

$$\mathcal{F}_{\boldsymbol{k}'} \mathcal{F}_{\boldsymbol{k}'}^\dagger = (\mathcal{U}_{\boldsymbol{k}}^{\mathrm{I}})^* \mathcal{F}_{\boldsymbol{k}} \mathcal{F}_{\boldsymbol{k}}^\dagger (\mathcal{U}_{\boldsymbol{k}}^{\mathrm{I}})^T \tag{A.37}$$

In the main text, we defined a $\mathcal{U}$ matrix at each momentum point to diagonalize the $\mathcal{F}\mathcal{F}^\dagger$ matrix. The relation above implies that

$$\mathcal{U}_{\boldsymbol{k}'} = \mathcal{U}_{\boldsymbol{k}} (\mathcal{U}_{\boldsymbol{k}}^{\mathrm{I}})^T \tag{A.38}$$

up to some unimportant gauge choice.

Utilizing Eqs. (A.36) and (A.38), we can verify easily that for the valence-band Bloch states defined in Eq (3.23), $|\Psi(\boldsymbol{k}, \alpha)\rangle = |\Psi(\boldsymbol{k}', \alpha)\rangle$ up to a gauge choice. Thus, the insulator that we defined as the adiabatic path preserves the correct symmetry.

APPENDIX B

Finite-size scaling of ground-state overlaps beyond Anderson orthogonality catastrophe

B.1 Central charge of the critical $O(n)$-loop model

The partition function of the $O(n)$-loop model on the honeycomb lattice is

$$Z_{O(n)} = \sum_{\text{DW config.}} x^L n^l \tag{B.1}$$

for general values of x and $n \in [-2, 2]$. The critical line of this model is $x_c = \left[2 + (2-n)^{1/2}\right]^{-1/2}$ [169]. For $x > x_c$ which contains the point $x = 1, n = -1$, this loop model is also critical [151]. And the central charges of both cases are given by [151, 152]

$$c = 1 - \frac{6(g-1)^2}{g} \tag{B.2}$$

where g is defined by $n = -2\cos(\pi g)$. The branches $g \in [0, 1]$ and $g \in [1, 2]$ correspond to $x > x_c$ and $x = x_c$ systems respectively. The central charge for $x = 1, n = -1$ is found through Eq. (B.2) by setting $g = 1/3$, which leads to $c = -7$ (numerically verified in Blöte et al [153]).

Actually, the denominator $\mathcal{N}/2$ of the overlap (5.16) of the main text can also be considered trivially as a critical $O(n)$-loop model at $x = 1, n = 1$. Then the same formula gives $c = 0$, implying no logarithmic term correction in the "free energy". This is consistent with $\mathcal{N}/2 = 2^{N-1}$ we got from direct counting.

B.2 Slater determinants from Laughlin wave-function expansion are mutually orthogonal

A typical Slater determinant in the expansion of Laughlin wave functions is as follows,

$$\begin{aligned}\mathcal{D}_\lambda &= \begin{vmatrix} z_1^{\lambda_1} & z_1^{\lambda_2} & \cdots & z_1^{\lambda_N} \\ z_2^{\lambda_1} & z_2^{\lambda_2} & \cdots & z_2^{\lambda_N} \\ \vdots & \vdots & \vdots & \vdots \\ z_N^{\lambda_1} & z_N^{\lambda_2} & \cdots & z_N^{\lambda_N} \end{vmatrix} \exp\left(-\sum_{i=1}^{N} \frac{|z_i|^2}{4}\right) \\ &= \sum_{\sigma \in S^N} \mathrm{sgn}(\sigma) z_1^{\sigma(\lambda_1)} z_2^{\sigma(\lambda_2)} \cdots z_N^{\sigma(\lambda_N)} e^{-\frac{1}{4}\sum_i r_i^2}\end{aligned} \tag{B.3}$$

where $\lambda = (\lambda_1, \lambda_2, \ldots, \lambda_N)$ is a partition of $J = mN(N-1)/2$. Another partition $\mu \neq \lambda$ corresponds to a different Slater determinant in the expansion. Their inner product is given by

$$
\begin{aligned}
&\int \prod_{i=1}^{N} dz_i \mathcal{D}_{\lambda}^{(1)} D_{\mu} \\
&= \int \prod_{i=1}^{N} dz_i \left[\sum_{\sigma_\lambda \in S^N} \mathrm{sgn}(\sigma_\lambda) (z_1^*)^{\sigma_\lambda(\lambda_1)} (z_2^*)^{\sigma_\lambda(\lambda_2)} \cdots (z_N^*)^{\sigma_\lambda(\lambda_N)} e^{-\frac{1}{4}\sum_i r_i^2} \right] \\
&\quad \left[\sum_{\sigma_\mu \in S^N} \mathrm{sgn}(\sigma_\mu) z_1^{\sigma_\mu(\mu_1)} z_2^{\sigma_\mu(\mu_2)} \cdots z_N^{\sigma_\mu(\mu_N)} e^{-\frac{1}{4}\sum_i r_i^2} \right] \\
&= \int \prod_{i=1}^{N} (r_i dr_i d\phi_i) \, \mathrm{sgn}(\sigma_\lambda \sigma_\mu) r_1^{\sigma_\lambda(\lambda_1)+\sigma_\mu(\mu_1)} r_2^{\sigma_\lambda(\lambda_2)+\sigma_\mu(\mu_2)} \cdots r_N^{\sigma_\lambda(\lambda_N)+\sigma_\mu(\mu_N)} \\
&\quad e^{i(\sigma_\mu(\mu_1)-\sigma_\lambda(\lambda_1))\phi_1} e^{i(\sigma_\mu(\mu_2)-\sigma_\lambda(\lambda_2))\phi_2} \cdots e^{i(\sigma_\mu(\mu_N)-\sigma_\lambda(\lambda_N))\phi_N} e^{-\frac{1}{2}\sum_i r_i^2}
\end{aligned}
\tag{B.4}
$$

Clearly, the integral over polar angles vanishes unless $\sigma_\mu(\mu_i) - \sigma_\lambda(\lambda_i) = 0$ for all $i \in \{1, 2, \ldots, N\}$. But if this condition is true, then $\lambda = \mu$ which contradicts with our assumption that λ and μ are different partitions of $J = mN(N-1)$. Therefore the integral must vanish and all the Slater determinants in the expansion of Laughlin wave functions are mutually orthogonal.

B.3 One component plasma on a disk

This section is based on Sari et al [170].

One component plasma (OCP) on a disk consists of N identical particles with charge e and a neutralizing background with uniform charge distribution. The Hamiltonian is $H = T + V$ where

$$
T = \sum_{i=1}^{N} \frac{p_i^2}{2M} \tag{B.5}
$$

is the kinetic term and the potential term V consists of background-background in-

teraction, particle-background interaction and particle-particle interaction.

$$\begin{aligned} V &= V_{bb} + V_{pb} + V_{pp} \\ &= -\frac{e^2 n^2}{2} \int d^2 z d^2 w \ln \left| \frac{z-w}{L} \right| + e^2 n \sum_i \int d^2 w \ln \left| \frac{w - z_i}{L} \right| \\ &\quad - \frac{e^2}{2} \sum_{i \neq j} \ln \left| \frac{z_i - z_j}{L} \right| \end{aligned} \tag{B.6}$$

where L is an arbitrary length scale.

After the integration and using the relation $n = N/(\pi R^2)$ we find

$$\begin{aligned} V_{bb} =& -\frac{e^2 N^2}{2} \left[\ln \left(\frac{R}{L} \right) - \frac{1}{4} \right], \\ V_{pb} =& \frac{e^2 N}{2} \sum_i \left[2 \ln \left(\frac{R}{L} \right) - 1 + \left(\frac{r_i}{R} \right)^2 \right] \\ =& \frac{e^2 N^2}{2} \left[2 \ln \left(\frac{R}{L} \right) - 1 \right] - \frac{e^2 N}{2} \sum_i \left(\frac{r_i}{R} \right)^2 . \end{aligned} \tag{B.7}$$

So

$$\begin{aligned} V =& -\frac{e^2 N^2}{2} \left[\frac{3}{4} - \ln \left(\frac{R}{L} \right) \right] + \frac{e^2 N}{2} \sum_i \left(\frac{r_i}{R} \right)^2 \\ & - \frac{e^2}{2} \sum_{i \neq j} \ln \left| \frac{z_i - z_j}{L} \right| . \end{aligned} \tag{B.8}$$

Then the canonical partition function could be calculated by

$$Z = \mathrm{tr}(e^{-\beta H}). \tag{B.9}$$

The kinetic term $T = \sum_i p_i^2/(2M)$ contributes as the partition function of ideal gas. Integrate out the momenta first and we obtain

$$\begin{aligned} & \frac{1}{N!} \prod_i \int \frac{d^2 z_i d^2 p_i}{h^2} \exp \left(-\beta \frac{p_i^2}{2M} \right) \\ =& \frac{1}{N!} \left(\frac{2M\pi}{\beta h^2} \right)^N \prod_i \int d^2 z_i \end{aligned} \tag{B.10}$$

where we leave the integral over particle positions untouched because the potential part of the plasma depends on positions.

To relate OCP partition function with Laughlin wave function, we assume the particle density $n = \frac{1}{2\pi m}$, electric charge $e = m$ and $\beta = 1/(k_B T) = 2/m$. Then the partition function Z_D of the OCP on a disk is

$$\begin{aligned} Z_D \equiv & A(N) Z_d \\ A(N) = & \frac{L^{mN}}{N!} e^{\frac{3mN^2}{4}} (2mN)^{-mN^2/2} \left(\frac{m\pi M}{h^2}\right)^N \\ Z_d = & \int d^2 z_1 \cdots \int d^2 z_N e^{-\frac{1}{2}\sum_i r_i^2} \prod_{i<j} |z_i - z_j|^{2m} \end{aligned} \tag{B.11}$$

where Z_d is exactly the normalization factor of Laughlin wave function and $A(N)$ is the prefactor independent of the integral.

B.4 Scaling of $A(N)Z_d^{(1)}$ in the disk case

To obtain the scaling of $A(N)Z_d^{(1)}$ in the numerator of the overlap function (5.32) in the main text, the only difficulty comes from the evaluation of $\prod_{i=1}^N [m(i-1)]!$. We first take logarithm of this term to convert it to a summation $\sum_{i=1}^N \ln[m(i-1)]!$ and then use Euler-Maclaurin formula to change the summation to an integral with a controlled error term. The Euler-Maclaurin formula reads

$$\begin{aligned} \sum_{i=m+1}^{n} f(i) = & \int_m^n f(x)dx + \sum_{k=1}^{p} \frac{B_k}{k!} (f^{(k-1)}(n) - f^{(k-1)}(m)) \\ & + \text{higher order error terms} \end{aligned} \tag{B.12}$$

where B_k is the k-th Bernoulli number and the error term depends on which term p we stop the expansion. For our purpose, knowing $B_1 = \frac{1}{2}, B_2 = \frac{1}{6}$ is enough.

But before we can finish the calculation, $\ln[m(i-1)]!$ must be evaluated first using

Stirling's formula (or Euler-Maclaurin formula)

$$\begin{aligned} & f(i) = \ln[m(i-1)]! \\ =& m(i-1)\ln[m(i-1)] - m(i-1) + \frac{1}{2}\ln[m(i-1)] \\ & + \frac{1}{2}\ln(2\pi) + \frac{1}{12m(i-1)} + \cdots \end{aligned} \tag{B.13}$$

Taking the derivative of this equation we find

$$\frac{df(i)}{di} = m\ln[m(i-1)] + \frac{1}{2(i-1)} + \cdots . \tag{B.14}$$

Plug these into the Euler-Maclaurin formula, we find

$$\begin{aligned} & \sum_{i=1}^{N} \ln[m(i-1)]! - \ln[m!] \\ =& \int_{i=2}^{N} \left\{ m(i-1)\ln[m(i-1)] - m(i-1) + \frac{1}{2}\ln[m(i-1)] + \frac{1}{2}\ln(2\pi) + \frac{1}{12m(i-1)} \right\} \\ & + \frac{1}{2}\left\{ m(N-1)\ln[m(N-1)] - m(N-1) + \frac{1}{2}\ln[m(N-1)] - \ln[m!] \right\} \\ & + \frac{1}{12}\{m\ln[m(N-1)] - m\ln m\} + O(1) \\ =& -\frac{m}{2}N^2\ln N + \frac{2m\ln m - 3m}{4}N^2 - \frac{m-1}{2}N\ln N - \frac{1}{2}[(m-1)(\ln m - 1) - \ln(2\pi)]N \\ & + \frac{m^2 - 3m + 1}{12m}\ln N + O(1). \end{aligned} \tag{B.15}$$

Then it is an easy calculation to find the scaling of the overlap as in the main text.

B.5 One component plasma on a sphere

Similar to the OCP on a disk, the Hamiltonian of the OCP on a sphere consists of a kinetic term $K = \sum_{i=1}^{N} p_i^2/(2M)$ and potential term U coming from background-background interaction, particle-background interaction and particle-particle interaction. In the following, the distance between two points on the sphere are calculated by embedding the sphere into a 3D Euclidean space.

$$\begin{aligned}
U =& U_{bb} + U_{pb} + U_{pp} \\
U_{bb} =& -\frac{e^2 n^2}{2} \int R^2 d\Omega_x R^2 d\Omega_y \ln \left| \frac{\boldsymbol{x} - \boldsymbol{y}}{L} \right| \\
=& -\frac{e^2 N^2}{4} \left[2 \ln \left(\frac{2R}{L} \right) - 1 \right] \\
U_{pb} =& e^2 n \sum_i \int R^2 d\Omega_x \ln \left| \frac{\boldsymbol{x}_i - \boldsymbol{x}}{L} \right| \\
=& \frac{e^2 N^2}{2} \left[2 \ln \left(\frac{2R}{L} \right) - 1 \right] \\
U_{pp} =& -e^2 \sum_{i<j} \ln \left| \frac{\boldsymbol{x}_i - \boldsymbol{x}_j}{L} \right| \\
=& -e^2 \sum_{i<j} \ln \left| \frac{2R}{L} (u_i v_j - u_j v_i) \right|
\end{aligned} \tag{B.16}$$

where $u = \cos\frac{\theta}{2} e^{i\phi/2}, v = \sin\frac{\theta}{2} e^{-i\phi/2}$.

In the Laughlin plasma analogy, $\beta = 2/m$ and $e = m, n = 1/(2\pi m)$. So the

partition function (including the ideal gas part) is

$$\begin{aligned} Z_{S^2} = \mathrm{tr}[e^{-\beta(K+U)}] = & \frac{e^{mN^2/2}}{N!}\left(\frac{mM\pi}{h^2}\right)^N \left(\frac{L}{2R}\right)^{mN^2} \\ & \int R^2 d\Omega_1 \cdots R^2 d\Omega_N \prod_{i<j}\left[\frac{2R}{L}|u_i v_j - u_j v_i|\right]^{2m} \\ = & \frac{e^{mN^2/2}}{N!}\left(\frac{mM\pi}{h^2}\right)^N \left(\frac{L}{2}\right)^{mN} \left(\frac{mN}{2}\right)^{\frac{(2-m)N}{2}} \\ & \int d\Omega_1 \cdots d\Omega_N \prod_{k=1}^{N} |u_k|^{2m(N-1)} \prod_{i<j}\left|\frac{v_j}{u_j} - \frac{v_i}{u_i}\right|^{2m} \end{aligned} \tag{B.17}$$

Then we recognize that the integral part is the normalization factor Z_s of Laughlin wave functions and the prefactor is $B(N)$.

B.6 Scaling of $B(N)Z_s^{(1)}$ in the sphere case

In the main text, the scaling of factorial part of $Z_s^{(1)}$ in Eq. (5.43) is the only difficulty for finding the scaling of $B(N)Z_s^{(1)}$ in the overlap (5.41).

$$\begin{aligned} & \ln Z_s^{(1)} = \ln N! + N\ln(4\pi) + \\ & \sum_{i=1}^{N}\{\ln[m(i-1)]! + \ln[m(N-i)]! - \ln[m(N-1)+1]!\} \end{aligned} \tag{B.18}$$

As described in the disk case, the factorials can be approximated using the Stirling's formula

$$\ln N! = N\ln N - N + \frac{1}{2}\ln N + \frac{1}{2}\ln(2\pi) + \frac{1}{12N} + \cdots . \tag{B.19}$$

And the summation could be converted to integral using the Euler-Maclaurin formula Eq.(B.12) where $f(i)$ is now defined as follows,

$$
\begin{aligned}
& f(i) = \ln[m(i-1)]! + \ln[m(N-i)]! \\
=& \left\{ m(i-1)\ln[m(i-1)] - m(i-1) + \frac{1}{2}\ln[m(i-1)] + \frac{1}{2}\ln(2\pi) + \frac{1}{12m(i-1)} \right\} + \\
& \left\{ m(N-i)\ln[m(N-i)] - m(N-i) + \frac{1}{2}\ln[m(N-i)] + \frac{1}{2}\ln(2\pi) + \frac{1}{12m(N-i)} \right\}.
\end{aligned} \tag{B.20}
$$

And its derivative is

$$
\frac{df(i)}{di} = m\ln[m(i-1)] + \frac{1}{2(i-1)} - m\ln[m(N-i)] + \cdots . \tag{B.21}
$$

Plug these into the Euler-Maclaurin formula, we find the summation part of Eq. (B.18)

$$
\begin{aligned}
& \sum_{i=1}^{N} \{\ln[m(i-1)]! + \ln[m(N-i)]! - \ln[m(N-1)+1]!\} \\
=& \sum_{i=1}^{N} f(i) - N\{[m(N-1)+1]\ln[m(N-1)+1] - [m(N-1)+1] + \\
& \frac{1}{2}\ln[m(N-1)+1] + \frac{1}{2}\ln(2\pi) + \frac{1}{12[m(N-1)+1]}\} + O(1) \\
=& -\frac{m}{2}N^2 - \frac{1}{2}N\ln N + \frac{1}{2}[2(m-1)+\ln(2\pi)]N + \frac{m^2-3m+1}{6m}\ln N + O(1).
\end{aligned} \tag{B.22}
$$

Inserting this result in the expression of $B(N)Z_s^{(1)}$ one can easily find the overlap scaling as Eq. (5.44) in the main text.

B.7 Further calculations for Laughlin states

B.7.1 Question 1

Which terms in the finite-size scaling would change if we replace $\exp(-\frac{1}{4}r^2)$ *in* Ψ^I *by* $\exp(-\frac{C}{4}r^2)$ *where* C *is an arbitrary number?*

Answer:

We will have an extra term N^2 and the coefficients of $N, \sqrt{N}$ will be modified. Nothing will be changed for $N \ln N$ and $\ln N$ terms.

Detail of calculation:

Denote the modified trivial wave function (un-normalized) as

$$\tilde{\mathcal{D}}_{\lambda^{(1)}} = \begin{vmatrix} z_1^{m(N-1)} & z_1^{m(N-2)} & \cdots & 1 \\ z_2^{m(N-1)} & z_2^{m(N-2)} & \cdots & 1 \\ \vdots & \vdots & \vdots & \vdots \\ z_N^{m(N-1)} & z_N^{m(N-2)} & \cdots & 1 \end{vmatrix} \exp\left(-\sum_{i=1}^{N} \frac{C|z_i|^2}{4} \right) \tag{B.23}$$

Then the overlap is

$$\langle \tilde{\Psi}^I | \Psi^{II} \rangle = \frac{\sum_i a_i \langle \tilde{\mathcal{D}}_{\lambda^{(1)}} | \mathcal{D}_i \rangle}{\sqrt{\tilde{Z}_d^{(1)} Z_d}} = \frac{\langle \tilde{\mathcal{D}}_{\lambda^{(1)}} | \mathcal{D}_i \rangle}{\sqrt{\tilde{Z}_d^{(1)} Z_d}} \tag{B.24}$$

where $\tilde{Z}_d^{(1)}$ is the normalization factor for the wave function of system I. Following the same argument as in the main text, the terms that contribute to $\tilde{Z}_d^{(1)}$ and $\langle \tilde{\mathcal{D}}_{\lambda^{(1)}} | \mathcal{D}_i \rangle$

are those with zero phase for each particle coordinate z_i in the integrand.

$$\begin{aligned}
\tilde{Z}_d^{(1)} &= (2\pi)^N \int_0^R r_1 dr_1 \cdots \int_0^R r_N dr_N \exp\left(-\frac{C}{2}\sum_i r_i^2\right) \sum_{\sigma\in S_N} r_{\sigma(1)}^0 r_{\sigma(2)}^m \cdots r_{\sigma(N)}^{m(N-1)} \\
&= (2\pi)^N N! \int_0^R r_1 dr_1 \cdots \int_0^R r_N dr_N \exp\left(-\frac{C}{2}\sum_i r_i^2\right) r_1^0 r_2^{2m} \cdots r_N^{2m(N-1)} \\
&= (2\pi)^N N! 2^{\frac{m(N-1)N}{2}} \prod_{i=1}^N \int_0^{mN} dx_i e^{-Cx_i} x_i^{m(i-1)} \\
&= (2\pi)^N 2^{\frac{m(N-1)N}{2}} \prod_{j=1}^N [m(j-1)]! N! \prod_{i=1}^N \left(\frac{1}{[m(i-1)]!} \int_0^{CmN} dy_i e^{-y_i} y_i^{m(i-1)}\right) \\
&\quad C^{-mN^2/2+(m-2)N/2}
\end{aligned} \tag{B.25}$$

where we used the change of variables $x_i = r_i^2/2$ and $y_i = Cx_i$ in the last two steps respectively. By comparing the the calculation of $Z_d^{(1)}$ we realize that the only change is the factor $C^{-mN^2/2+(m-2)N/2}$ (which only contributes to the N^2, N terms) and the integral limit CmN (which only contributes to the boundary term $\sqrt{N}$).

Similarly, the numerator is calculated as follows.

$$\begin{aligned}
\langle \tilde{\mathcal{D}}_{\lambda^{(1)}} | \mathcal{D}_i \rangle &= (2\pi)^N \int_0^R r_1 dr_1 \cdots \int_0^R r_N dr_N \exp\left(-\frac{1+C}{4}\sum_i r_i^2\right) \sum_{\sigma\in S_N} r_{\sigma(1)}^0 r_{\sigma(2)}^m \cdots r_{\sigma(N)}^{m(N-1)} \\
&= (2\pi)^N N! \int_0^R r_1 dr_1 \cdots \int_0^R r_N dr_N \exp\left(-\frac{1+C}{4}\sum_i r_i^2\right) r_1^0 r_2^{2m} \cdots r_N^{2m(N-1)} \\
&= (2\pi)^N N! 2^{\frac{m(N-1)N}{2}} \prod_{i=1}^N \int_0^{mN} dx_i e^{-(1+C)x_i/2} x_i^{m(i-1)} \\
&= (2\pi)^N 2^{\frac{m(N-1)N}{2}} \prod_{j=1}^N [m(j-1)]! N! \prod_{i=1}^N \left(\frac{1}{[m(i-1)]!} \int_0^{(1+C)mN/2} dy_i e^{-y_i} y_i^{m(i-1)}\right) \\
&\quad \left(\frac{1+C}{2}\right)^{-mN^2/2+(m-2)N/2}
\end{aligned} \tag{B.26}$$

Again, the only change to the numerator is also the terms related to N^2, N and $\sqrt{N}$.

Therefore we obtained a N^2 term and modified $N, \sqrt{N}$ terms, but didn't change those terms related to $N \ln N, \ln N$.

B.7.2 Question 2

Are the logarithmic terms really universal for all choices of Slater determinant as the trivial wave function? Can the scaling be higher order, N^2 for example?

Answer:

No. In general, both $N \ln N$ and $\ln N$ terms vary as we choose different Slater determinants. But as in the main text, the coefficient of $\ln N$ term is proportional to the Euler characteristic of the real space manifold. So it is only universal in the topological sense.

Yes, the scaling could be of order N^2. It was proven that the lower bound of the overlap scaling is power law with some negative exponent. But no upper bound has been found in the literature. So there is no contradiction even if N^2 exists.

Calculation detail:

Here we give an example for $m = 3$ in the overlap calculation. Choose $\lambda' = (2N-2, 2N-3, \ldots, N-1)$ instead of $\lambda^{(1)}$ as in the main text. The corresponding Slater determinant in the expansion is

$$\mathcal{D}_{\lambda'} = \begin{vmatrix} z_1^{2N-2} & z_1^{2N-3} & \cdots & z_1^{N-1} \\ z_2^{2N-2} & z_2^{2N-3} & \cdots & z_2^{N-1} \\ \vdots & \vdots & \vdots & \vdots \\ z_N^{2N-2} & z_N^{2N-3} & \cdots & z_N^{N-1} \end{vmatrix} \exp\left(-\sum_{i=1}^{N} \frac{|z_i|^2}{4}\right) \tag{B.27}$$

It has been shown in equation (55) of [154] that the coefficient of such a term is

$a_{\lambda'} = (-1)^{[N/2]}(2N-1)!!$. So the overlap is

$$|\langle\Psi^I|\Psi^{II}\rangle| = \left|\frac{\sum_i a_i \langle\mathcal{D}_{\lambda'}|\mathcal{D}_i\rangle}{\sqrt{\tilde{Z}_d^{(1)} Z_d}}\right| = |a_{\lambda'}|\sqrt{\frac{Z_d^{(1)}}{Z_d}} = \sqrt{\frac{a_{\lambda'}^2 A(N) Z_d^{(1)}}{Z_D}} \tag{B.28}$$

where $Z_D = A(N)Z_d$ and $A(N)$ is the same as that in the main text. The same argument as before gives the non-zero contribution to $Z_d^{(1)}$ as

$$\begin{aligned}
Z_d^{(1)} =& (2\pi)^N \int_0^R r_1 dr_1 \cdots \int_0^R r_N dr_N \exp\left(-\frac{1}{2}\sum_i r_i^2\right) \sum_{\sigma\in S_N} r_{\sigma(1)}^{2(N-1)} r_{\sigma(2)}^{2N} \ldots r_{\sigma(N)}^{2(2N-2)} \\
=& (2\pi)^N N! \int_0^R r_1 dr_1 \cdots \int_0^R r_N dr_N \exp\left(-\frac{1}{2}\sum_i r_i^2\right) r_1^{2(N-1)} r_2^{2N} \ldots r_N^{2(2N-2)} \\
=& (2\pi)^N N! 2^{3N(N-1)/2} \prod_{i=1}^N \int_0^{3N} dx_i e^{-x_i} x_i^{N+i-2} \\
=& (2\pi)^N 2^{3N(N-1)/2} \prod_{j=1}^N [N+j-2)]! N! \prod_{i=1}^N \left(\frac{1}{[N+i-2)]!} \int_0^{3N} dx_i e^{-x_i} x_i^{N+i-2}\right)
\end{aligned} \tag{B.29}$$

where the last product with integral inside only contributes to the boundary term $\sqrt{N}$ in the finite-size scaling. The factorials could be evaluated by Euler-Maclaurin formula as in previous discussion. Ignoring the boundary term contribution, it can be shown that the logarithm of the numerator $a_{\lambda'}^2 A(N) Z_d^{(1)}$ is

$$\ln[a_{\lambda'}^2 A(N) Z_d^{(1)}] = \left(-\frac{3}{2}\ln 3 + \ln 4\right) N^2 + N\ln N + \left(\ln\left(\frac{3\pi^{5/2} M}{h^2}\right) - 1\right) N + O(1), \tag{B.30}$$

which produces a higher order N^2 term. And if the coefficients of $N\ln N, \ln N$ were universal, then they should be $-1, \frac{1}{12}$ respectively (consider the numerator part only since the denominators are the same for this example and the calculation in the main text). But the coefficients are $1, 0$ in the above expression. So they are not universal when we change the trivial wave function Ψ^I.

However, the dependence of $\ln N$ term on the topology of real space manifold should be valid. That would be the only "universal" part.

BIBLIOGRAPHY

BIBLIOGRAPHY

[1] N.W. Ashcroft and N.D. Mermin. *Solid State Physics*. Saunders College, Philadelphia, 1976.

[2] Ado Jorio Mildred S. Dresselhaus, Gene Dresselhaus. *Group Theory*. Springer-Verlag Berlin Heidelberg, 2008. ISBN 978-3-540-32897-1. doi: 10.1007/978-3-540-32899-5.

[3] L. D. Landau. *Phys. Z. Sowjetunion 11*, pages 26–35, 1937.

[4] V. L. Ginzburg and L. D. Landau. On the Theory of superconductivity. *Zh. Eksp. Teor. Fiz.*, 20:1064–1082, 1950.

[5] L. D. Landau and E. M. Lifshitz. *Statistical Physics (Part 1)*. Pergamon Press, Oxford, 1958. Course of Theoretical Physics, Vol. 5.

[6] Mehran Kardar. *Statistical Physics of Fields*. Cambridge University Press, 2007. doi: 10.1017/CBO9780511815881.

[7] Philippe Di Francesco, Pierre Mathieu, and David Snchal. *Conformal field theory*. Graduate texts in contemporary physics. Springer, New York, NY, 1997. URL `https://cds.cern.ch/record/639405`.

[8] K. von Klitzing, G. Dorda, and M. Pepper. New method for high-accuracy determination of the fine-structure constant based on quantized hall resistance. *Phys. Rev. Lett.*, 45(6):494–497, Aug 1980. doi: 10.1103/PhysRevLett.45.494.

[9] D. C. Tsui, H. L. Stormer, and A. C. Gossard. Two-dimensional magneto-transport in the extreme quantum limit. *Phys. Rev. Lett.*, 48:1559–1562, May 1982. doi: 10.1103/PhysRevLett.48.1559. URL `http://link.aps.org/doi/10.1103/PhysRevLett.48.1559`.

[10] R. Willett, J. P. Eisenstein, H. L. Störmer, D. C. Tsui, A. C. Gossard, and J. H. English. Observation of an even-denominator quantum number in the fractional quantum hall effect. *Phys. Rev. Lett.*, 59:1776–1779, Oct 1987. doi: 10.1103/PhysRevLett.59.1776. URL `https://link.aps.org/doi/10.1103/PhysRevLett.59.1776`.

[11] Iuliana P. Radu, J. B. Miller, C. M. Marcus, M. A. Kastner, L. N. Pfeiffer, and K. W. West. Quasi-particle properties from tunneling in the v = 5/2 fractional

quantum hall state. *Science*, 320(5878):899–902, 2008. ISSN 0036-8075. doi: 10.1126/science.1157560. URL https://science.sciencemag.org/content/320/5878/899.

[12] Horst L. Stormer, Daniel C. Tsui, and Arthur C. Gossard. The fractional quantum hall effect. *Rev. Mod. Phys.*, 71:S298–S305, Mar 1999. doi: 10.1103/RevModPhys.71.S298. URL https://link.aps.org/doi/10.1103/RevModPhys.71.S298.

[13] D. J. Thouless, M. Kohmoto, M. P. Nightingale, and M. den Nijs. Quantized hall conductance in a two-dimensional periodic potential. *Phys. Rev. Lett.*, 49 (6):405–408, Aug 1982. doi: 10.1103/PhysRevLett.49.405.

[14] F. D. M. Haldane. Model for a quantum hall effect without landau levels: Condensed-matter realization of the "parity anomaly". *Phys. Rev. Lett.*, 61: 2015–2018, Oct 1988. doi: 10.1103/PhysRevLett.61.2015. URL https://link.aps.org/doi/10.1103/PhysRevLett.61.2015.

[15] X. G. Wen. Vacuum degeneracy of chiral spin states in compactified space. *Phys. Rev. B*, 40:7387–7390, Oct 1989. doi: 10.1103/PhysRevB.40.7387. URL https://link.aps.org/doi/10.1103/PhysRevB.40.7387.

[16] X. G. Wen. Topological orders in rigid states. *Int. J. Mod. Phys. B*, page 239, 1990.

[17] Xie Chen, Zheng-Cheng Gu, and Xiao-Gang Wen. Local unitary transformation, long-range quantum entanglement, wave function renormalization, and topological order. *Phys. Rev. B*, 82:155138, Oct 2010. doi: 10.1103/PhysRevB.82.155138. URL https://link.aps.org/doi/10.1103/PhysRevB.82.155138.

[18] Xie Chen, Zheng-Cheng Gu, Zheng-Xin Liu, and Xiao-Gang Wen. Symmetry protected topological orders and the group cohomology of their symmetry group. *Phys. Rev. B*, 87:155114, Apr 2013. doi: 10.1103/PhysRevB.87.155114. URL https://link.aps.org/doi/10.1103/PhysRevB.87.155114.

[19] Xiao-Gang Wen. Classifying gauge anomalies through symmetry-protected trivial orders and classifying gravitational anomalies through topological orders. *Phys. Rev.*, D88(4):045013, 2013. doi: 10.1103/PhysRevD.88.045013.

[20] F.D.M. Haldane. Continuum dynamics of the 1-d heisenberg antiferromagnet: Identification with the o(3) nonlinear sigma model. *Physics Letters A*, 93(9):464 – 468, 1983. ISSN 0375-9601. doi: https://doi.org/10.1016/0375-9601(83)90631-X. URL http://www.sciencedirect.com/science/article/pii/037596018390631X.

[21] F. D. M. Haldane. Nonlinear field theory of large-spin heisenberg antiferromagnets: Semiclassically quantized solitons of the one-dimensional easy-axis néel state. *Phys. Rev. Lett.*, 50:1153–1156, Apr 1983. doi: 10.1103/PhysRevLett.50.1153. URL https://link.aps.org/doi/10.1103/PhysRevLett.50.1153.

[22] F. D. M. Haldane. physics and quantum spin chains (abstract). *Journal of Applied Physics*, 57(8):3359–3359, 1985. doi: 10.1063/1.335096. URL https://doi.org/10.1063/1.335096.

[23] Ian Affleck, Tom Kennedy, Elliott H. Lieb, and Hal Tasaki. Valence bond ground states in isotropic quantum antiferromagnets. *Communications in Mathematical Physics*, 115(3):477–528, Sep 1988. ISSN 1432-0916. doi: 10.1007/BF01218021. URL https://doi.org/10.1007/BF01218021.

[24] C. L. Kane and E. J. Mele. Z_2 topological order and the quantum spin hall effect. *Phys. Rev. Lett.*, 95:146802, Sep 2005. doi: 10.1103/PhysRevLett.95.146802. URL https://link.aps.org/doi/10.1103/PhysRevLett.95.146802.

[25] C. L. Kane and E. J. Mele. Quantum spin hall effect in graphene. *Phys. Rev. Lett.*, 95:226801, Nov 2005. doi: 10.1103/PhysRevLett.95.226801. URL https://link.aps.org/doi/10.1103/PhysRevLett.95.226801.

[26] Liang Fu and C. L. Kane. Topological insulators with inversion symmetry. *Phys. Rev. B*, 76:045302, Jul 2007. doi: 10.1103/PhysRevB.76.045302. URL https://link.aps.org/doi/10.1103/PhysRevB.76.045302.

[27] Liang Fu, C. L. Kane, and E. J. Mele. Topological insulators in three dimensions. *Phys. Rev. Lett.*, 98:106803, Mar 2007. doi: 10.1103/PhysRevLett.98.106803. URL https://link.aps.org/doi/10.1103/PhysRevLett.98.106803.

[28] J. E. Moore and L. Balents. Topological invariants of time-reversal-invariant band structures. *Phys. Rev. B*, 75:121306, Mar 2007. doi: 10.1103/PhysRevB.75.121306. URL https://link.aps.org/doi/10.1103/PhysRevB.75.121306.

[29] Rahul Roy. Z_2 classification of quantum spin hall systems: An approach using time-reversal invariance. *Phys. Rev. B*, 79:195321, May 2009. doi: 10.1103/PhysRevB.79.195321. URL https://link.aps.org/doi/10.1103/PhysRevB.79.195321.

[30] Rahul Roy. Topological phases and the quantum spin hall effect in three dimensions. *Phys. Rev. B*, 79:195322, May 2009. doi: 10.1103/PhysRevB.79.195322. URL https://link.aps.org/doi/10.1103/PhysRevB.79.195322.

[31] B. Andrei Bernevig, Taylor L. Hughes, and Shou-Cheng Zhang. Quantum spin hall effect and topological phase transition in hgte quantum wells. *Science*, 314 (5806):1757–1761, 2006. ISSN 0036-8075. doi: 10.1126/science.1133734. URL http://science.sciencemag.org/content/314/5806/1757.

[32] Markus König, Steffen Wiedmann, Christoph Brüne, Andreas Roth, Hartmut Buhmann, Laurens W. Molenkamp, Xiao-Liang Qi, and Shou-Cheng Zhang. Quantum spin hall insulator state in hgte quantum wells. *Science*, 318(5851): 766–770, 2007. ISSN 0036-8075. doi: 10.1126/science.1148047. URL https://science.sciencemag.org/content/318/5851/766.

[33] D Hsieh, Dong Qian, L Wray, Yiman Xia, Y S. Hor, R J. Cava, and M. Zahid Hasan. A topological dirac insulator in a quantum spin hall phase : Experimental observation of first strong topological insulator. 02 2009.

[34] Y. Xia et al. Observation of a large-gap topological-insulator class with a single Dirac cone on the surface. *Nature Phys.*, 5:398–402, 2009. doi: 10.1038/nphys1274.

[35] Haijun Zhang, Chao-Xing Liu, Xiao-Liang Qi, Xi Dai, Zhong Fang, and Shou-Cheng Zhang. Topological insulators in bi2se3, bi2te3 and sb2te3 with a single dirac cone on the surface. *Nature Physics*, 5:438–442, 05 2009. doi: 10.1038/nphys1270.

[36] Maxim Dzero, Kai Sun, Piers Coleman, and Victor Galitski. Theory of topological kondo insulators. *Phys. Rev. B*, 85:045130, Jan 2012. doi: 10.1103/PhysRevB.85.045130. URL https://link.aps.org/doi/10.1103/PhysRevB.85.045130.

[37] G. Li, Z. Xiang, F. Yu, T. Asaba, B. Lawson, P. Cai, C. Tinsman, A. Berkley, S. Wolgast, Y. S. Eo, Dae-Jeong Kim, C. Kurdak, J. W. Allen, K. Sun, X. H. Chen, Y. Y. Wang, Z. Fisk, and Lu Li. Two-dimensional fermi surfaces in kondo insulator smb6. *Science*, 346(6214):1208–1212, 2014. ISSN 0036-8075. doi: 10.1126/science.1250366. URL https://science.sciencemag.org/content/346/6214/1208.

[38] Steven Wolgast, Çağlı yan Kurdak, Kai Sun, J. W. Allen, Dae-Jeong Kim, and Zachary Fisk. Low-temperature surface conduction in the kondo insulator smb_6. *Phys. Rev. B*, 88:180405, Nov 2013. doi: 10.1103/PhysRevB.88.180405. URL https://link.aps.org/doi/10.1103/PhysRevB.88.180405.

[39] Zheng-Cheng Gu and Xiao-Gang Wen. Symmetry-protected topological orders for interacting fermions: Fermionic topological nonlinear σ models and a special group supercohomology theory. *Phys. Rev. B*, 90:115141, Sep 2014. doi: 10.1103/PhysRevB.90.115141. URL https://link.aps.org/doi/10.1103/PhysRevB.90.115141.

[40] V. Kalmeyer and R. B. Laughlin. Equivalence of the resonating-valence-bond and fractional quantum hall states. *Phys. Rev. Lett.*, 59:2095–2098, Nov 1987. doi: 10.1103/PhysRevLett.59.2095. URL https://link.aps.org/doi/10.1103/PhysRevLett.59.2095.

[41] X. G. Wen, Frank Wilczek, and A. Zee. Chiral spin states and superconductivity. *Phys. Rev. B*, 39:11413–11423, Jun 1989. doi: 10.1103/PhysRevB.39.11413. URL https://link.aps.org/doi/10.1103/PhysRevB.39.11413.

[42] N. Read and Subir Sachdev. Large-n expansion for frustrated quantum antiferromagnets. *Phys. Rev. Lett.*, 66:1773–1776, Apr 1991. doi:

10.1103/PhysRevLett.66.1773. URL https://link.aps.org/doi/10.1103/PhysRevLett.66.1773.

[43] X. G. Wen. Mean-field theory of spin-liquid states with finite energy gap and topological orders. *Phys. Rev. B*, 44:2664–2672, Aug 1991. doi: 10.1103/PhysRevB.44.2664. URL https://link.aps.org/doi/10.1103/PhysRevB.44.2664.

[44] R. Moessner and S. L. Sondhi. Resonating valence bond phase in the triangular lattice quantum dimer model. *Phys. Rev. Lett.*, 86:1881–1884, Feb 2001. doi: 10.1103/PhysRevLett.86.1881. URL https://link.aps.org/doi/10.1103/PhysRevLett.86.1881.

[45] R. B. Laughlin. Anomalous quantum hall effect: An incompressible quantum fluid with fractionally charged excitations. *Phys. Rev. Lett.*, 50:1395–1398, May 1983. doi: 10.1103/PhysRevLett.50.1395. URL https://link.aps.org/doi/10.1103/PhysRevLett.50.1395.

[46] Gregory Moore and Nicholas Read. Nonabelions in the fractional quantum hall effect. *Nuclear Physics B*, 360(2):362 – 396, 1991. ISSN 0550-3213. doi: https://doi.org/10.1016/0550-3213(91)90407-O. URL http://www.sciencedirect.com/science/article/pii/055032139190407O.

[47] X. G. Wen. Non-abelian statistics in the fractional quantum hall states. *Phys. Rev. Lett.*, 66:802–805, Feb 1991. doi: 10.1103/PhysRevLett.66.802. URL https://link.aps.org/doi/10.1103/PhysRevLett.66.802.

[48] Xie Chen, Zheng-Cheng Gu, and Xiao-Gang Wen. Classification of gapped symmetric phases in one-dimensional spin systems. *Phys. Rev. B*, 83:035107, Jan 2011. doi: 10.1103/PhysRevB.83.035107. URL https://link.aps.org/doi/10.1103/PhysRevB.83.035107.

[49] Norbert Schuch, David Pérez-García, and Ignacio Cirac. Classifying quantum phases using matrix product states and projected entangled pair states. *Phys. Rev. B*, 84:165139, Oct 2011. doi: 10.1103/PhysRevB.84.165139. URL https://link.aps.org/doi/10.1103/PhysRevB.84.165139.

[50] Xie Chen, Zheng-Cheng Gu, and Xiao-Gang Wen. Complete classification of one-dimensional gapped quantum phases in interacting spin systems. *Phys. Rev. B*, 84:235128, Dec 2011. doi: 10.1103/PhysRevB.84.235128. URL https://link.aps.org/doi/10.1103/PhysRevB.84.235128.

[51] Frank Pollmann, Ari M. Turner, Erez Berg, and Masaki Oshikawa. Entanglement spectrum of a topological phase in one dimension. *Phys. Rev. B*, 81:064439, Feb 2010. doi: 10.1103/PhysRevB.81.064439. URL https://link.aps.org/doi/10.1103/PhysRevB.81.064439.

[52] Ari M. Turner, Frank Pollmann, and Erez Berg. Topological phases of one-dimensional fermions: An entanglement point of view. *Phys. Rev. B*, 83:075102, Feb 2011. doi: 10.1103/PhysRevB.83.075102. URL https://link.aps.org/doi/10.1103/PhysRevB.83.075102.

[53] Lukasz Fidkowski and Alexei Kitaev. Topological phases of fermions in one dimension. *Phys. Rev. B*, 83:075103, Feb 2011. doi: 10.1103/PhysRevB.83.075103. URL https://link.aps.org/doi/10.1103/PhysRevB.83.075103.

[54] Alexei Kitaev. Periodic table for topological insulators and superconductors. *AIP Conf. Proc.*, 1134(1):22–30, 2009. doi: 10.1063/1.3149495.

[55] Meng Cheng, Zhen Bi, Yi-Zhuang You, and Zheng-Cheng Gu. Classification of symmetry-protected phases for interacting fermions in two dimensions. *Phys. Rev. B*, 97:205109, May 2018. doi: 10.1103/PhysRevB.97.205109. URL https://link.aps.org/doi/10.1103/PhysRevB.97.205109.

[56] Qing-Rui Wang and Zheng-Cheng Gu. Towards a complete classification of symmetry-protected topological phases for interacting fermions in three dimensions and a general group supercohomology theory. *Phys. Rev. X*, 8:011055, Mar 2018. doi: 10.1103/PhysRevX.8.011055. URL https://link.aps.org/doi/10.1103/PhysRevX.8.011055.

[57] J M Kosterlitz and D J Thouless. Ordering, metastability and phase transitions in two-dimensional systems. *Journal of Physics C: Solid State Physics*, 6(7): 1181, 1973. URL http://stacks.iop.org/0022-3719/6/i=7/a=010.

[58] J Villain. Spin glass with non-random interactions. *Journal of Physics C: Solid State Physics*, 10(10):1717, 1977. URL http://stacks.iop.org/0022-3719/10/i=10/a=014.

[59] J Villain. Two-level systems in a spin-glass model. i. general formalism and two-dimensional model. *Journal of Physics C: Solid State Physics*, 10(23):4793, 1977. URL http://stacks.iop.org/0022-3719/10/i=23/a=013.

[60] Mark Yosefin and Eytan Domany. Phase transitions in fully frustrated spin systems. *Phys. Rev. B*, 32:1778–1795, Aug 1985. doi: 10.1103/PhysRevB.32.1778. URL https://link.aps.org/doi/10.1103/PhysRevB.32.1778.

[61] M. Y. Choi and S. Doniach. Phase transitions in uniformly frustrated xy models. *Phys. Rev. B*, 31:4516–4526, Apr 1985. doi: 10.1103/PhysRevB.31.4516. URL https://link.aps.org/doi/10.1103/PhysRevB.31.4516.

[62] D. Loison and K.D. Schotte. First and second order transition in frustrated xy systems. *The European Physical Journal B - Condensed Matter and Complex Systems*, 5(3):735–743, Oct 1998. ISSN 1434-6036. doi: 10.1007/s100510050497. URL https://doi.org/10.1007/s100510050497.

[63] Piero Martinoli and Chris Leemann. Two dimensional josephson junction arrays. *Journal of Low Temperature Physics*, 118(5):699–731, Mar 2000. ISSN 1573-7357. doi: 10.1023/A:1004651730459. URL https://doi.org/10.1023/A:1004651730459.

[64] S. Teitel and C. Jayaprakash. Phase transtions in frustrated two-dimensional XY models. *Phys. Rev. B*, 27:598–601, Jan 1983. doi: 10.1103/PhysRevB.27.598. URL https://link.aps.org/doi/10.1103/PhysRevB.27.598.

[65] S. Teitel and C. Jayaprakash. Josephson-junction arrays in transverse magnetic fields. *Phys. Rev. Lett.*, 51:1999–2002, Nov 1983. doi: 10.1103/PhysRevLett.51.1999. URL https://link.aps.org/doi/10.1103/PhysRevLett.51.1999.

[66] Hikaru Kawamura. Renormalization-group analysis of chiral transitions. *Phys. Rev. B*, 38:4916–4928, Sep 1988. doi: 10.1103/PhysRevB.38.4916. URL https://link.aps.org/doi/10.1103/PhysRevB.38.4916.

[67] T Garel and S Doniach. On the critical behaviour of two-dimensional xy helimagnets. *Journal of Physics C: Solid State Physics*, 13(31):L887, 1980. URL http://stacks.iop.org/0022-3719/13/i=31/a=003.

[68] N. D. Mermin. The topological theory of defects in ordered media. *Rev. Mod. Phys.*, 51:591–648, Jul 1979. doi: 10.1103/RevModPhys.51.591. URL https://link.aps.org/doi/10.1103/RevModPhys.51.591.

[69] Martin Hasenbusch, Andrea Pelissetto, and Ettore Vicari. Critical behavior of two-dimensional fully frustrated xy systems. *Journal of Physics: Conference Series*, 42(1):124, 2006. URL http://stacks.iop.org/1742-6596/42/i=1/a=013.

[70] Martin Hasenbusch, Andrea Pelissetto, and Ettore Vicari. Multicritical behaviour in the fully frustrated xy model and related systems. *Journal of Statistical Mechanics: Theory and Experiment*, 2005(12):P12002, 2005. URL http://stacks.iop.org/1742-5468/2005/i=12/a=P12002.

[71] Martin Hasenbusch, Andrea Pelissetto, and Ettore Vicari. Transitions and crossover phenomena in fully frustrated *xy* systems. *Phys. Rev. B*, 72:184502, Nov 2005. doi: 10.1103/PhysRevB.72.184502. URL https://link.aps.org/doi/10.1103/PhysRevB.72.184502.

[72] Pasquale Calabrese and Pietro Parruccini. Critical behavior of two-dimensional frustrated spin models with noncollinear order. *Phys. Rev. B*, 64:184408, Oct 2001. doi: 10.1103/PhysRevB.64.184408. URL https://link.aps.org/doi/10.1103/PhysRevB.64.184408.

[73] Hikaru Kawamura. Universality of phase transitions of frustrated antiferromagnets. *Journal of Physics: Condensed Matter*, 10(22):4707, 1998. URL http://stacks.iop.org/0953-8984/10/i=22/a=004.

[74] H. Kawamura. Phase transitions in heisenberg antiferromagnets on triangular and layeredtriangular lattices (invited). *Journal of Applied Physics*, 61(8):3590–3594, 1987. doi: 10.1063/1.338936. URL http://dx.doi.org/10.1063/1.338936.

[75] Hikaru Kawamura. Renormalization-group approach to the frustrated heisenberg antiferromagnet on the layered-triangular lattice. *Journal of the Physical Society of Japan*, 55(7):2157–2165, 1986. doi: 10.1143/JPSJ.55.2157. URL http://dx.doi.org/10.1143/JPSJ.55.2157.

[76] Yurij Holovatch, Dmytro Ivaneyko, and Bertrand Delamotte. On the criticality of frustrated spin systems with noncollinear order. *Journal of Physics A: Mathematical and General*, 37(11):3569, 2004. URL http://stacks.iop.org/0305-4470/37/i=11/a=002.

[77] B. Delamotte, M. Dudka, D. Mouhanna, and S. Yabunaka. Functional renormalization group approach to noncollinear magnets. *Phys. Rev. B*, 93:064405, Feb 2016. doi: 10.1103/PhysRevB.93.064405. URL https://link.aps.org/doi/10.1103/PhysRevB.93.064405.

[78] D. D. Betts. The exact solution of some lattice statistics models with four states per site. *Canadian Journal of Physics*, 42(8):1564–1572, 1964. doi: 10.1139/p64-142. URL https://doi.org/10.1139/p64-142.

[79] P. W. Kasteleyn. *Report in Aachen Conference on Statistical Mechanics*, 1964.

[80] Sooyeul Lee and Koo-Chul Lee. Phase transitions in the fully frustrated xy model studied with use of the microcanonical monte carlo technique. *Phys. Rev. B*, 49:15184–15189, Jun 1994. doi: 10.1103/PhysRevB.49.15184. URL https://link.aps.org/doi/10.1103/PhysRevB.49.15184.

[81] Peter Olsson. Two phase transitions in the fully frustrated XY model. *Phys. Rev. Lett.*, 75:2758–2761, Oct 1995. doi: 10.1103/PhysRevLett.75.2758. URL https://link.aps.org/doi/10.1103/PhysRevLett.75.2758.

[82] H-J Xu and B W Southern. Phase transitions in the classical xy antiferromagnet on the triangular lattice. *Journal of Physics A: Mathematical and General*, 29 (5):L133, 1996. URL http://stacks.iop.org/0305-4470/29/i=5/a=009.

[83] Sooyeul Lee and Koo-Chul Lee. Phase transitions in the fully frustrated triangular XY model. *Phys. Rev. B*, 57:8472–8477, Apr 1998. doi: 10.1103/PhysRevB.57.8472. URL https://link.aps.org/doi/10.1103/PhysRevB.57.8472.

[84] Luca Capriotti, Ruggero Vaia, Alessandro Cuccoli, and Valerio Tognetti. Phase transitions induced by easy-plane anisotropy in the classical heisenberg antiferromagnet on a triangular lattice: A monte carlo simulation. *Phys. Rev. B*, 58:273–281, Jul 1998. doi: 10.1103/PhysRevB.58.273. URL https://link.aps.org/doi/10.1103/PhysRevB.58.273.

[85] S. E. Korshunov. Kink pairs unbinding on domain walls and the sequence of phase transitions in fully frustrated XY models. *Phys. Rev. Lett.*, 88:167007, Apr 2002. doi: 10.1103/PhysRevLett.88.167007. URL https://link.aps.org/doi/10.1103/PhysRevLett.88.167007.

[86] Soichirou Okumura, Hajime Yoshino, and Hikaru Kawamura. Spin-chirality decoupling and critical properties of a two-dimensional fully frustrated XY model. *Phys. Rev. B*, 83:094429, Mar 2011. doi: 10.1103/PhysRevB.83.094429. URL https://link.aps.org/doi/10.1103/PhysRevB.83.094429.

[87] Tomoyuki Obuchi and Hikaru Kawamura. Spin and chiral orderings of the antiferromagnetic xy model on the triangular lattice and their critical properties. *Journal of the Physical Society of Japan*, 81(5):054003, 2012. doi: 10.1143/JPSJ.81.054003. URL http://dx.doi.org/10.1143/JPSJ.81.054003.

[88] V. L. Berezinskii. Destruction of long-range order in one-dimensional and two-dimensional systems having a continuous symmetry group i. classical systems. *Sov. Phys. JETP*, 32:493, 1971.

[89] J M Kosterlitz. The critical properties of the two-dimensional xy model. *Journal of Physics C: Solid State Physics*, 7(6):1046, 1974. URL http://stacks.iop.org/0022-3719/7/i=6/a=005.

[90] Peter Olsson and S. Teitel. Kink-antikink unbinding transition in the two-dimensional fully frustrated xy model. *Phys. Rev. B*, 71:104423, Mar 2005. doi: 10.1103/PhysRevB.71.104423. URL https://link.aps.org/doi/10.1103/PhysRevB.71.104423.

[91] John Cardy. *Scaling and Renormalization in Statistical Physics*. Cambridge Lecture Notes in Physics. Cambridge University Press, 1996. doi: 10.1017/CBO9781316036440.

[92] Mitsuhiro Itakura. Monte carlo renormalization group study of the heisenberg and the xy antiferromagnet on the stacked triangular lattice and the chiral 4 model. *Journal of the Physical Society of Japan*, 72(1):74–82, 2003. doi: 10.1143/JPSJ.72.74. URL http://dx.doi.org/10.1143/JPSJ.72.74.

[93] H. T. Diep. Magnetic transitions in helimagnets. *Phys. Rev. B*, 39:397–404, Jan 1989. doi: 10.1103/PhysRevB.39.397. URL https://link.aps.org/doi/10.1103/PhysRevB.39.397.

[94] G. Quirion, X. Han, M. L. Plumer, and M. Poirier. First order phase transition in the frustrated triangular antiferromagnet $csnicl_3$. *Phys. Rev. Lett.*, 97:077202, Aug 2006. doi: 10.1103/PhysRevLett.97.077202. URL https://link.aps.org/doi/10.1103/PhysRevLett.97.077202.

[95] S. Bekhechi, B. W. Southern, A. Peles, and D. Mouhanna. Short-time dynamics of a family of xy noncollinear magnets. *Phys. Rev. E*, 74:016109, Jul

2006. doi: 10.1103/PhysRevE.74.016109. URL https://link.aps.org/doi/10.1103/PhysRevE.74.016109.

[96] A. Peles, B. W. Southern, B. Delamotte, D. Mouhanna, and M. Tissier. Critical properties of a continuous family of xy noncollinear magnets. *Phys. Rev. B*, 69: 220408, Jun 2004. doi: 10.1103/PhysRevB.69.220408. URL https://link.aps.org/doi/10.1103/PhysRevB.69.220408.

[97] V. Thanh Ngo and H. T. Diep. Stacked triangular xy antiferromagnets: End of a controversial issue on the phase transition. *Journal of Applied Physics*, 103(7):07C712, 2008. doi: 10.1063/1.2837281. URL http://dx.doi.org/10.1063/1.2837281.

[98] S.A. Antonenko, A.I. Sokolov, and K.B. Varnashev. Chiral transitions in three-dimensional magnets and higher order expansion. *Physics Letters A*, 208(1):161 – 164, 1995. ISSN 0375-9601. doi: http://dx.doi.org/10.1016/0375-9601(95)00736-M. URL http://www.sciencedirect.com/science/article/pii/037596019500736M.

[99] Andrea Pelissetto, Paolo Rossi, and Ettore Vicari. Critical behavior of frustrated spin models with noncollinear order. *Phys. Rev. B*, 63:140414, Mar 2001. doi: 10.1103/PhysRevB.63.140414. URL https://link.aps.org/doi/10.1103/PhysRevB.63.140414.

[100] Andrea Pelissetto and Ettore Vicari. Critical phenomena and renormalization-group theory. *Physics Reports*, 368(6):549 – 727, 2002. ISSN 0370-1573. doi: http://dx.doi.org/10.1016/S0370-1573(02)00219-3. URL http://www.sciencedirect.com/science/article/pii/S0370157302002193.

[101] B. Delamotte, M. Dudka, Yu. Holovatch, and D. Mouhanna. Relevance of the fixed dimension perturbative approach to frustrated magnets in two and three dimensions. *Phys. Rev. B*, 82:104432, Sep 2010. doi: 10.1103/PhysRevB.82.104432. URL https://link.aps.org/doi/10.1103/PhysRevB.82.104432.

[102] M. Tissier, B. Delamotte, and D. Mouhanna. XY. *Phys. Rev. B*, 67:134422, Apr 2003. doi: 10.1103/PhysRevB.67.134422. URL https://link.aps.org/doi/10.1103/PhysRevB.67.134422.

[103] B. Delamotte, D. Mouhanna, and M. Tissier. Nonperturbative renormalization-group approach to frustrated magnets. *Phys. Rev. B*, 69:134413, Apr 2004. doi: 10.1103/PhysRevB.69.134413. URL https://link.aps.org/doi/10.1103/PhysRevB.69.134413.

[104] B Delamotte, D Mouhanna, and M Tissier. Frustrated magnets in three dimensions: a nonperturbative approach. *Journal of Physics: Condensed Matter*, 16 (11):S883, 2004. URL http://stacks.iop.org/0953-8984/16/i=11/a=044.

[105] Subir Sachdev. *Quantum Phase Transitions*. Cambridge University Press, Cambridge, UK, 1999.

[106] M. Z. Hasan and C. L. Kane. Colloquium: Topological insulators. *Rev. Mod. Phys.*, 82(4):3045–3067, Nov 2010. doi: 10.1103/RevModPhys.82.3045.

[107] Xiao-Liang Qi and Shou-Cheng Zhang. Topological insulators and superconductors. *Rev. Mod. Phys.*, 83:1057–1110, Oct 2011.

[108] B. A. Bernevig and T. L. Hughes. *Topological Insulators and Topological Superconductors*. Princeton University Press, 2013. ISBN 9780691151755.

[109] Andreas P. Schnyder, Shinsei Ryu, Akira Furusaki, and Andreas W. W. Ludwig. Classification of topological insulators and superconductors in three spatial dimensions. *Phys. Rev. B*, 78(19):195125, Nov 2008. doi: 10.1103/PhysRevB.78.195125.

[110] Joel E. Moore, Ying Ran, and Xiao-Gang Wen. Topological surface states in three-dimensional magnetic insulators. *Phys. Rev. Lett.*, 101:186805, Oct 2008. doi: 10.1103/PhysRevLett.101.186805. URL `http://link.aps.org/doi/10.1103/PhysRevLett.101.186805`.

[111] Liang Fu. Topological crystalline insulators. *Phys. Rev. Lett.*, 106:106802, Mar 2011. doi: 10.1103/PhysRevLett.106.106802. URL `http://link.aps.org/doi/10.1103/PhysRevLett.106.106802`.

[112] P. W. Anderson. Infrared catastrophe in fermi gases with local scattering potentials. *Phys. Rev. Lett.*, 18:1049–1051, Jun 1967. doi: 10.1103/PhysRevLett.18.1049. URL `https://link.aps.org/doi/10.1103/PhysRevLett.18.1049`.

[113] A. Kol and N. Read. Fractional quantum Hall effect in a periodic potential. *Phys. Rev. B*, 48:8890, 1993.

[114] Anders S. Sørensen, Eugene Demler, and Mikhail D. Lukin. Fractional quantum hall states of atoms in optical lattices. *Phys. Rev. Lett.*, 94:086803, Mar 2005. doi: 10.1103/PhysRevLett.94.086803. URL `http://link.aps.org/doi/10.1103/PhysRevLett.94.086803`.

[115] G. Möller and N. R. Cooper. Composite fermion theory for bosonic quantum hall states on lattices. *Phys. Rev. Lett.*, 103:105303, Sep 2009. doi: 10.1103/PhysRevLett.103.105303. URL `http://link.aps.org/doi/10.1103/PhysRevLett.103.105303`.

[116] Evelyn Tang, Jia-Wei Mei, and Xiao-Gang Wen. High-temperature fractional quantum hall states. *Phys. Rev. Lett.*, 106:236802, Jun 2011. doi: 10.1103/PhysRevLett.106.236802. URL `http://link.aps.org/doi/10.1103/PhysRevLett.106.236802`.

[117] Kai Sun, Zhengcheng Gu, Hosho Katsura, and S. Das Sarma. Nearly flatbands with nontrivial topology. *Phys. Rev. Lett.*, 106:236803, Jun 2011. doi: 10.1103/PhysRevLett.106.236803. URL http://link.aps.org/doi/10.1103/PhysRevLett.106.236803.

[118] Titus Neupert, Luiz Santos, Claudio Chamon, and Christopher Mudry. Fractional quantum hall states at zero magnetic field. *Phys. Rev. Lett.*, 106:236804, Jun 2011. doi: 10.1103/PhysRevLett.106.236804. URL http://link.aps.org/doi/10.1103/PhysRevLett.106.236804.

[119] D. N. Sheng, Zheng-Cheng Gu, Kai Sun, and L. Sheng. Fractional quantum hall effect in the absence of landau levels. *Nat. Commun.*, 2:389, 2011.

[120] N. Regnault and B. Andrei Bernevig. Fractional chern insulator. *Phys. Rev. X*, 1:021014, Dec 2011. doi: 10.1103/PhysRevX.1.021014. URL http://link.aps.org/doi/10.1103/PhysRevX.1.021014.

[121] Siddharth A. Parameswaran, Rahul Roy, and Shivaji L. Sondhi. Fractional quantum Hall physics in topological flat bands. *Comptes Rendus Physique*, 14: 816, 2013.

[122] E. I. Blount. In Frederick Seitz and David Turnbull, editors, *Solid State Physics*, volume 13. Academic, New York, 1962.

[123] Yi-Zhuang You, Zhen Bi, Alex Rasmussen, Kevin Slagle, and Cenke Xu. Wave function and strange correlator of short-range entangled states. *Phys. Rev. Lett.*, 112:247202, Jun 2014. doi: 10.1103/PhysRevLett.112.247202. URL http://link.aps.org/doi/10.1103/PhysRevLett.112.247202.

[124] Bohm-Jung Yang, Mohammad Saeed Bahramy, and Naoto Nagaosa. Topological protection of bound states against the hybridization. *Nature Communications*, 4, Feb 2013. ISSN 1434-6036. doi: 10.1038/ncomms2524. URL http://dx.doi.org/10.1038/ncomms2524.

[125] Qian Niu, D. J. Thouless, and Yong-Shi Wu. Quantized hall conductance as a topological invariant. *Phys. Rev. B*, 31:3372–3377, Mar 1985. doi: 10.1103/PhysRevB.31.3372. URL https://link.aps.org/doi/10.1103/PhysRevB.31.3372.

[126] W. P. Su, J. R. Schrieffer, and A. J. Heeger. Solitons in polyacetylene. *Phys. Rev. Lett.*, 42:1698–1701, Jun 1979. doi: 10.1103/PhysRevLett.42.1698. URL http://link.aps.org/doi/10.1103/PhysRevLett.42.1698.

[127] Kai Sun. Topological insulators part iii: tight-binding models. 2013. URL http://www-personal.umich.edu/~sunkai/teaching/Fall_2013/chapter5.pdf.

[128] Liang Fu and C. L. Kane. Time reversal polarization and a Z_2 adiabatic spin pump. *Phys. Rev. B*, 74:195312, Nov 2006. doi: 10.1103/PhysRevB.74.195312. URL https://link.aps.org/doi/10.1103/PhysRevB.74.195312.

[129] D. N. Sheng, Xin Wan, E. H. Rezayi, Kun Yang, R. N. Bhatt, and F. D. M. Haldane. Disorder-driven collapse of the mobility gap and transition to an insulator in the fractional quantum hall effect. *Phys. Rev. Lett.*, 90:256802, Jun 2003. doi: 10.1103/PhysRevLett.90.256802. URL http://link.aps.org/doi/10.1103/PhysRevLett.90.256802.

[130] Christopher N. Varney, Kai Sun, Victor Galitski, and Marcos Rigol. Kaleidoscope of exotic quantum phases in a frustrated xy model. *Phys. Rev. Lett.*, 107 (7):077201, Aug 2011. doi: 10.1103/PhysRevLett.107.077201.

[131] Christopher N. Varney, Kai Sun, Marcos Rigol, and Victor Galitski. Topological phase transitions for interacting finite systems. *Phys. Rev. B*, 84:241105, Dec 2011. doi: 10.1103/PhysRevB.84.241105. URL https://link.aps.org/doi/10.1103/PhysRevB.84.241105.

[132] Paolo Zanardi and Nikola Paunković. Ground state overlap and quantum phase transitions. *Phys. Rev. E*, 74:031123, Sep 2006. doi: 10.1103/PhysRevE.74.031123. URL https://link.aps.org/doi/10.1103/PhysRevE.74.031123.

[133] Lorenzo Campos Venuti and Paolo Zanardi. Quantum critical scaling of the geometric tensors. *Phys. Rev. Lett.*, 99(9):095701, Aug 2007. doi: 10.1103/PhysRevLett.99.095701.

[134] Marcos Rigol, B. Sriram Shastry, and Stephan Haas. Fidelity and superconductivity in two-dimensional t-J models. *Phys. Rev. B*, 80(9):094529, Sep 2009. doi: 10.1103/PhysRevB.80.094529.

[135] Yuan-Yao He, Han-Qing Wu, Yi-Zhuang You, Cenke Xu, Zi Yang Meng, and Zhong-Yi Lu. Bona fide interaction-driven topological phase transition in correlated symmetry-protected topological states. *Phys. Rev. B*, 93:115150, Mar 2016. doi: 10.1103/PhysRevB.93.115150. URL http://link.aps.org/doi/10.1103/PhysRevB.93.115150.

[136] Tzu-Chieh Wei and Paul M. Goldbart. Geometric measure of entanglement and applications to bipartite and multipartite quantum states. *Phys. Rev. A*, 68:042307, Oct 2003. doi: 10.1103/PhysRevA.68.042307. URL https://link.aps.org/doi/10.1103/PhysRevA.68.042307.

[137] M. Blasone, F. Dell'Anno, S. De Siena, and F. Illuminati. Hierarchies of geometric entanglement. *Phys. Rev. A*, 77:062304, Jun 2008. doi: 10.1103/PhysRevA.77.062304. URL https://link.aps.org/doi/10.1103/PhysRevA.77.062304.

[138] Romn Ors, Tzu-Chieh Wei, Oliver Buerschaper, and Maarten Van den Nest. Geometric entanglement in topologically ordered states. *New Journal of Physics*, 16(1):013015, 2014. URL http://stacks.iop.org/1367-2630/16/i=1/a=013015.

[139] Jiahua Gu and Kai Sun. Adiabatic continuity, wave-function overlap, and topological phase transitions. *Phys. Rev. B*, 94:125111, Sep 2016. doi: 10.1103/PhysRevB.94.125111. URL http://link.aps.org/doi/10.1103/PhysRevB.94.125111.

[140] Shi-Jian Gu. Fidelity approach to quantum phase transitions. *International Journal of Modern Physics B*, 24(23):4371–4458, 2010. doi: 10.1142/S0217979210056335. URL http://www.worldscientific.com/doi/abs/10.1142/S0217979210056335.

[141] Christopher N. Varney, Kai Sun, Marcos Rigol, and Victor Galitski. Interaction effects and quantum phase transitions in topological insulators. *Phys. Rev. B*, 82:115125, Sep 2010. doi: 10.1103/PhysRevB.82.115125. URL https://link.aps.org/doi/10.1103/PhysRevB.82.115125.

[142] E. J. König, A. Levchenko, and N. Sedlmayr. Universal fidelity near quantum and topological phase transitions in finite one-dimensional systems. *Phys. Rev. B*, 93:235160, Jun 2016. doi: 10.1103/PhysRevB.93.235160. URL https://link.aps.org/doi/10.1103/PhysRevB.93.235160.

[143] Michael Levin and Zheng-Cheng Gu. Braiding statistics approach to symmetry-protected topological phases. *Phys. Rev. B*, 86:115109, Sep 2012. doi: 10.1103/PhysRevB.86.115109. URL http://link.aps.org/doi/10.1103/PhysRevB.86.115109.

[144] John L. Cardy and Ingo Peschel. Finite-size dependence of the free energy in two-dimensional critical systems. *Nuclear Physics B*, 300:377 – 392, 1988. ISSN 0550-3213. doi: http://dx.doi.org/10.1016/0550-3213(88)90604-9. URL http://www.sciencedirect.com/science/article/pii/0550321388906049.

[145] Zhen Bi, Alex Rasmussen, Kevin Slagle, and Cenke Xu. Classification and description of bosonic symmetry protected topological phases with semiclassical nonlinear sigma models. *Phys. Rev. B*, 91:134404, Apr 2015. doi: 10.1103/PhysRevB.91.134404. URL https://link.aps.org/doi/10.1103/PhysRevB.91.134404.

[146] Xie Chen, Zheng-Cheng Gu, Zheng-Xin Liu, and Xiao-Gang Wen. Symmetry-protected topological orders in interacting bosonic systems. *Science*, 338(6114):1604–1606, 2012. ISSN 0036-8075. doi: 10.1126/science.1227224. URL http://science.sciencemag.org/content/338/6114/1604.

[147] Xie Chen, Zheng-Xin Liu, and Xiao-Gang Wen. Two-dimensional symmetry-protected topological orders and their protected gapless edge excitations. *Phys. Rev. B*, 84:235141, Dec 2011. doi: 10.1103/PhysRevB.84.235141. URL https://link.aps.org/doi/10.1103/PhysRevB.84.235141.

[148] Zheng-Xin Liu and Xiao-Gang Wen. Symmetry-protected quantum spin hall phases in two dimensions. *Phys. Rev. Lett.*, 110:067205, Feb 2013. doi: 10.

1103/PhysRevLett.110.067205. URL https://link.aps.org/doi/10.1103/PhysRevLett.110.067205.

[149] Edward Witten. Global aspects of current algebra. *Nuclear Physics B*, 223(2):422 – 432, 1983. ISSN 0550-3213. doi: https://doi.org/10.1016/0550-3213(83)90063-9. URL http://www.sciencedirect.com/science/article/pii/0550321383900639.

[150] Edward Witten. Non-abelian bosonization in two dimensions. *Communications in Mathematical Physics*, 92(4):455–472, Dec 1984. ISSN 1432-0916. doi: 10.1007/BF01215276. URL https://doi.org/10.1007/BF01215276.

[151] P. Di Francesco, H. Saleur, and J.B. Zuber. Modular invariance in non-minimal two-dimensional conformal theories. *Nuclear Physics B*, 285:454 – 480, 1987. ISSN 0550-3213. doi: http://dx.doi.org/10.1016/0550-3213(87)90349-X. URL http://www.sciencedirect.com/science/article/pii/055032138790349X.

[152] P. di Francesco, H. Saleur, and J. B. Zuber. Relations between the coulomb gas picture and conformal invariance of two-dimensional critical models. *Journal of Statistical Physics*, 49(1):57–79, 1987. ISSN 1572-9613. doi: 10.1007/BF01009954. URL http://dx.doi.org/10.1007/BF01009954.

[153] Henk W J Blöte, Yougang Wang, and Wenan Guo. The completely packed o(n) loop model on the square lattice. *Journal of Physics A: Mathematical and Theoretical*, 45(49):494016, 2012. URL http://stacks.iop.org/1751-8121/45/i=49/a=494016.

[154] Gerald V. Dunne. Slater decomposition of laughlin states. *International Journal of Modern Physics B*, 07(28):4783–4813, 1993. doi: 10.1142/S0217979293003838. URL http://www.worldscientific.com/doi/abs/10.1142/S0217979293003838.

[155] B. Jancovici, G. Manificat, and C. Pisani. Coulomb systems seen as critical systems: Finite-size effects in two dimensions. *Journal of Statistical Physics*, 76 (1), 1994. ISSN 1572-9613. doi: 10.1007/BF02188664. URL http://dx.doi.org/10.1007/BF02188664.

[156] B. Jancovici and G. Téllez. Coulomb systems seen as critical systems: Ideal conductor boundaries. *Journal of Statistical Physics*, 82(3):609–632, 1996. ISSN 1572-9613. doi: 10.1007/BF02179788. URL http://dx.doi.org/10.1007/BF02179788.

[157] G. Téllez and P. J. Forrester. Exact finite-size study of the 2d ocp at γ=4 and γ=6. *Journal of Statistical Physics*, 97(3):489–521, 1999. ISSN 1572-9613. doi: 10.1023/A:1004654923170. URL http://dx.doi.org/10.1023/A:1004654923170.

[158] Bernard Jancovici and Emmanuel Trizac. Universal free energy correction for the two-dimensional one-component plasma. *Physica A: Statistical Mechanics and its Applications*, 284(14):241 – 245, 2000. ISSN 0378-4371. doi: http://dx.doi.org/10.1016/S0378-4371(00)00216-8. URL http://www.sciencedirect.com/science/article/pii/S0378437100002168.

[159] Caillol, J.M. Exact results for a two-dimensional one-component plasma on a sphere. *J. Physique Lett.*, 42(12):245–247, 1981. doi: 10.1051/jphyslet:019810042012024500. URL https://doi.org/10.1051/jphyslet:019810042012024500.

[160] Richard B. Paris. Incomplete gamma and related functions. 2010. URL http://dlmf.nist.gov/8.11.

[161] Alastuey, A. and Jancovici, B. On the classical two-dimensional one-component coulomb plasma. *J. Phys. France*, 42(1):1–12, 1981. doi: 10.1051/jphys:019810042010100. URL https://doi.org/10.1051/jphys:019810042010100.

[162] Ashvin Vishwanath and T. Senthil. Physics of three-dimensional bosonic topological insulators: Surface-deconfined criticality and quantized magnetoelectric effect. *Phys. Rev. X*, 3:011016, Feb 2013. doi: 10.1103/PhysRevX.3.011016. URL https://link.aps.org/doi/10.1103/PhysRevX.3.011016.

[163] F. J. Burnell, Xie Chen, Lukasz Fidkowski, and Ashvin Vishwanath. Exactly soluble model of a three-dimensional symmetry-protected topological phase of bosons with surface topological order. *Phys. Rev. B*, 90:245122, Dec 2014. doi: 10.1103/PhysRevB.90.245122. URL https://link.aps.org/doi/10.1103/PhysRevB.90.245122.

[164] Lukasz Fidkowski, Xie Chen, and Ashvin Vishwanath. Non-abelian topological order on the surface of a 3d topological superconductor from an exactly solved model. *Phys. Rev. X*, 3:041016, Nov 2013. doi: 10.1103/PhysRevX.3.041016. URL https://link.aps.org/doi/10.1103/PhysRevX.3.041016.

[165] Xie Chen, Lukasz Fidkowski, and Ashvin Vishwanath. Symmetry enforced non-abelian topological order at the surface of a topological insulator. *Phys. Rev. B*, 89:165132, Apr 2014. doi: 10.1103/PhysRevB.89.165132. URL https://link.aps.org/doi/10.1103/PhysRevB.89.165132.

[166] Max A. Metlitski, C. L. Kane, and Matthew P. A. Fisher. Symmetry-respecting topologically ordered surface phase of three-dimensional electron topological insulators. *Phys. Rev. B*, 92:125111, Sep 2015. doi: 10.1103/PhysRevB.92.125111. URL https://link.aps.org/doi/10.1103/PhysRevB.92.125111.

[167] Michael Levin and Xiao-Gang Wen. Detecting topological order in a ground state wave function. *Phys. Rev. Lett.*, 96:110405, Mar 2006. doi: 10.1103/PhysRevLett.96.110405. URL https://link.aps.org/doi/10.1103/PhysRevLett.96.110405.

[168] Alexei Kitaev and John Preskill. Topological entanglement entropy. *Phys. Rev. Lett.*, 96:110404, Mar 2006. doi: 10.1103/PhysRevLett.96.110404. URL https://link.aps.org/doi/10.1103/PhysRevLett.96.110404.

[169] Bernard Nienhuis. Exact critical point and critical exponents of O(n) models in two dimensions. *Phys. Rev. Lett.*, 49:1062–1065, Oct 1982. doi: 10.1103/PhysRevLett.49.1062. URL http://link.aps.org/doi/10.1103/PhysRevLett.49.1062.

[170] R R Sari, D Merlini, and R Calinon. On the ground state of the one-component classical plasma. *Journal of Physics A: Mathematical and General*, 9(9):1539, 1976. URL http://stacks.iop.org/0305-4470/9/i=9/a=014.